universität wien

DISSERTATION

Titel der Dissertation

Novel strategies of maintaining and transmitting specific microbial symbionts in marine flatworms

Verfasser

Diplom Biologe Ulrich Dirks

angestrebter akademischer Grad

Doktor der Naturwissenschaften (Dr. rer. nat.)

Wien, 14.09.2011

Studienkennzahl (lt. Studienblatt):	A 091-444
Dissertationsgebiet (lt. Studienblatt):	Ökologie
Betreuerin / Betreuer:	Univ. Prof. i.R. Dr. Jörg Ott

Table of Contents

INTRODUCTION

Symbiosis and Mutualism

In 1879 the german researcher Heinrich Anton de Bary published the article "Die Erscheinung der Symbiose" in which he defined "the living together of unlike organisms" as symbiosis (based on the ancient-greek words *"sýn*" = with/together and "*bíōsis"* = living). Since then, various kinds of long-term associations between two or more different organisms are termed symbiosis. Parasitism is a special case of symbiosis in which only one partner, the parasite, benefits at the expense of the other partner, the host. In contrast the opposite type of symbiosis termed "mutualism", which is a central topic of this PhD-thesis, stands for an interaction from which both partners, host (usually the bigger partner) and symbiont, benefit. However, it is often not possible to define the exact borders between parasitism and mutualism since life is a dynamic process and small changes in the environment may also affect the interactions between the symbiotic partners.

Symbiotic relationships can be found between organisms of all domains of life. While the general public thinks for example of birds cleaning the teeth of crocodiles or the well-known clownfish-anemone symbiosis, the scientific community is rather focused on associations of microbes among themselves or with eukaryotes. In case the symbionts reside outside of their host´s body they are termed ectosymbionts (e.g. the beneficial bacteria on the human's skin), those inside of their host´s body are termed endosymbionts (e.g. the human gut microbiota). Endosymbionts can further be divided into extra- or intracellular forms.

How microbial symbiosis allowed eukaryotes to conquer new habitats

Mutualistic symbiosis between organisms with different metabolic or mechanical abilities increases the fitness of both partners and can extend their range of suitable habitats significantly (Boucher et al. 1982). For example the acquisition of the mitochondrion about 2 billion years ago increased the efficiency of the

heterotrophic lifestyle in the eukaryote progenitor cell; the uptake of the plastid progenitor enabled the eukaryotic cell to live photoautotrophic. Both of these microbial uptake-events had lasting consequences on the tree of life. Today mitochondria and plastids are called "cell-organelles" due to their deep integration into the eukaryotic cell and their incapability to survive independently (see for example Martin and Russell 2003).

Eukaryotic cells (containing organelles) possess a set of metabolic core-features. In addition many eukaryotes have established symbiotic associations with microbes that further increased their fitness and thus allowed them to conquer new habitats, which both symbiotic partners are unable to inhabit individually (Dale and Moran 2006). The microbial symbionts profit from a fairly stable environment, a reliable supply of specific nutrients and motility and/or other mechanical skills of the eukaryotic host to access sheltered resources. In turn the host profits from the diverse metabolic capabilities of the microbes. In strong contrast to the organelles, which are found in most cells of their hosts (with some exceptions), the associations between animals/plants and their symbionts are often restricted to certain cell types or organs and in many cases also to a certain stage of life (reviewed in Bright and Bulgheresi 2010).

Chemosynthetic symbionts of marine animals

Oceans cover more than 70% of the earth´s surface with a mean depth of 3800m. However, due to the attenuation of light in the water column photosynthesis is restricted to the surface waters down to a maximum depth of 200m and to the top millimeters of the shallow water sediments. Although phototrophic organisms are responsible for the bulk of the primary production in marine waters, not all organisms in the "Dark Ocean" or within sediments live heterotrophically. Many microorganisms are capable of chemosynthesis; they are primary producers using the energy from the oxidation of reduced inorganic compounds like sulfide, ammonium or methane to fix inorganic carbon (usually CO_2). Animals of various taxa in different marine environments from the coast to the deep sea were found to build symbioses with chemosynthetic symbionts (Figure 1) (reviewed in Dubilier et al. 2008).

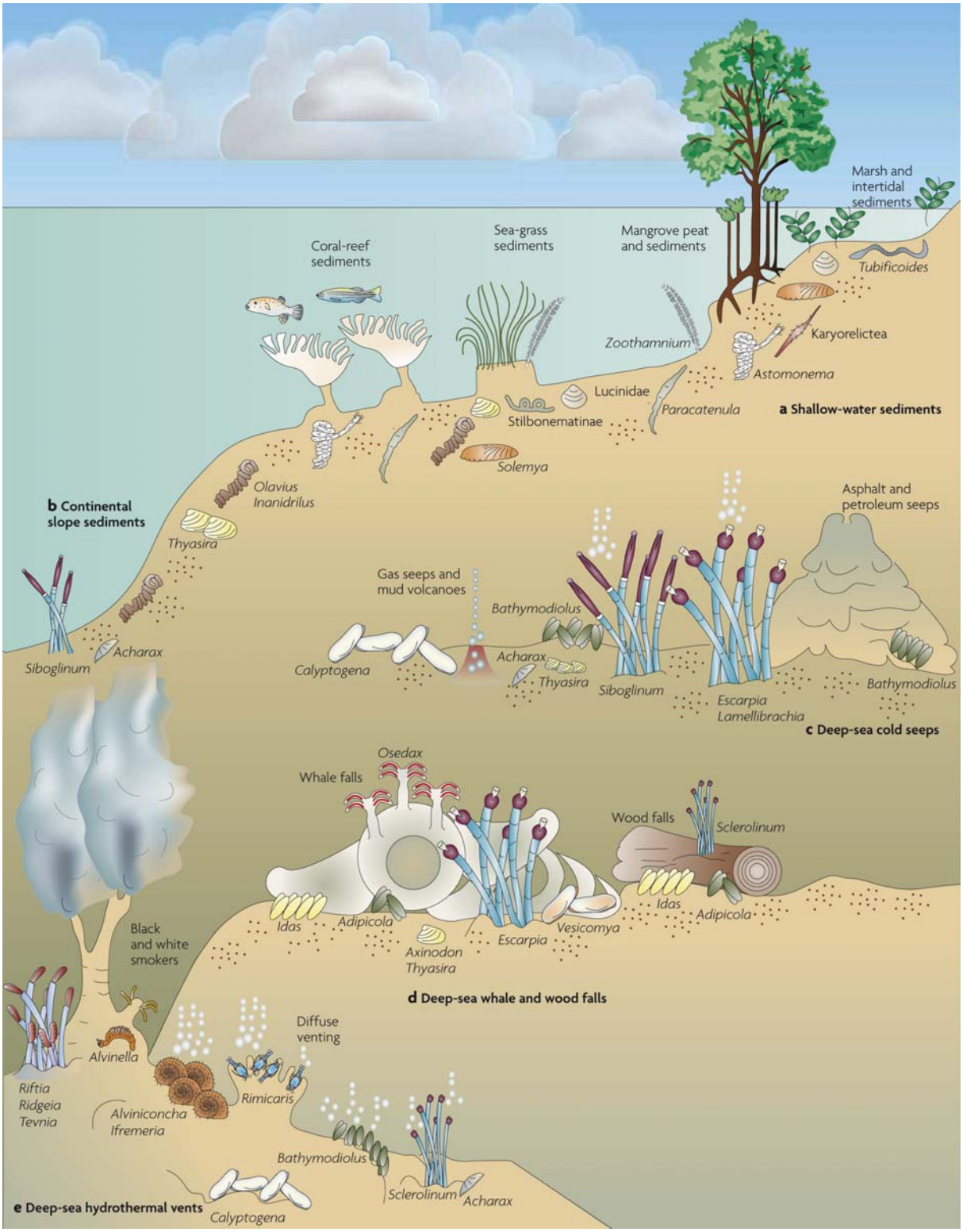

Figure 1: Chemosynthetic symbioses in different marine habitats. Chemosynthetic symbioses occur in a wide range of marine habitats, including shallow-water sediments (a), continental slope sediments (b), cold seeps (c), whale and wood falls (d), and hydrothermal vents (e). Some host groups are found in only one habitat (such as *Osedax* on whale bones), whereas others occur in several different environments (such as thyasirid clams, which are found in shallow-water sea-grass sediments and in the deep sea at cold seeps, whale falls and hydrothermal vents). The animals are not drawn to scale; for example, *Idas* and *Adipicola* mussels are much smaller than *Bathymodiolus* mussels. (from Dubilier et al., 2008).

Paracatenula: An exceptional genus of marine flatworms

In 1974 Sterrer & Rieger published the description of a new family within the most basal group of the Plathyhelmintes, the Catenulida. This family, which they called Retronectidae due to the ability of their members to swim backwards by reversing the ciliary beat, contains two genera: *Retronectes* and *Paracatenula*. Retronectidae were found in marine shallow water sediments of tropical to temperate regions. Possessing most of the typical features *Retronectes*-species were doubtlessly assigned to the catenulids while *Paracatenula*-species, however, appeared to be catenulids completely lacking mouth, pharynx and gut lumen (Figure 2A). Instead, Sterrer and Rieger (1974) described peculiar large turgescent cells containing little granular bodies which almost filled the complete posterior body region (Figure 2B). Ten years later Ott et al. (1982) published a reinvestigation of *Paracatenula* in which they identified the

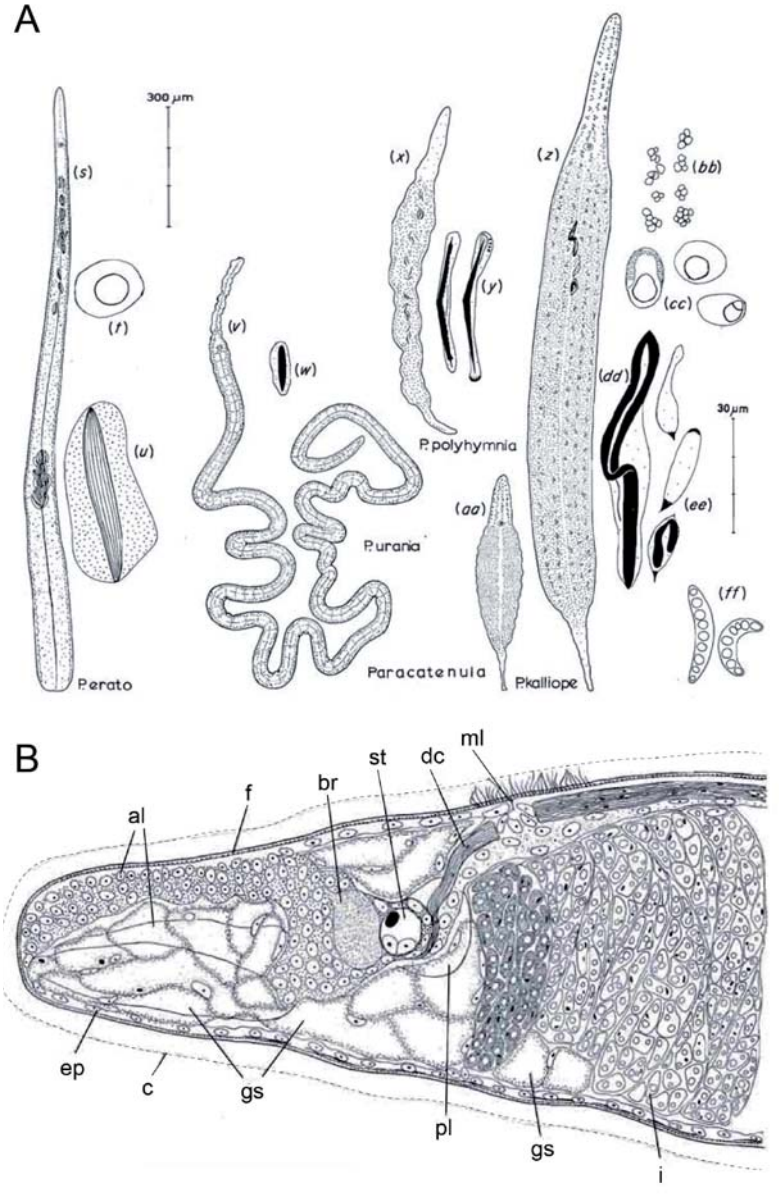

Figure 2: Modified drawings from the original description of the genus *Paracatenula* by Sterrer and Rieger, 1974. (A) *Paracatenula*, general morphology drawn from live specimens. All organizations are in one scale, all details in the other. (s-u) *Paracatenula erato* sp. n.: (s) organization: (t) statocyst: (u) sperm. (v, w) *Paracatenula urania* sp. n.: (v) organization; (w) sperm. (x, y) *Paracatenula polyhymnia* sp. n.: (x) organization; (y) sperm. (z, aa - ff) *Paracatenula kalliope* sp. n.: (z) organization: (aa) juvenile specimen; (bb) inclusions from rostrum: (cc) statocysts of three specimens: (dd) sperm; (ee) spermatids: (ff) inclusions from parenchyma. (B) *Paracatenula* erato sp. n. organization of anterior body region, lateral view. ml: male opening; dc: dorsal cord; st: statocyst; br: brain; f: fibrillose structures in the epidermis; al: anterior gangliar lobes of the brain; ep: epidermis; c: cilia; gs: granular strands; pl: posterior gangliar lobes of the brain; i: gut; Scale bars in A: see label, in B: 40 µm.

"little granular bodies" as intracellular symbiotic bacteria. To date species of the genus *Paracatenula* are still the only known free-living and symbiotic Platyhelminthes lacking mouth and gut. A detailed investigation of this symbiosis, which still remained to be conducted, was the central aim of this thesis.

Aims of symbiosis research

Symbioses are unique systems to study interactions between different organisms because they are, in contrast to other inter-organism-associations, long lasting and intimate. Two of the major research questions are: "How do host and symbiont selectively establish and maintain an association without becoming target of the immune defense of the counterpart?" and "How do mutualistic partners profit from their association?" Recent research showed that the strategies which symbionts and hosts use to circumvent their mutual immune systems are in many ways similar to those in pathogenic interactions (reviewed in Dale and Moran 2006). Furthermore, the cooperation of different organisms stimulates the field of biotechnology to derive benefit from this. For example microbial symbionts in sponges and other marine invertebrates produce diverse compounds that are promising candidates as anti-cancer or anti-inflammatory agents (reviewed in Taylor et al. 2007). Likewise, also genetic engineered symbiosis e.g. of mycorrhiza (fungal root-symbionts of nearly all land plants) will gain importance in the near future in order to increase crop yields (Ferrol et al. 2004). Beyond a doubt symbiosis has a tremendous future potential for the disciplines of medicine and food production (reviewed in Smith 2001).

Thesis outline

The general aim of this thesis was to investigate the mechanisms which symbiotic flatworms of the genus *Paracatenula* use to maintain the symbiotic association during growth and development (ontogenesis) and to transmit or reestablish the association during reproduction. The material and data that were collected since November 2007 are so far included in four manuscripts of which two are published or in press, one is under review and one is "ready for submission". In the following I provide short summaries of the four manuscripts (Chapters 1-4) and briefly describe which questions were addressed and results accomplished. The central work of this thesis is included in chapter 3. At the beginning of each chapter a statement on my personal contribution to manuscript/publication is provided.

Chapter 1: One goal of this thesis was to identify a *Paracatenula* species which can be sampled reliably (or cultivated) and is suitable to perform incubation experiments and different kinds of stainings. In the article "A new species of symbiotic flatworms, *Paracatenula galateia* sp. nov. (Platyhelminthes: Catenulida: *Retronectidae*) from Belize (Central America)" (in press in Marine Biology Research; DOI 10.1080/17451000.2011.574880) we describe a newly discovered *Paracatenula*-species which has become the most promising flatworm model system in our laboratory. Among the high diversity of species we found on various sampling trips (see Chapter 2), *P. galateia* appeared to be best suitable for experimental work and it could be reliably sampled on well accessible spots. The cultivation attempts, however, were not successful.

Chapter 2: In the second study included in this thesis "*Paracatenula*, an ancient symbiosis between thiotrophic *Alphaproteobacteria* and catenulid flatworms" (published in Proceedings of the National Academy of Sciences, 2011) I contributed essential experimental data to the work of my colleague Mag. Harald R. Gruber-Vodicka who used molecular techniques to investigate the phylogeny of *Paracatenula* host-species and their specific symbionts. On six fieldtrips we sampled a diversity of 16 species. Using ribosomal RNA sequence based molecular phylogeny and fluorescence *in situ* hybridization we show that each *Paracatenula*-species harbors specific symbionts and that both partners tightly coevolve, a phenomenon known from other symbioses in which the symbionts are vertically transmitted (inherited) through host generations. In addition we provide a detailed description of the first known thiotrophic symbionts among the *Alphaproteobacteria*.

Chapter 3 is the central work of this thesis. The question addressed here was how *Paracatenula*-hosts maintain their symbionts during growth and development and how the offspring acquires the obligate symbionts. In the manuscript "Continued *de novo* formation and asexual transmission of bacteriocytes in the symbiotic flatworm *Paracatenula galateia*" (under review in The ISME Journal) we present data that answer these questions and may explain the tight coevolution between host and symbionts. The data includes a first characterization of *P. galateia´*s neoblast stem cell system and its regenerative potential. In addition a to date unknown way of vertical symbiont transmission was documented. Summarized chapter 3 describes the previously unknown strategies these flatworms use to maintain contact to their intracellular symbionts during growth and reproduction.

Chapter 4: In the previous chapter we showed that *Paracatenula*-worms are capable to regenerate lost body parts. In chapter 4 named "Proliferation pattern of neoblasts during rostrum regeneration of the symbiotic flatworm *Paracatenula galateia* – a pulse-chase-pulse analysis" (ready for submission to Cell and Tissue Research) the processes underlying regeneration were analyzed in detail. The data presented in this chapter clearly identify neoblast stem cells as the major drivers of rostrum regeneration in decapitated *P. galateia*. With an Edu-BrdU double-labelling approach we detected and traced the S-phase cells during different stages of regeneration. In addition also the regeneration of the brain was observed.

References

Boucher DH, James S, Keeler KH (1982). The Ecology of Mutualism. *Annual Review of Ecology and Systematics* **13:** 315-347.

Bright M, Bulgheresi S (2010). A complex journey: transmission of microbial symbionts. *Nat Rev Micro* **8:** 218-230.

Dale C, Moran NA (2006). Molecular interactions between bacterial symbionts and their hosts. *Cell* **126:** 453-465.

de Bary A (1879). *Die Entstehung der Symbiose*. Verlag von Karl, J. Trübner, Strassburg.

Dubilier N, Bergin C, Lott C (2008). Symbiotic diversity in marine animals: the art of harnessing chemosynthesis. *Nature reviews* **6:** 725-740.

Ferrol N, Bago B, Franken P, Gollotte A, González-Guerrero M, Alexandra Harrier L et al. (2004). Genomics of arbuscular mycorrhizal fungi. In: Dilip KA, George GK (eds). *Applied Mycology and Biotechnology*. Elsevier. pp 379-403.

Martin W, Russell MJ (2003). On the origins of cells: a hypothesis for the evolutionary transitions from abiotic geochemistry to chemoautotrophic prokaryotes, and from prokaryotes to nucleated cells. *Philos Trans R Soc Lond B Biol Sci* **358:** 59-83; discussion 83-55.

Ott JA, Rieger G, Rieger R, Enderes F (1982). New mouthless interstitial worms from the sulfide system: Symbiosis with Prokaryotes. *PSZN I: Mar Ecol* **3:** 313-333.

Smith DC (2001). Symbiosis research at the end of the millenium. *Hydrobiologia* **461:** 49-54.

Sterrer W, Rieger R (1974). Retronectidae - a new cosmopolitan marine family of Catenulida (Turbellaria). In: Riser N, Morse M (eds). *Biology of the Turbellaria*. McGraw-Hill: New York. pp 63-92.

Taylor MW, Radax R, Steger D, Wagner M (2007). Sponge-associated microorganisms: evolution, ecology, and biotechnological potential. *Microbiol Mol Biol Rev* **71:** 295-347.

CHAPTER 1

A new species of symbiotic flatworms, *Paracatenula galateia* sp. nov. (Platyhelminthes: Catenulida: Retronectidae) from Belize (Central America) †

Authors: Ulrich Dirks[$], Harald R. Gruber-Vodicka[$], Nikolaus Leisch, Wolfgang Sterrer & Jörg A. Ott

[$] these authors contributed equally

Keywords: interstitial meiofauna, subtidal sand, intracellular symbiosis

Publication status: Article in press in Marine Biology Research (MBR) (accepted 2011-02-26).

Detailed description of UD´s contribution: UD attended the field trips to Carrie Bow Caye (Belize) during which the material was collected ; UD contributed light microscopical data and measurements for the statistical analysis; UD established protocols for immunofluorescence and phalloidin stainings of *P. galateia* and performed all stainings included in this manuscript; UD contributed the semithin cross-sections; UD wrote the manuscript together with HRGV and JAO.

Abstract

Paracatenula galateia sp. nov. is a mouthless marine catenulid platyhelminth with bacterial intracellular endosymbionts. The worms live in shallow back-reef sands in the Belize Barrier Reef system and are distinguished from the four previously described members of the genus by their large size combined with a ribbon-shaped body and characteristic bipartite inclusions in cells, which are interpreted as sperm. The bacteria are presumed to be sulphur oxidizing chemoautotrophs. They are found in bacteriocytes which fill the body region ("trophosome region") posterior to the brain, whereas the anterior part of the worm (rostrum) is bacteria free. Phalloidin staining reveals a delicate system of subepitheliar circular and longitudinal muscles and dorsoventral fibers. The serotonergic nervous system consists of a brain at the base of the rostrum and longitudinal fibers extending both anteriorly and posteriorly, the latter being concentrated in a structure called the "dorsal cord".

Introduction

Catenulida are an order of small, free-living Platyhelminthes ('Turbellaria', Tyler et al. 2006-2010). Originally thought to occur exclusively in freshwater except for the questionable *Tyrrheniella sigillata* (Riedl 1959), they were first reported from marine sandy bottoms by Sterrer (1966). Sterrer & Rieger (1974) described nine marine species from NE and W Atlantic coasts, belonging to two new genera (*Retronectes* and *Paracatenula*) for which they erected the family Retronectidae, named for their ability to swim backward by reversing the ciliary beat. Usually found only as isolated, fragile specimens, and difficult to identify for their paucity of consistent morphometric features, retronectids are characterized by an often polylithophorous statocyst (which may be lacking in some species or specimens), and a simple, anterio-dorsally opening mixed gonad. Reproductive biology is as yet unresolved: oocytes were observed in only one, and a mature egg in another species of *Retronectes* of at least 50 specimens studied (Sterrer and Rieger 1974). A small proportion of specimens contained cells with distinctly shaped inclusions that have been interpreted as spermatozoa and their nuclei; spermatids contain ciliary rudiments (Rieger 1978). In *Paracatenula,* distinct gonads are apparently lacking; in fact no oocytes or eggs have ever been found. Instead, cells containing characteristic rod-, ribbon-, banana- or even spicule-shaped inclusions were found along a strand of tissue named "dorsal cord" (Sterrer and Rieger 1974), which extends throughout the body in median position. These inclusions often clustered behind the brain (in a *vesicula seminalis*?), where a dorsal pore to the outside may be located.

The peculiar retronectid gonad with its large, oocyte-like sperm prompted Sterrer & Rieger (1974) to suggest "a completely new mode of reproduction – such as parthenogenesis from sperm" along the transformation of male cells into oocytes described by Borkott (1970) for the freshwater catenulid *Stenostomum*; see also Schuchert & Rieger (1990) – and further "underlines the isolated position of the Catenulida within the Turbellaria and the Platyhelminthes" (Rieger 1978). Recent multilocus phylogenetic studies corroborate the placement of the genus *Paracatenula* within the Catenulida and also the status of the Catenulida as the basal taxon of Platyhelminthes (Larsson and Jondelius 2008).

While members of *Retronectes* have a mouth, ciliated pharynx, and gut lumen, those of *Paracatenula* were described to lack mouth, pharynx, and gut lumen; the tissue filling most of the body volume rather consists of large turgescent cells containing "granular bodies". These have been identified as intracellular

bacteria in *P. erato* Sterrer and Rieger, 1974 (Ott et al. 1982). Subsequent investigations have shown that this is the case for all members of the genus *Paracatenula* (own unpublished observations). The bacteria are presumably symbiotic sulphur oxidizers, since the bacteria from two *Paracatenula* species have been shown to possess a reverse dissimilatory sulphite reductase (DsrAB) gene, an important gene in bacterial sulphur metabolism, which clustered with the sequences of other sulphur oxidizing bacteria (Loy et al. 2009). In addition, the bacteria contain highly refractive granules, appearing white in incident light, which resemble the elemental sulphur storage granules known from many sulphur oxidizing bacteria (Pasteris et al. 2001). Members of *Paracatenula* have a symbiont-free anterior body region (rostrum) and a posterior body region filled by symbiont-containing cells (bacteriocytes), which together form a distinct organ, which we call "trophosome" in analogy to the symbiont-containing organ in the vestimentiferan annelids.

Only three more species of Retronectidae have been described since Sterrer & Rieger's (1974) original nine: one new genus*, Myoretronectes paranensis* Noreña-Jansson and Faubel, 1996 from Argentina, and two species of *Retronectes* - *R. sterreri* Faubel, 1976 from the North Sea and *R. atypica* Doe and Rieger, 1977 from North Carolina. During investigations of the meiofauna in back reef sediments of the Mesoamerican barrier reef system at Belize, a large, conspicuous new species was found to be common in subtidal sands close to the field station of the US National Museum of Natural History (Washington DC) on the island of Carrie Bow Cay (Rützler and Macintyre 1982). This species is currently subject to intensive studies of its biology and ecology. Here we present the description of this species new to science.

Materials and Methods

Specimens were collected between 2007 and 2010 at several locations in the vicinity of the field station of the US National Museum of Natural History (Washington DC) on the island of Carrie Bow Cay (Fig. 1). The worms were extracted by shaking sand samples in seawater and pouring the supernatant through a 32-µm-pore-size mesh. Individual specimens were picked by hand and inspected using a dissecting microscope. Squeeze preparations of live animals were analyzed using bright field and phase contrast microscopy at 16x to 1000x magnification. Digital photomicrographs were collected and used for measurements with the analysis tool of Adobe Photoshop CS5.

Fluorescent staining of whole mounts

Musculature in whole mounts of individual worms was made visible by staining F-actin with fluorescently labeled phalloidin (Alexa Fluor 568; Invitrogen, Austria); the nervous system by staining of serotonergic nerves with an anti-serotonin antiserum produced in rabbit (Sigma Aldrich, Austria) followed by a staining with an Alexa Fluor 568-conjugated secondary antibody. Freshly collected specimens were first relaxed in a magnesium chloride solution isotonic to sea water, fixed for 12 h in 4% (w/v) formaldehyde at 4°C, rinsed in PBS (phosphate buffered saline) and stored in PBS at 4°C (for phalloidin staining) or in Methanol at -20°C (for serotonin staining). For phalloidin staining the specimens were washed and permeabilized in PBS with 0.2% (v/v) Triton X-100 (PBS-T) and then stained for 30 min with phalloidin-Alexa 568 diluted 1:200 in PBS-T. After 3 washes in PBS and a DAPI staining for 5 min the specimens were mounted on slides in Vecta shield (Vector Laboratories). For antibody staining the fixed animals were transferred into PBS-T and digested for 6 min at room temperature in 0,1 mg/ml Proteinase K in PBS-T. Digestion was stopped by adding 2 N hydrochloric acid. Animals were then washed in PBS-T and blocked in BSA-T (bovine serum albumin plus 0.2% Triton X-100) for 30 min. Serotonin was stained with the anti-serotonin antiserum 1:2000 diluted in BSA-T overnight at 4° C. After three washing steps in PBS-T an Alexa 547 conjugated secondary antibody was applied for 1 h at room temperature at 1:300 dilution in BSA-T. DAPI staining and mounting was done as described above. Slides were either scanned with a confocal laser-scanning microscope (Zeiss LSM 510) or examined and photographed with an epifluorescence microscope (Zeiss Axio Imager).

DNA extraction, PCR amplification and sequencing

DNA was extracted from ten worms using the Blood and Tissue DNA extraction kit (Qiagen, Germany) and 2 µl of each extraction was used as PCR template. Fragments of the 18S and 28S rRNA-gene (1750 and 1350 nt-long, respectively) were amplified for each worm by PCR with the general eukaryotic primers 1f (5'-CTGGTTGATYCTGCCAGT-3') and 2023r (5'-GGTTCACCTACGGAAACC-3) for 18S (Pradillon et al. 2007) and the Primers D1a (5'-CCC(C/G)CGTAA(T/C)TTAAGCATAT-3') and D5b2 (5'-CGCCAGTTCTGCTTACC-3) initially developed for Arthropoda for 28S (von Reumont et al. 2009). Cycling conditions for both genes were: 94°C for 3 min followed by 40 cycles of 94°C for 45 s, 49°C for 30 s, 72°C for 1 min, and a final elongation step of 72°C for 10 min. The PCR products obtained were

purified using the MinElute PCR purification kit (Qiagen) and directly sequenced with the PCR primers. All sequences were deposited in Genbank, accession numbers HQ231330 - HQ231344.

rRNA-genes based phylogenetic analysis

18S and 28S rRNA gene datasets were constructed with our sequences and selected Catenulida sequences available in Genbank. The 18S and 28S rRNA gene datasets were separately aligned using MAFFT Q-INS-i which considers secondary structure of RNA (Katoh et al. 2005). The 5' and 3' ends of both alignments were trimmed, final length of alignments were 1816 nt (18S) and 1676 nt (28S). The nucleotide sequence identity between individuals was calculated based on these alignments using Geneious 5 (Drummond et al. 2010). The alignments were concatenated and we reconstructed the phylogenies using maximum likelihood- (PHYML at the phylogeny.fr web service; Guindon and Gascuel 2003; Dereeper et al. 2008) and Bayesian inference-based (MrBayes; Ronquist and Huelsenbeck 2003) algorithms. Substitution models for both genes were evaluated using MrModeltest 2.3 (Nylander 2008). The GTR+I+G model was chosen using the Akaike information criterion. MrBayes was run for 5 Mio generations using 4 chains. Convergence was evaluated by plotting the generations versus logL and the burn-in was set to 2 Mio generations. Node stability was evaluated using posterior probabilities (pp - Bayesian inference) and aLRT (maximum likelihood; Anisimova and Gascuel 2006; Guindon et al. 2010). Sequences of Macrostomida served as out-group.

Results

Taxonomy

***Paracatenula galateia* sp. nov.**

Material: Of more than 100 individuals from back reef sediments at a variety of sampling sites in the vicinity of Carrie Bow Cay (Belize) (see Fig. 1), nineteen adults were studied live in squeeze preparation, six by serial semi-thin sections, and about ten each as whole mounts stained with phalloidin and serotonin antibody, respectively.

Type specimens: Holotype: 1 specimen fixed in formaldehyde 4% and mounted on a microscope slide embedded in glycerol; USNM 1154145

Paratype: 2 specimens fixed in Bouin's fluid in separate vials; USNM 1154146 and 1154147

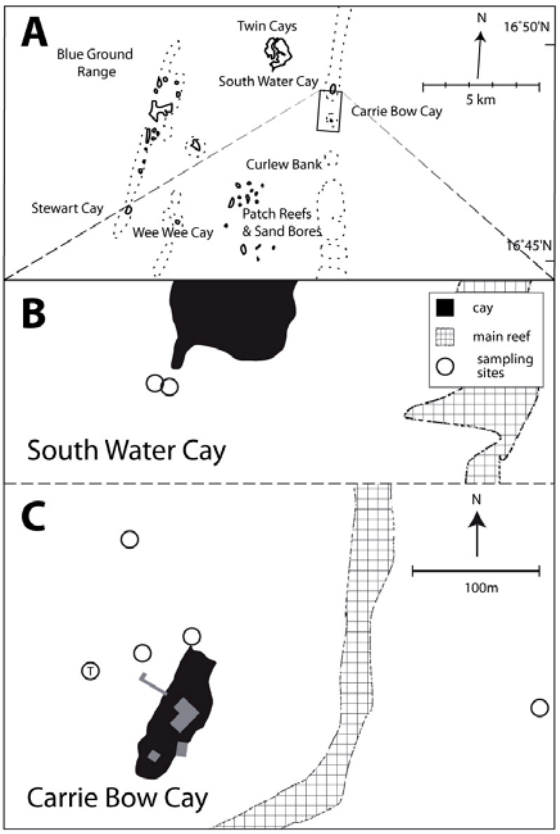

Figure 1: A. Map of the southern part of the Belize Barrier Reef. B and C. Sample locations in the vicinity of Carrie Bow Cay where *Paracatenula galateia* sp. nov. was found. T = type location.

Type locality: Carrie Bow Cay, Belize Barrier Reef (16° 48' 10.50'' N, 88°04' 56.30'' W). Subtidal sand in approximately 1 m water depth, 50 m west of the island in front of the pier (Fig. 1).

Etymology: *Galateia* refers to the silky, milky-white appearance of the worm under incident light. In Greek mythology this is an attribute of the skin of the nymph Galateia (Greek Γαλατεία „the milky white").

Diagnosis: Ribbon-shaped *Paracatenula* up to 6 mm long, with or without a statocyst. Inclusions bipartite, with conical to ladyfinger-shaped parts, 12-19 µm long and 3 µm wide.

External appearance: *Paracatenula galateia* is a ribbon-shaped worm up to 6 mm long (Fig. 2 A, Fig. 3). The length of the animals is extremely variable because the fragile worms tend to break, probably due to the extraction process. Only rarely are individuals found that are apparently complete and show an

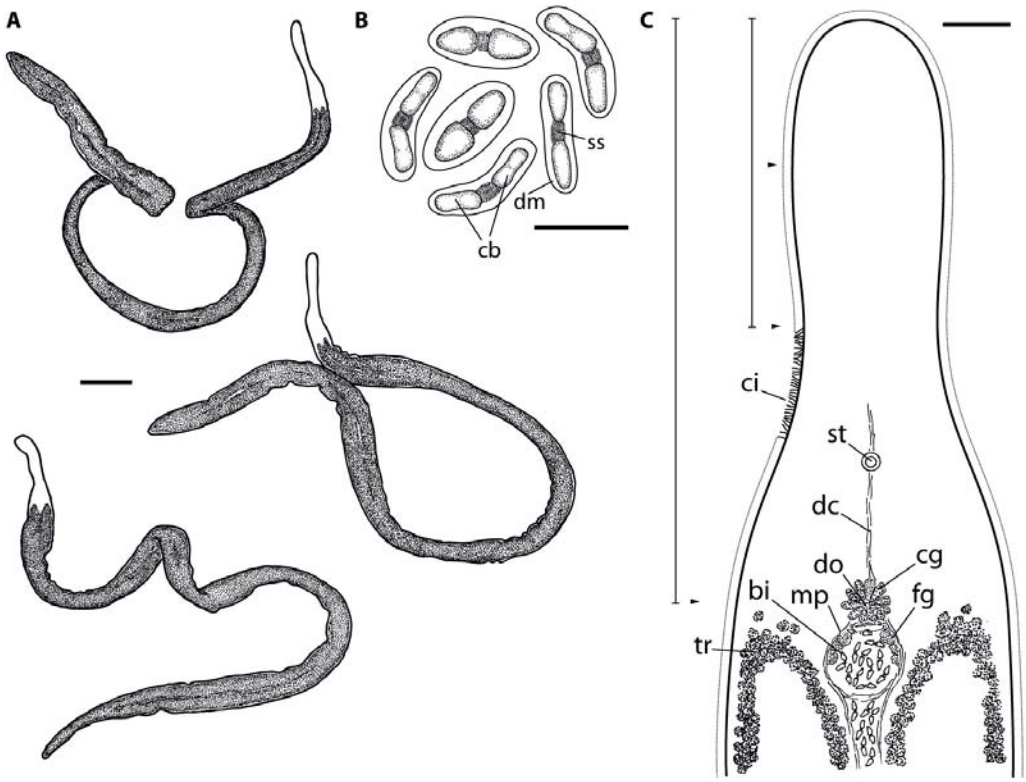

Figure 2: *Paracatenula galateia* sp. nov. A. Habitus of live specimens. B. Drawings of bipartite inclusions showing the conical to ladyfinger-shaped bodies (cb) connected by a short strand (ss) and surrounded by a dense matrix (dm). C. Morphology and organization of the rostrum showing the ciliated epidermis (ci), the monolithophorous statocyst (st), the dorsal cord (dc), the trophosome (tr), the dorsal opening (do) with surrounding gland cells with coarse granules (cg) adjacent to the muscular pouch (mp) which is filled with bipartite inclusions (bi) and has gland cells with fine granules (fg). The positions where measurements of width (arrowheads) and length (bars) were taken are indicated. Scale bars indicate 250 µm (A), 10 µm (B) and 50 µm (C).

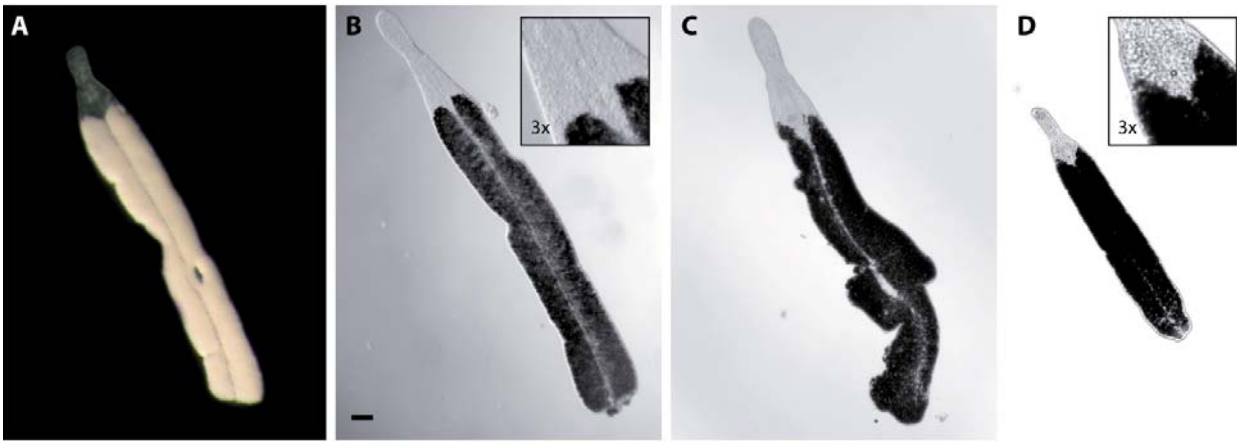

Figure 3: *Paracatenula galateia* sp. nov. Micrographs of live specimens. A. Incident light showing smooth silky appearance of trophosome. B. Transmitted light showing characteristic shape of extended rostrum and dorsal chord. C. Specimen with irregular outline and constriction. D. Small (juvenile?) specimen. Note position of the statocysts in inserts to B and D. A - D at same scale, bar indicates 100 µm.

undamaged posterior end. Many worms show constrictions or an irregular outline (Fig. 3 C). The width of the trophosome region, which makes up the largest part of the animal, is 225-315 µm (271 ± 30.6 mm, n= 19); its dorso-ventral height, however, is much smaller, and difficult to measure or even estimate in living worms. Fixed specimens have a width/height ratio of approximately 4.6-5.5. The trophosome is pinkish-white in incident light and has a characteristic silky appearance (Fig. 3 A). The transparent dorsal cord appears to divide the trophosome into two parts along the midline (Fig. 3 and Fig. 9 A).

The rostrum is 330-460 µm (398 ± 37.5 µm, n=19) long and has a characteristic shape. The anterior part is cylindrical or club-shaped, with a rounded tip (Fig. 2 A, C and Fig 3). Its diameter is 100-176 µm (129 ± 17.7 µm, n=19). The posterior part is conical and widens to match the width of the trophosome region. This widening begins at about 60% of the length of the rostrum, where it has its minimum diameter of 94-

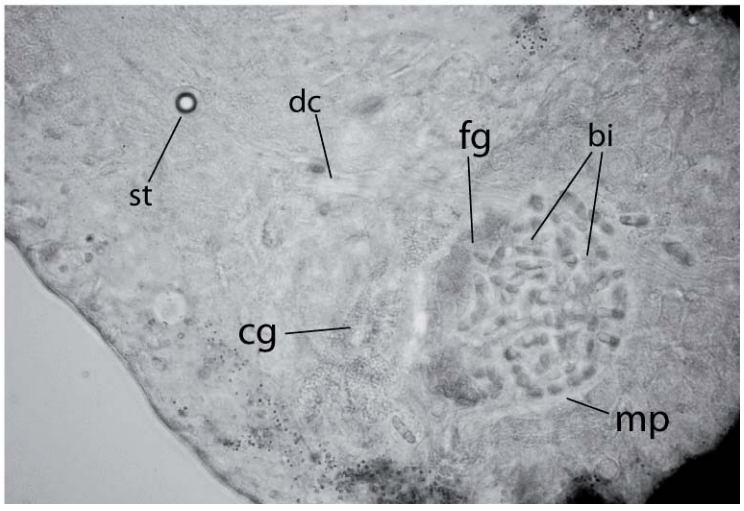

Figure 4: *Paracatenula galateia* sp. nov. Statocyst (st) anterior of brain connected to the dorsal cord (dc), gland cells with coarse granules (cg) adjacent to the muscular pouch (mp) filled with bipartite inclusions (bi) and gland cells with fine granules (fg). Scale bar 25µm.

145 µm (119 ± 14.9 µm, n=19). In five out of nineteen specimens studied in detail, the rostrum contained a monolithophorous statocyst (Fig. 4) of 12.8 ± 0.63 µm in diameter; diameter of the statolith was 6.5±0.43 µm. In small (juvenile?) worms the statocyst lies close to the brain (Fig. 3 D), which nestles between the anterior tips of the two trophosome parts, whereas in large (adult?) animals it is in a more forward position (Fig. 3 B).

Anatomy: A cross section in the trophosome region (Fig. 5) shows a thin (3.7-4.7 µm thick), ciliated epidermis. The nuclei of the epidermis cells are sunk into the underlying muscle layer that consists of fine longitudinal and even finer circular muscle fibres (Fig. 6 A, B). Numerous dorso-ventral muscle fibres run through the body. The 'dorsal cord' is a muscular strand that also contains the major longitudinal nerves. The remainder of the body is filled with the bacteriocytes. Approximately 50 bacteriocytes can be distinguished in a cross section; each bacteriocyte contains numerous bacteria. The symbionts show different shapes in the section (Fig. 7). When squeezed out of the worm they attain a coccoid shape with a diameter of 8.26 ± 0.63 µm (n=10). The refractive granules are contained in vacuoles and are approximately 0.5 µm in diameter.

The serotonergic nervous system (Fig. 8) is centralized in a brain, which is located at the boundary of trophosome and rostrum. Originating in the brain there are four nerve cords innervating the rostrum in an anterior direction, two on the dorsal and two on the ventral side. In the median of the DV-axis we find two prominent nerves originating in the brain that extend laterally and innervate the sub-epidermal or sub-

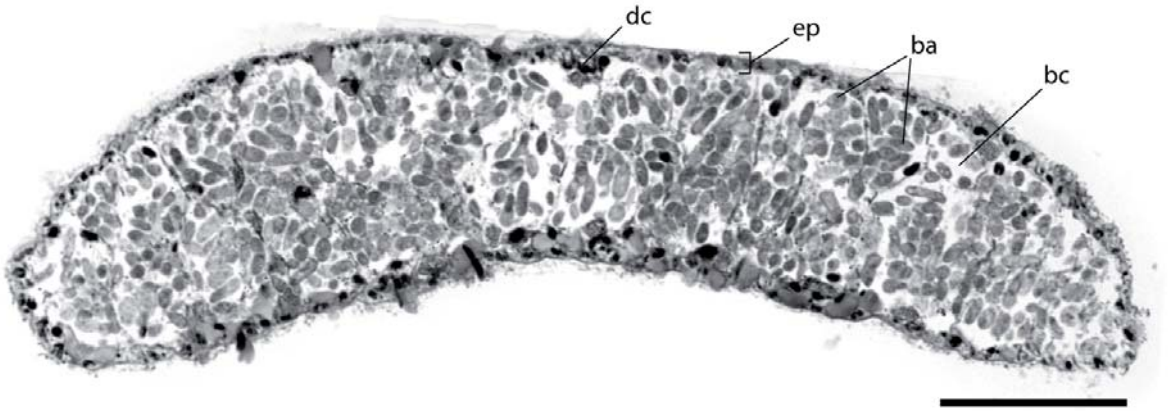

Figure 5: *Paracatenula galateia* sp. nov. Semi-thin cross section through trophosome region showing the thin epidermis (ep), the dorsal cord (dc), the bacteriocytes (bc) filling most of the body and the symbiotic bacteria (ba) within the bacteriocytes. Scale bar 50 µm.

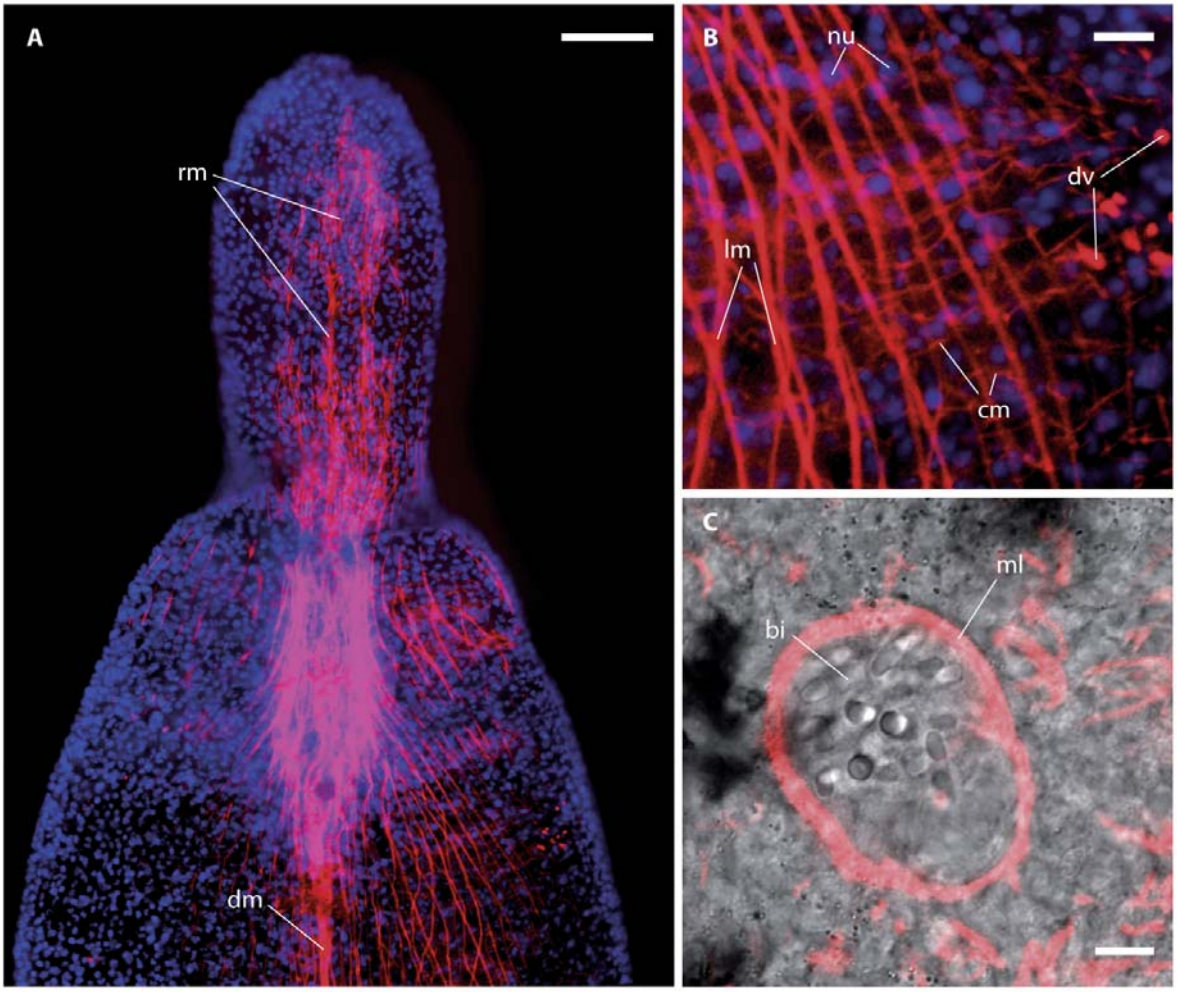

Figure 6: *Paracatenula galateia* sp. nov. Phalloidin staining of muscles (red). A. Anterior region showing rostrum muscles (rm) and dorsal cord muscles (dm); DAPI staining in blue. B. Detail showing longitudinal fibres (lm), thin circular fibres (cm), nuclei of the epidermis (nu) sunken into the muscle sheath and dorso-ventral fibres (dv). C. Muscular layer (ml) surrounding the pouch that contains the bipartite inclusions (bi). Scale bars 50 µm (A) and 5 µm (B, C).

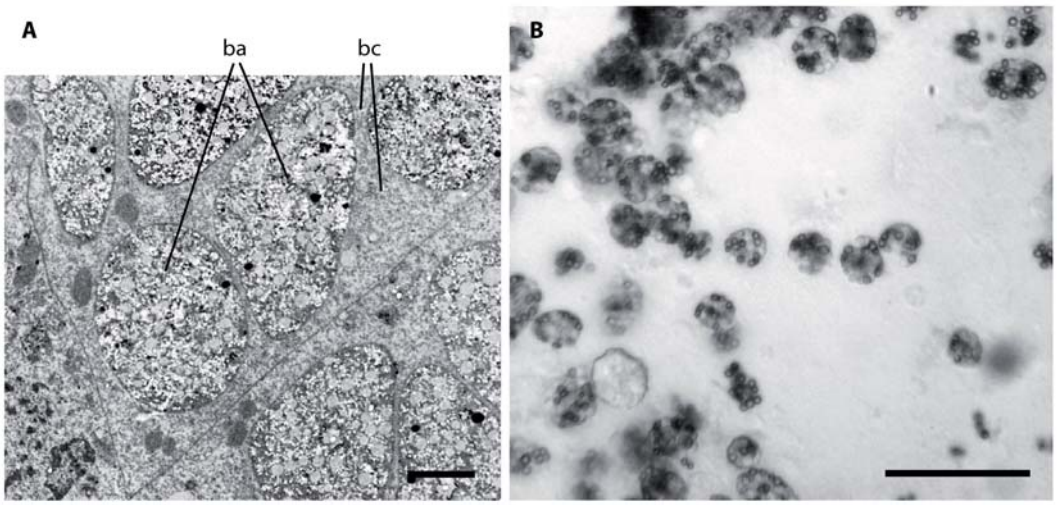

Figure. 7: *Paracatenula galateia* sp. nov. symbiotic bacteria. TEM section of the trophosome region with several bacteria (ba) localized in a bacteriocyte (bc). Scale bar 2 µm.

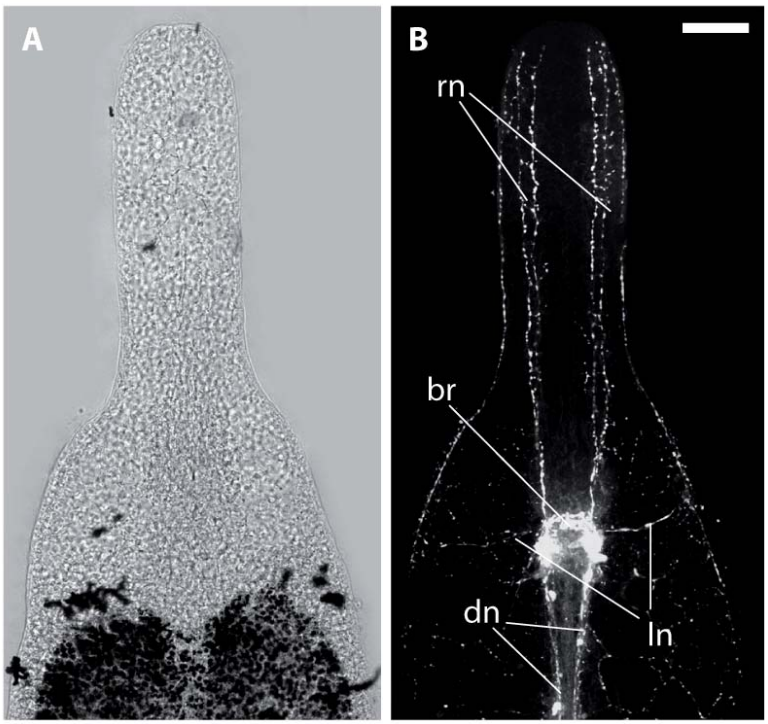

Figure 8: *Paracatenula galateia* sp. nov. Serotonin staining of the nervous system in the anterior region. A. Light micrograph of anterior end. B. Projection of several immunofluorescent micrographs of the same specimen showing the brain (br), rostrum nerves (rn), lateral nerves (ln) and dorsal cord nerves (dn). Scale bar 50 µm.

muscular nerve nets. The region posterior to the brain has two kinds of nerves showing strong serotonin signals. There is a very strong staining of two main nerve cords that are direct extensions of the dorsal parts of the brain. These main nerves are associated with the 'dorsal cord' and extend through the entire posterior part of the worm. The other type of serotonergic nerve in the posterior part of the animal is the sub-epidermal or sub-muscular nerve net, which is ubiquitous and evenly distributed.

Cells containing characteristic bipartite inclusions (Fig. 2 B, 4, 6 C, 9 A and B), which could be interpreted as spermatozoa, were encountered in five of nineteen large specimens. They are distributed throughout the trophosome region, especially along the dorsal cord (Fig. 9 A), but are concentrated behind the brain, between the anterior ends of the trophosome lobes, in a round pouch enclosed by a muscle layer (Fig. 4, 6 C, 9 A), which we interpret as a *vesicula seminalis*. The rostral wall of the pouch is made up of fine-grained gland cells. Anterior and connected to this pouch there is a circular dorsal opening to the outside (genital pore?), which is surrounded by gland cells containing coarse granules (Fig. 9 A).

The inclusion containing cells are oval, 20-24 µm long and 7-15 µm wide. The inclusion are made up of

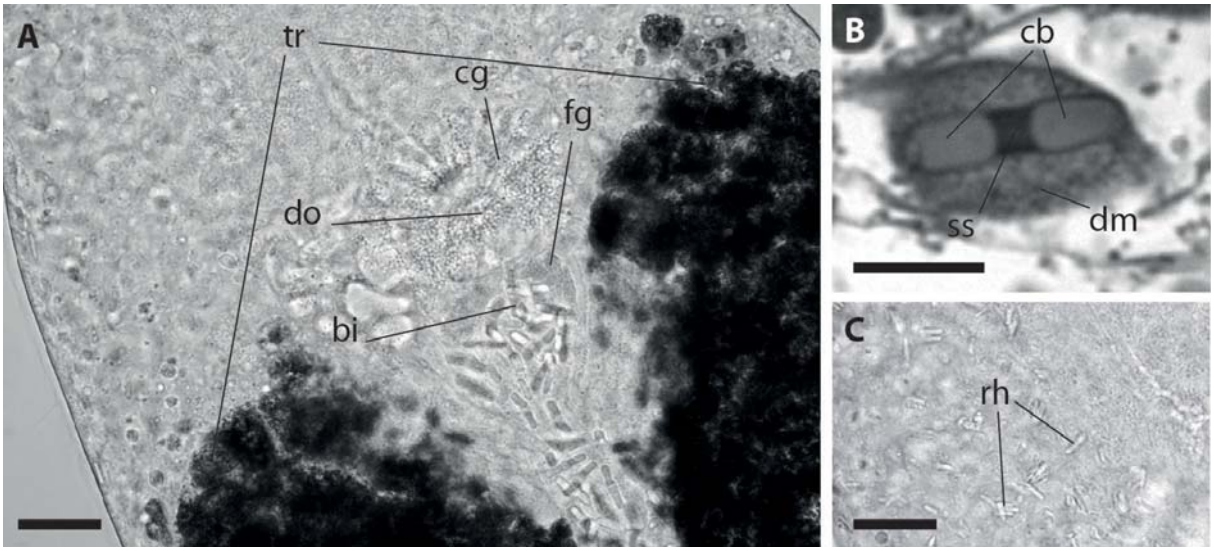

Figure 9: *Paracatenula galateia* sp. nov. bipartite inclusions and rhabdoids. (A) Anterior end of trophosome (tr) region. Focus on dorsal side showing the bipartite inclusions (bi) along the dorsal chord and concentrated in the circular pouch with finely granulated glands (fg), the dorsal opening (do) and the surrounding glands with coarse granules (cg). (B) Bipartite inclusion in a semi thin section showing two slightly cone-shaped bodies (cb) connected by a short strand (ss) surrounded by a dense matrix (dm). (C) Same region as A; focus on ventral side, showing bundles of rhabdoids (rh). Scale bars 25 µm (A, C) and 10 µm (B).

a pair of conical or ladyfinger-shaped bodies (Fig. 2 B, 4, 6 C, 9 A and B) that are arranged in either a straight line or at a 160º angle, without touching each other but joined together by a short bond; each pair measures 11.2-13.5 µm (mean 12.2 µm) in length and 2.6-3.6 µm (mean 3.0 µm) in width. The conical or ladyfinger-shaped bodies are 3-6.1 µm long; the connecting bond is a 1.6-3.3 µm long electron-dense strand.

Bundles of 2-6 rhabdoids, rounded rods 10-12 µm long and 1-2 µm wide, may be found throughout the animal (Fig. 9 C).

Molecular phylogenetic analysis

Of ten individuals of *Paracatenula galateia* sp. nov. sequences of the 18S and 28S rRNA gene were obtained. They are highly similar, with 99.9% and 99.7 % pairwise identity. Phylogenetic analysis based on a concatenated alignment of 18S and 28S rRNA genes from *Paracatenula galateia* and selected Catenulida as well as Macrostomida (Fig. 10) shows that (1) our reconstruction of the Catenulida internal phylogeny supports the phylogeny presented by Larsson et al. (2008) (2) all sequences from the genus *Paracatenula* form one clade within the Catenulida (3) sequences from *P. galateia* form a highly supported and well

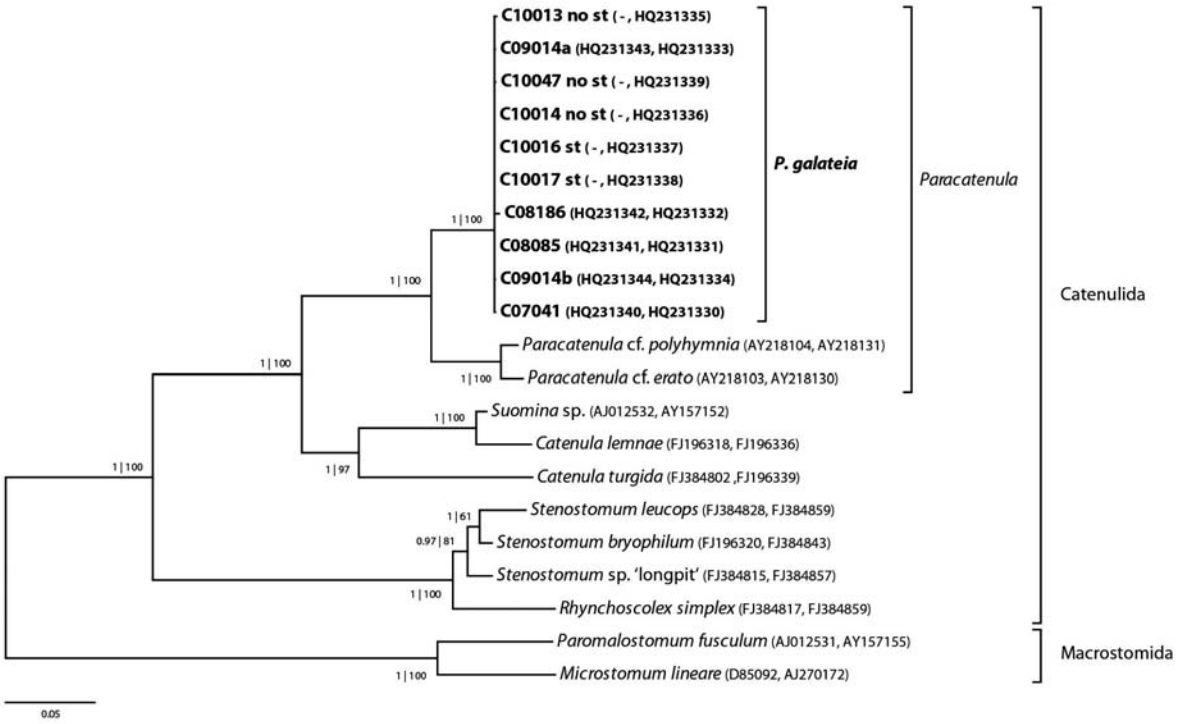

Figure 10: 18S and 28S rRNA-gene based phylogenetic reconstruction showing the position of the sequenced individuals of *P. galateia* sp. nov. in the Catenulida. The tree is based on the most likely PHYML tree (GTR+I+G model of substitution). Support in MrBayes and PHYML analysis is indicated (pp | aRLT) for each node. Microstomidae were used as outgroup. GenBank accession numbers are given in parentheses (first 18S and then 28S rRNA gene). Scale bar represents 5% estimated sequence divergence. st=statocyst.

separated cluster within the genus meriting the designation of a new species and (4) there is no separation of sequences from individuals with statocyst to individuals without statocyst, showing that all specimens studied belong to the same species.

Discussion

The lack of mouth and pharynx together with the molecular data define the new species as belonging to the genus *Paracatenula. P. galateia* sp. nov. is the most massive species described so far. The width of the similarly long *P. urania* Sterrer and Rieger, 1974 is only a tenth of that of the new species. A comparison of biometric data is given in Table 1. Furthermore, *P. galateia* sp. nov. is clearly distinguished from the four species described by Sterrer & Rieger (1974) by the structure of its "sperm nucleus", which is spindle-shaped in *P. urania* and *P. erato*, spicule-shaped in *P. polyhymnia* Sterrer and Rieger, 1974, and possibly ribbon-shaped in the less-known *P. kalliope* Sterrer and Rieger, 1974. The fact that in *P. galateia* sp. nov.

the two ”ladyfingers” often diverge at a 160º angle might suggest an affinity with *P. polyhymnia* where the two arms of the spicules as a rule enclose a 160º angle (Sterrer and Rieger 1974, Fig 13g). However, the nature of the peculiar cells containing the variously shaped inclusions is still unclear. In *P. galateia* sp. nov. the location of the cells, and their concentration in a muscular pouch with a dorsal opening, strongly suggests them to be sperm. Attempts to stain the presumed nucleus with DAPI, however, failed. Most puzzling are the spicule shaped inclusions in *P. polyhymnia* and several other not yet described species (own unpublished observations) that seem to have a mineral nature.

Table 1: Biometric comparison of the *Paracatenula* species

	P. galateia	*P. urania*	*P. erato*	*P. polyhymnia*	*P. kalliope*
maximal length	6 mm	3-7 mm	1.9 mm	0.83 mm	2.2 mm
maximal width	271 µm	30 µm	100 µm	100 µm	170 µm
cross section	ribbon	round?	ribbon?	?	ribbon
rostrum	398 µm	220 µm	130 µm	200 µm	400 µm
tail	no	no	?	100 µm	200 µm
inclusion shape	bipartite	spindle	spindle	spicule	ribbon
inclusion length	11-14 µm	10 µm	45 µm	34-36 µm	65 µm
inclusion width	3 µm	1.5 µm	5 µm	1.5 µm	6 µm

Acknowledgements

This work was supported by the Austrian Science Fund (FWF) project 20394-B03 (JO, HG, NL and UD). We thank Renate Hodinka for suggesting the species name. Part of this work was carried out by using the resources of the Computational Biology Service Unit from Cornell University which is partially funded by The Microsoft Corporation.

References

Anisimova M, Gascuel O. 2006. Approximate Likelihood-Ratio Test for Branches: A Fast, Accurate, and Powerful Alternative. Systematic Biology 55:539-552.

Borkott H. 1970. Geschlechtliche Organisation, Fortpflanzungsverhalten und Ursachen der sexuellen Vermehrung von *Stenostomum sthenum*; nov. spec. (Turbellaria, Catenulida). Zoomorphology 67:183-262.

Dereeper A, Guignon V, Blanc G, Audic S, Buffet S, Chevenet F, Dufayard J-F, Guindon S, Lefort V, Lescot M, Claverie J-M, Gascuel O. 2008. Phylogeny.fr: robust phylogenetic analysis for the non-specialist. Nucleic Acids Research 36:W465-469.

Doe D, Rieger RM. 1977. A new species of the genus Retronectes (Turbellaria, Catenulida) from the coast of North Carolina, U.S.A. Mikrofauna des Meeresbodens 66:1-10.

Drummond A, Ashton B, Buxton S, Cheung M, Cooper A, Heled J, Kearse M, Moir R, Stones-Havas S, Sturrock S, Thierer T, Wilson A. 2010. Geneious v5.1, available from http://www.geneious.com/. Computer Software.

Faubel A. 1976. Eine neue Art der Gattung *Retronectes* (Turbeliaria, Catenulida) aus dem Küstengrundwasser der Nordseeinsel Sylt. Zoologica Scripta 5:217-220.

Guindon S, Dufayard J-F, Lefort V, Anisimova M, Hordijk W, Gascuel O. 2010. New Algorithms and Methods to Estimate Maximum-Likelihood Phylogenies: Assessing the Performance of PhyML 3.0. Systematic Biology 59:307-321.

Guindon S, Gascuel O. 2003. A Simple, Fast, and Accurate Algorithm to Estimate Large Phylogenies by Maximum Likelihood. Systematic Biology 52:696-704.

Katoh K, Kuma K-i, Toh H, Miyata T. 2005. MAFFT version 5: improvement in accuracy of multiple sequence alignment. Nucleic Acids Research 33:511-518.

Larsson K, Jondelius U. 2008. Phylogeny of Catenulida and support for Platyhelminthes. Organisms Diversity & Evolution 8:378-387.

Loy A, Duller S, Baranyi C, Mussmann M, Ott J, Sharon I, Beja O, Le Paslier D, Dahl C, Wagner M. 2009. Reverse dissimilatory sulfite reductase as phylogenetic marker for a subgroup of sulfur-oxidizing prokaryotes. Environmental Microbiology 11:289-299.

Noreña-Janssen C, Faubel A. 1996. *Myoretronectes paranaensis* n. gen. et sp., a new freshwater genus of the family Retronectidae (Turbellaria, Catenulida) from the Paraná, Argentina. Hydrobiologia 330:111-118.

Nylander JAA. 2008. MrModeltest v2.3, Program distributed by the author, Evolutionary Biology Centre, Uppsala University. Computer Software.

Ott JA, Rieger G, Rieger R, Enderes F. 1982. New mouthless interstitial worms from the sulfide system: Symbiosis with Prokaryotes. Pubblicazioni Stazione Zoologica Napoli I: Marine Ecology 3:313-333.

Pasteris JD, Freeman JJ, Goffredi SK, Buck KR. 2001. Raman spectroscopic and laser scanning confocal microscopic analysis of sulfur in living sulfur-precipitating marine bacteria. Chemical Geology 180:3-18.

Pradillon F, Schmidt A, Peplies J, Dubilier N. 2007. Species identification of marine invertebrate early stages by whole-larvae in situ hybridisation of 18S ribosomal RNA. Marine Ecology Progress Series 333:103-116.

Riedl R. 1959. Turbellarien aus submarinen Höhlen. I. Archoophora. Pubblicazioni Stazione Zoologica Napoli Supplement 30:178-208.

Rieger PM. 1978. Multiple ciliary stuctures in developing spermatozoa of marine Catenulida (Turbellaria). Zoomorphology 89:229-236.

Ronquist F, Huelsenbeck JP. 2003. MrBayes 3: Bayesian phylogenetic inference under mixed models. Bioinformatics 19:1572-1574.

Rützler K, Macintyre I. 1982. The Atlantic Barrier Reef Ecosystem at Carrie Bow Cay, Belize, I. Structure and Communities. Washington: Smithsonian Institution Press. 539 pages.

Schuchert P, Rieger RM. 1990. Ultrastructural examination of spermatogenesis in *Retronectes atypica* (Catenulida, Platyhelminthes). Journal of Submicroscopical Cytology & Pathology 22:379-387.

Sterrer W. 1966. New polylithophorus marine Turbellaria. Nature 210:436.

Sterrer W, Rieger RM. 1974. Retronectidae - a new cosmopolitan marine family of Catenulida (Turbellaria). In: Riser N, Morse M (eds) Biology of the Turbellaria. New York: McGraw-Hill, p 63-92.

Tyler S, Schilling S, Hooge M, Bush L. 2006-2010. Turbellarian taxonomic database Version 1.6, available at http://turbellaria.umaine.edu.

von Reumont B, Meusemann K, Szucsich N, Dell'Ampio E, Gowri-Shankar V, Bartel D, Simon S, Letsch H, Stocsits R, Luan Y-x, Wagele J, Pass G, Hadrys H, Misof B. 2009. Can comprehensive background knowledge be incorporated into substitution models to improve phylogenetic analyses? A case study on major arthropod relationships. BMC Evolutionary Biology 9:119.

CHAPTER 2

Paracatenula, an ancient symbiosis between thiotrophic *Alphaproteobacteria* and catenulid flatworms

Authors: Harald R. Gruber-Vodicka, Ulrich Dirks, Nikolaus Leisch, Christian Baranyi, Kilian Stoecker, Silvia Bulgheresi, Niels R. Heindl, Matthias Horn, Christian Lott, Alexander Loy, Michael Wagner, Jörg A. Ott

Keywords: intracellular symbiosis, marine catenulid, meiofauna, subtidal sand

Publication status: Article published in Proceedings of the National Academy of Sciences (PNAS).

Detailed description of UD´s contribution: UD attended six field trips and contributed to the collection of the material; UD planned and conducted the fluorescence in situ hybridisation (FISH) experiments; UD contributed to the sequencing of 16S and 18S ribosomal RNA genes; UD provided sections for the area measurements; UD edited and approved the manuscript.

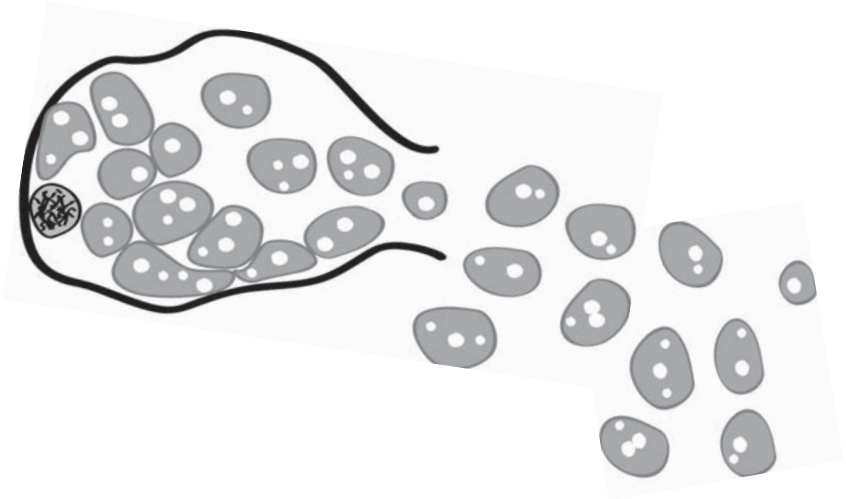

Paracatenula, an ancient symbiosis between thiotrophic *Alphaproteobacteria* and catenulid flatworms

Harald Ronald Gruber-Vodicka[a,1], Ulrich Dirks[a], Nikolaus Leisch[a], Christian Baranyi[b,2], Kilian Stoecker[b,3], Silvia Bulgheresi[c], Niels Robert Heindl[a,c], Matthias Horn[b], Christian Lott[d,e], Alexander Loy[b], Michael Wagner[b], and Jörg Ott[a]

Departments of [a]Marine Biology, [b]Microbial Ecology, and [c]Genetics in Ecology, University of Vienna, A-1090 Vienna, Austria; [d]Symbiosis Group, Max Planck Institute for Marine Microbiology, D-28359 Bremen, Germany; and [e]Elba Field Station, Hydra Institute for Marine Sciences, I-57034 Campo nell'Elba, Italy

Edited by Nancy A. Moran, Yale University, West Haven, CT, and approved May 31, 2011 (received for review April 8, 2011)

Harnessing chemosynthetic symbionts is a recurring evolutionary strategy. Eukaryotes from six phyla as well as one archaeon have acquired chemoautotrophic sulfur-oxidizing bacteria. In contrast to this broad host diversity, known bacterial partners apparently belong to two classes of bacteria—the *Gamma*- and *Epsilonproteobacteria*. Here, we characterize the intracellular endosymbionts of the mouthless catenulid flatworm genus *Paracatenula* as chemoautotrophic sulfur-oxidizing *Alphaproteobacteria*. The symbionts of *Paracatenula galateia* are provisionally classified as "*Candidatus* Riegeria galateiae" based on 16S ribosomal RNA sequencing confirmed by fluorescence in situ hybridization together with functional gene and sulfur metabolite evidence. 16S rRNA gene phylogenetic analysis shows that all 16 *Paracatenula* species examined harbor host species-specific intracellular *Candidatus* Riegeria bacteria that form a monophyletic group within the order *Rhodospirillales*. Comparing host and symbiont phylogenies reveals strict cocladogenesis and points to vertical transmission of the symbionts. Between 33% and 50% of the body volume of the various worm species is composed of bacterial symbionts, by far the highest proportion among all known endosymbiotic associations between bacteria and metazoans. This symbiosis, which likely originated more than 500 Mya during the early evolution of flatworms, is the oldest known animal–chemoautotrophic bacteria association. The distant phylogenetic position of the symbionts compared with other mutualistic or parasitic *Alphaproteobacteria* promises to illuminate the common genetic predispositions that have allowed several members of this class to successfully colonize eukaryote cells.

intracellular symbiosis | marine catenulid | meiofauna | subtidal sand

Marine catenulid flatworms of the genus *Paracatenula* have no mouth or gut (1). Instead, they harbor intracellular microbial endosymbionts in bacteriocytes (2) that form a tissue known as the trophosome (Fig. 1*A*) in functional analogy to the trophosome of the mouthless Siboglinidae (Annelida) (3). The trophosome almost completely fills the posterior part of the body behind the brain (2, 3). The worms inhabit the interstitial space of warm temperate to tropical subtidal sands together with other animals such as nematodes, gutless oligochaetes, and lucinid or solemyid bivalves that all harbor chemoautotrophic sulfur-oxidizing bacteria (SOB). By migrating through the redox potential gradient in the uppermost 5- to 15-cm sediment layer, millimeter-sized worms can supply chemoautotrophic symbiotic bacteria alternately with spatially separated electron donors and acceptors such as sulfide and oxygen, as has been described for Nematoda and Oligochaeta (4, 5).

Chemosynthetic carbon fixation by using reduced sulfur compounds (i.e., thiotrophy) is widespread in free-living members of the microbial domains *Bacteria* and *Archaea*. This metabolic capability has been found in members of the *Actinobacteria*, *Aquificae*, *Bacilli*, *Chloroflexi*, *Chlorobi*, and *Spirochaeta*, and all classes of the *Proteobacteria* and the archaeal order *Sulfolobales*. One archaeon, "*Candidatus* Giganthauma karukerense" (6), as well as a wide range of protists and animals, including Ciliata (e.g., *Zoothamnium*), Nematoda (Stilbonematinae and *Astomonema*), Arthropoda (*Rimicaris* and *Kiwa*), Annelida (e.g., *Riftia* or *Olavius*), along with bivalve and gastropod Mollusca (e.g., *Solemya* or *Neomphalina*; reviewed in ref. 7), have established themselves as hosts in symbioses with SOB. They all derive some or all of their energy demands from the primary production of the symbionts (7). Interestingly, despite this great taxonomic variety of hosts—from habitats as divergent as deep-sea hydrothermal hot vents, cold seeps, whale or wood falls, and peat and shallow-water sediments—the SOB symbiont diversity seemed to be limited to *Proteobacteria* of the *Gamma* and *Epsilon* classes (7). Here, we present evidence that the symbionts of *Paracatenula* form an ancient clade of sulfur-oxidizing *Alphaproteobacteria* that are strictly coevolved with their hosts and that equal host biomass in the consortium.

Results and Discussion

The body plan of *Paracatenula* suggests that the symbionts make up a substantial proportion of the worms. To specify symbiont-to-host tissue ratios, cross-sections in the trophosome region of three species of *Paracatenula* were analyzed by transmission EM (TEM). The symbionts make up 36.7% of the cross section area in *Paracatenula galateia* (3) (Carrie Bow Cay, Belize), 41.2% in *P.* cf. *galateia* (Dahab, Egypt), and 51.9% in *P.* cf. *polyhymnia* (Dahab, Egypt; Fig. S1). The symbiont-housing trophosome region accounts for 90% to 98% of the total worm length: multiplying these two factors, we roughly estimate symbiont-to-host tissue ratios of 33% in *P. galateia*, 40% in *P.* cf. *galateia*, and 50% in *P.* cf. *polyhymnia*. These are the highest proportions of all known endosymbioses between bacteria and metazoans, far higher

Author contributions: H.R.G.-V., S.B., N.R.H., M.H., A.L., M.W., and J.O. designed research; H.R.G.-V., U.D., N.L., C.B., K.S., C.L., and J.O. performed research; M.W. contributed new reagents/analytic tools; H.R.G.-V., U.D., N.L., C.B., K.S., and J.O. analyzed data; and H.R.G.-V. wrote the paper.

The authors declare no conflict of interest.

This article is a PNAS Direct Submission.

Freely available online through the PNAS open access option.

Data deposition: The sequences reported in this paper have been deposited in the GenBank database [accession nos. HQ689139 (*aprA*); HQ840958 (*cbbM*); HQ689138 (*dsrAB*); HQ689029–HQ689053, HQ689087–HQ689095, HQ689123, HQ689124, HQ689128, HQ689129, and HQ845108–HQ845110 (16S rRNA); HQ689054–HQ689068, HQ689096–HQ689108, HQ689125, and HQ689130–HQ689133 (18S rRNA); and HQ689069–HQ689086, HQ689109–HQ689122, HQ689126, HQ689127, and HQ689134–HQ689137 (28S rRNA)].

[1]To whom correspondence should be addressed. E-mail: harald.gruber@univie.ac.at.

[2]Present address: Department of Marine Biology, University of Vienna, A-1090 Vienna, Austria.

[3]Present address: Project Group Bioresources, Fraunhofer Institute for Molecular Biology and Applied Ecology, D-35394 Giessen, Germany.

This article contains supporting information online at www.pnas.org/lookup/suppl/doi:10.1073/pnas.1105347108/-/DCSupplemental.

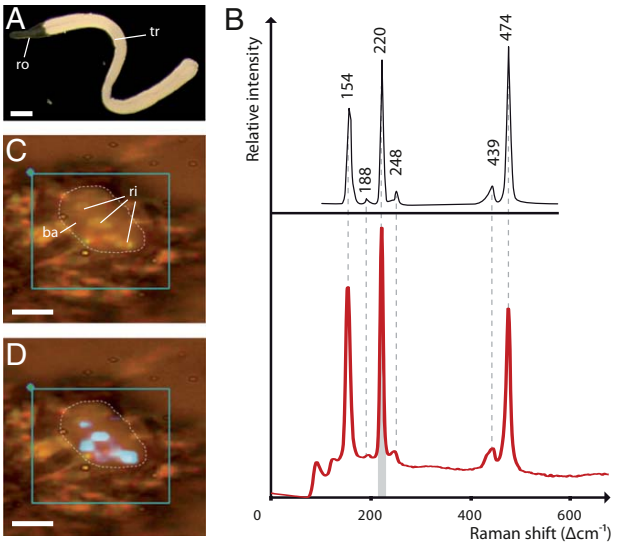

Fig. 1. Sulfur storage in *Candidatus* Riegeria galateiae. (*A*) Living specimen of *P. galateia*, with *Cand.* Riegeria galateiae endosymbionts in trophosome (tr) appearing white in incident light in contrast to the bacteria-free rostrum (ro). (Scale bar: 250 μm.) (*B*) Raman spectrum of individual cellular inclusion (red) with reference spectrum (black) of elemental sulfur in S_8 ring configuration. (*C*) Air-dried *Cand.* Riegeria galateiae cell (ba) with light refracticle inclusions (ri). (Scale bar: 5 μm.) (*D*) Mapping of the Raman sulfur spectrum peak indicated in *B* in gray onto *C*, with the mapped area indicated with turquoise rectangle. (Scale bar: 5 μm.)

than, e.g., in the deep-sea tubeworm *Riftia pachyptila*, in which bacteria make up only 24.1% of the trophosome, which in turn occupies less than one third of the body volume (8). The exceptional proportion of bacterial biomass in this intracellular symbiosis questions the common view that animals exploit the metabolic skills of their microbial partners because the *Paracatenula* worms in return appear to serve as a protective vehicle for their symbionts.

The bacteria of all *Paracatenula* species contain highly light refractive spherical inclusions (0.5–2 μm in diameter), which render the bacteria white in incident light (Fig. 1*A*). This white coloring, typical for SOB that store elemental sulfur (9), was an initial clue that the symbionts could be sulfur oxidizing (2). We selected the symbionts of *P. galateia* for a detailed analysis because the worms are abundant, comparatively large, and morphologically distinct (3). Sulfur oxidizing capabilities were assessed by examining sulfur storage and functional genes used in thiotrophy. All inclusions of extracted symbiont cells from *P. galateia* analyzed by Raman microspectroscopy consist of elemental sulfur in S_8 ring configuration (Fig. 1 *B–D*). Energy dispersive X-ray microanalysis shows that in the trophosome this bacterial sulfur storage can make up 5% to 19% of the tissue mass (Fig. S2). In many SOB that store elemental sulfur, the sirohaem dissimilatory sulfite reductase (i.e., DsrAB) enzyme system functioning in reverse is an important part of the sulfur oxidation machinery (10). Our phylogenetic analysis of a collection of dissimilatory sulfite reductase (i.e., DsrB) sequences from SOB, including the sequence of the *P. galateia* symbionts determined in the present study, demonstrates that the sequences of *Paracatenula* symbionts form a well supported monophyletic clade with sequences from other thiotrophic *Alphaproteobacteria* [approximate likelihood-ratio test (aLRT), 0.90; posterior probability (pp), 1.00; Fig. S3]. This corroborates the results from a previous study placing the DsrAB sequences from bacteria associated with two species of *Paracatenula* together with sequences of the alphaproteobacterial genus *Magnetospirillum*, albeit with weak node support (10). Additionally, the gene coding for AprA, the α-subunit of dissimilatory adenosine-5′-phosphosulfate (APS) reductase, another key enzyme in sulfur energy metabolism, was partially sequenced for the *P. galateia* symbionts. APS reductase is used by SOB to oxidize sulfite to APS and by sulfate-reducing microorganisms to reduce APS to sulfite (11). The symbionts' AprA sequence clusters with the AprA lineage II of SOB with good statistical support (aLRT, 0.89; pp, 1.00; Fig. S4). The Calvin–Benson–Basham pathway with ribulose-1,5-bisphosphate carboxylase/oxygenase (RubisCO) as the central enzyme is a key mechanism of carbon fixation in autotrophic organisms (12). The partial sequence coding for RubisCO form II (CbbM) sequenced for the *P. galateia* symbionts is related to sequences from the alphaproteobacterial genus *Magnetospirillum* and other chemoautotrophs (Fig. S5).

Taken together, three lines of evidence point to a chemoautotrophic sulfur-oxidizing lifestyle of the symbionts: (*i*) the habitat that *P. galateia* shares with many other hosts of thiotrophic bacteria, (*ii*) intracellular storage of elemental sulfur by the symbionts, and (*iii*) the presence of *cbbM* as well as *dsrAB* and *aprBA*, both related to sequences from SOB, in the symbionts' genome.

16S rRNA gene based approaches were used to assess the diversity within and between the symbiont populations of individual worms of *Paracatenula galateia*. The PCR products obtained separately from 10 specimens using general bacterial 16S rRNA gene primers comprise the same phylotype based on (*i*) clone libraries, (*ii*) direct sequencing, and (*iii*) denaturing gradient gel electrophoresis (DGGE) analysis [pairwise identity of 99.7–100; a species-level phylotype threshold of ≥99% 16S rRNA gene sequence identity was used (13)]. According to the ribosomal database project classifier (14) and our comprehensive phylogenetic analysis (as detailed later), this bacterial phylotype is a member of the alphaproteobacterial order *Rhodospirillales* (Fig. 2). FISH with a phylogenetically nested probe set specifically targeting most *Bacteria*, most *Alphaproteobacteria*, and the symbiont confirms that *P. galateia* contains only one alphaproteobacterial species-level phylotype (Fig. 3).

To infer host specificity of the symbionts from different *Paracatenula* hosts and to elucidate the symbionts' evolutionary relationships, we sequenced symbiont 16S rRNA genes from additional 31 worms belonging to 15 species, all morphologically distinct from *P. galateia*: five species from the Caribbean Sea (Carrie Bow Cay,

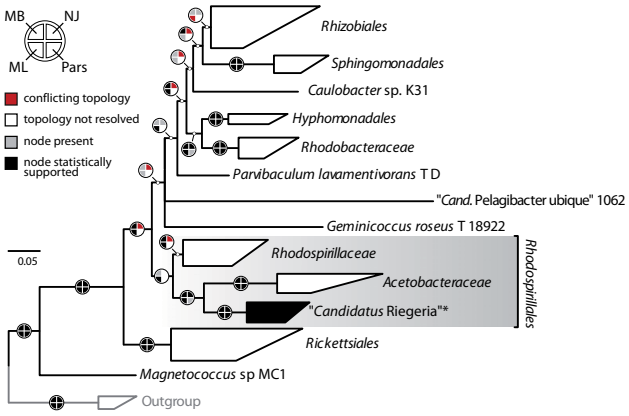

Fig. 2. Phylogeny of the family level *Candidatus* Riegeria clade in the *Alphaproteobacteria*. Based on comparative 16S rRNA gene analysis, the *Cand.* Riegeria clade is the sister group of the family *Acetobacteraceae* within the order *Rhodospirillales*. The tree shown was estimated by using MrBayes (MB), and node support is additionally indicated for three alternative methods (NJ, neighbor joining; Pars, parsimony; ML, maximum likelihood). **Cand.* Riegeria clade; the detailed phylogeny of this clade is shown in Fig. S6. (Scale bar: 5% estimated sequence divergence.)

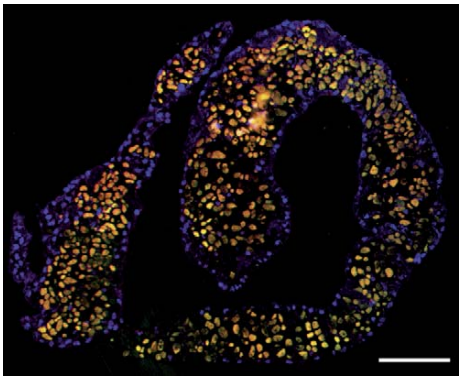

Fig. 3. *Candidatus* Riegeria galateiae in the host trophosome. Laser scanning confocal micrograph of FISH on LR-White cross-section; Overlay of three images with a bacteria-specific probe (green), symbiont-specific probe (red), and eukaryote-specific probe (blue). Because of the overlay of colors, the symbionts appear in yellow. (Scale bar: 50 μm.)

Belize), one from the Mediterranean Sea (Elba, Italy), five from the Red Sea (Dahab, Egypt), and four from the Pacific Ocean (Lizard Island, Australia). Our 16S rRNA gene-based tree of the *Alphaproteobacteria* (Fig. 2) is largely congruent with the topologies presented in recent phylogenomic studies of this class (15, 16). The placement of the symbiont sequences shows that (*i*) the symbionts form a distinct and well supported sister clade to the *Acetobacteraceae* within the order *Rhodospirillales* (Fig. 2), (*ii*) the symbionts are present in all worms (Fig. S6), and (*iii*) each host species harbors only one phylotype, which is specific for the respective host (Fig. S6). Based on these phylogenetic data and our detailed metabolic analysis, we propose the provisional classification (17) "*Candidatus* Riegeria galateiae" for the symbionts of *P. galateia*. Short description is as follows: coccoid alphaproteobacterium of the order *Rhodospirillales*, 5 to 8 μm in diameter with intracellular storage of elemental sulfur, present in bacteriocytes of the catenulid flatworm *Paracatenula galateia*. The basis of assignment is as follows: 16S rRNA gene, *cbbM*, *dsrAB*, and *aprA* sequences (HQ689043, HQ840958, HQ689138, and HQ689139, respectively) and hybridization with the phylotype-specific oligonucleotide probe PAR1151 (5′-CTT GTC ACC GGC AGT TCC CTC-3′). Riegeria refers to the late zoologist Reinhard Rieger, who described the host genus, together with W. Sterrer (1); and galateiae to its specific flatworm host *P. galateia*.

Our phylogenetic analysis also revealed that only a single 16S rRNA sequence in public databases (GQ402753) belongs to the clade of *Paracatenula* symbionts (Fig. S6). This clone was retrieved from a permanently waterlogged tropical peat swamp forest sample in Thailand (18), but only scarce details are available for the sample.

The maximum 16S rRNA gene sequence divergence within the symbiont clade is 12.7%, and members of the clade show a minimum sequence divergence of 11.5% to the next described relative *Elioraea tepidiphila* TU-7 (EF519867). This high degree of phylogenetic distinctness is in the range reported for other proteobacterial families (19) and would thus merit, from a 16S rRNA-based point of view, the proposal of a family within the *Rhodospirillales* to classify the *Paracatenula* symbionts.

With the exception of the genus *Paracatenula*, all groups of Catenulida have a cosmopolitan distribution ranging from tropical to cold temperate; several species of the marine catenulid genus *Retronectes*, which have no chemosynthetic symbionts, have been found as far north as Kristineberg on the Swedish west coast (1, 20). As all cultured *Rhodospirillales* related to the symbionts are mesophilic or slightly thermophilic (21), it is tempting to speculate that the limitation of *Paracatenula* to warm temperate or tropical waters reflects the temperature requirements of its symbionts.

To molecularly characterize the different hosts, we sequenced their 18S and 28S rRNA genes. Our phylogenetic analysis corroborates the placement of *Paracatenula* within the Catenulida as the monophyletic sister clade to the limnic *Catenula*/*Suomina* species complex (20) (Fig. S7). A strict consensus tree based on several phylogenetic methods using all hosts with both 18S and 28S rRNA genes sequenced (15 species) is highly congruent to the 16S rRNA gene tree obtained for their symbionts (Fig. 4). Bayesian inference-based reconstructions for this dataset are fully resolved on the host species level and completely congruent between host and symbiont (Fig. S6). The cocladogenesis of both groups indicates that a common ancestor of the host worms had acquired an alphaproteobacterial progenitor of the *Cand*. Riegeria clade and that this association has been stably maintained up to the present day by vertical transmission of the symbionts from one host generation to the next (22). In chemoautotrophic associations, vertical symbiont transmission has been reported

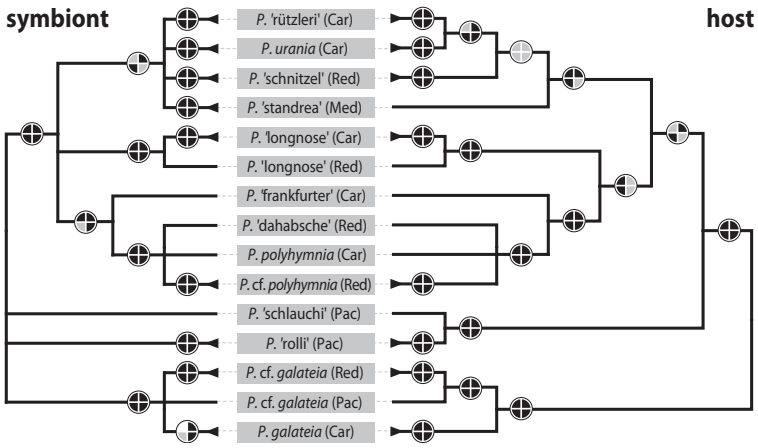

Fig. 4. Cocladogenesis between *Paracatenula* and *Candidatus* Riegeria. Tanglegram of strict consensus cladograms of four reconstruction methods for both symbiont 16S rRNA and host concatenated 18S and 28S rRNA. Node support is indicated as in Fig. 3. Provisional working names for undescribed species are given in parentheses. Sample origins: Car, Caribbean Sea; Med, Mediterranean Sea; Red, Red Sea; Pac, Pacific Ocean. No conflicting nodes are statistically supported in the results of the four phylogenetic reconstruction algorithms, indicating close coevolution between the partners.

only for the deep-sea clam family Vesicomyidae (23). Recent studies, however, have shown that host–symbiont phylogenies are decoupled for some vesicomyid clams, suggesting a mixed mode of symbiont transmission with vertical transmission occasionally interrupted with lateral symbiont acquisition (24, 25). Vertically transmitted symbionts tend to have an accelerated nucleotide substitution rate compared with free-living bacteria (26, 27). Sequence divergence of 16S rRNA for inheritable symbionts averages approximately 4% for every 100 million years (Ma), ranging from 2.5% to 11%, whereas free-living bacteria have rates ranging from 2% to 4% for 100 Ma (26, 28, 29). Based on this range of rates, the symbiosis in the ancestor of *Paracatenula* was established between 100 and 635 Mya. The maximum estimated divergence time for flatworms is 620 Ma and must be used as the maximum age of this symbiosis (30). As the *Cand*. Riegeria symbionts have no detectable nucleotide substitution rate heterogeneity in their 16S rRNA gene sequences compared with free-living *Acetobacteraceae* (Tajima rate test, $P > 0.05$ for all *Cand*. Riegeria against the *Acetobacteraceae* used in the phylogenetic analysis), we suppose a divergence rate of 2.5% in 100 Ma, as has been documented for symbionts with only slightly accelerated rates. This delimits the estimated age to 500 to 620 Ma. In comparison, the ancient solemyid and lucinid bivalve lineages in which all living taxa harbor chemoautotrophic symbionts have a paleontological record dating back to the late Ordovician/early Silurian 445 to 435 Mya (31). Even with the uncertainties involved when using evolutionary rates established for other groups of symbionts (29), the *Cand*. Riegeria–*Paracatenula* association can be considered the oldest known mutualistic bacteria–metazoan symbiosis, likely dating back to the early evolution of bilaterian diversity in the late Ediacaran/early Cambrian.

Coevolving inherited endosymbionts tend to have guanine and cytosine (GC) depleted genomes (27, 32). The alphaproteobacterial families closely related to the *Cand*. Riegeria clade, the *Acetobacteraceae* and *Rhodospirillaceae*, have a very high genomic guanine and cytosine content (gGC; 60–71% and 62–69%, respectively). Although there are no gGC data for *Cand*. Riegeria galateiae yet, the *dsrAB*, *aprA*, and *cbbM* genes combined have a GC content of 51.4%. This significantly lower GC content compared with closely related free-living groups has two possible non mutually exclusive explanations: (*i*) the intracellular symbiosis has relieved the symbionts from the selection pressure that leads to the high gGC in *Rhodospirillales* and the symbiont gGC therefore decreased to approximately 50%; or (*ii*) population bottlenecks leading to high genetic drift (33) have been driving the nucleotide bias in *Cand*. Riegeria galateiae, but at a much slower pace compared with that documented in the less than 50 Ma old symbiosis in vesicomyid clams (symbiont genome sizes of 1.02–1.16 Mb, gGC of 31.6–34%; closely related free-living *Thiomicrospira crunogena* genome size, 2.43 Mb, gGC of 43.1%) (23, 34, 35). The close coevolution of *Paracatenula* and *Cand*. Riegeria, in which each host maintains a monoculture of its specific symbiont, will allow comparative genomic studies to test these hypotheses and other theoretical predictions of genome evolution developed for intracellular symbionts (36). Moreover, this ancient clade of endosymbionts, with their distant phylogenetic position and their different function compared with other symbiotic *Alphaproteobacteria*, could help illuminate the common genetic predispositions that have allowed several members of this class to become successfully incorporated into eukaryotic cells—be it as intracellular parasites such as members of the order *Rickettsiales* or mutualists such as members of the order *Rhizobiales* or of the *Cand*. Riegeria clade.

Methods

TEM. TEM specimens were fixed in glutaraldehyde, postfixed with osmium tetroxide, and, after dehydration, embedded in Low Viscosity Resin (Agar Scientific). Complete ultrathin cross-sections mounted on formvar-coated slot grids were poststained with uranyl acetate and lead citrate. To estimate tissue ratios, digital images of the sections were merged and host and bacterial tissue were digitally traced into vector-based black and white representations. Area calculations were performed with ImageJ software based on these trace images using the "analyze particles" function.

SEM and Energy-Dispersive X-Ray Microanalysis. Specimens were immediately fixed as for TEM analysis. The samples were partly dehydrated in an acetone series up to 75% to preserve a maximum amount of sulfur (37). The samples were embedded in Spurr epoxy resin. Semithin cross sections (2.5 μm) of embedded samples were cut, mounted on carbon-padded stubs, and carbon-coated. The analysis was carried out on a Philips XL20 SEM with an EDAX P-505 sensor using EDAX eDXi V2.11 software. Sulfur was mapped against carbon and at least two other elements prominent in the given spectrum (e.g., phosphorous and osmium) to rule out structural and edge effects.

Raman Microspectroscopy. Extracted symbiont cells of PFA-fixed specimens were mounted on a calcium fluoride slide and analyzed with a LabRAM HR800 confocal Raman microspectroscope (HORIBA Jobin-Yvon). A 532-nm Nd:YAG laser provided the excitation for Raman scattering. Cells were selected haphazardly using a 50× objective, and the signal was acquired over a period of 5 s using a D0.6 intensity filter. The pinhole of the Peltier-cooled CCD detector was adjusted to 250 μm (optical slice, 4.6 μm). Spectra were measured between 0 and 2,000 cm^{-1}. They were baseline-corrected and normalized with LabSpec software 5.25.15 (HORIBA Jobin-Yvon). Reference spectra for elemental sulfur in S_8 ring configuration (Merck) were obtained by using the same settings and methods.

DNA Extraction, PCR Amplification, and Sequencing. DNA was extracted from individual worms by using the Blood and Tissue DNA extraction kit (Qiagen), and 2 μL of each extraction were used as PCR templates. Symbiont 16S rRNA-gene fragments (approximately 1,500 nt) were amplified with bacterial primers 616V (5′-AGAGTTTGATYMTGGCTC-3′) (38) and 1492R 5′-GGYTACCTTGTTACGACTT-3′ (39). PCR products were purified by using the MinElute PCR purification kit (Qiagen) and either directly sequenced with the PCR primers or cloned by using pCR2.1-TOPO and the TOPO TA Cloning Kit (Invitrogen Life Technologies). Host 18S and 28S rRNA-gene fragments (approximately 1,750 and 1,350 nt long, respectively) were amplified for each worm with general eukaryote primers 1f (5′-CTGGTTGATYCTGCCAGT-3′) and 2023r (5′-GGTTCACCTACGGAAACC-3) for 18S (40) and the primers D1a (5′-CCCSCGTAAYTTAAGCATAT-3′) and D5b2 (5′-CGCCAGTTCTGCTTACC-3) for 28S (41). PCR products were purified as described earlier and directly sequenced with the PCR primers. From *P. galateia* samples, *aprBA* was amplified with primers AprB-1-FW (5′-TGCGTGTAYATHTGYCC-3′) (11) and AprA-9-RV (5′-CKGWAGTAGTARCCSGGSYA-3′) (42), *dsrAB* was amplified with primers rDSR1Fa (5′-AARGGNTAYTGGAARG-3′) and rDSR4Rb (5′-GGRWARCAIGCNCCRCA-3′) (10), and *cbbM* was amplified with shortened primers after Blazejak et al. (43): CbbMF_bl_s (5′-ATCATCAARCCSAARCTSGGYC-3′) and CbbM1R_bl_s (5′-SGCRCCRTGRCCRGCMC-3′). We used touchdown PCR cycling programs for *cbbM*, *aprBA* and *dsrAB* as described for *aprBA* in Meyer and Kuever (42). The 395 nt-long *cbbM* fragment was directly sequenced by using the PCR primers, whereas the *aprBA* (2,178 nt) and *dsrAB* (1,911 nt) PCR products were gel purified using the MinElute gel extraction kit (Qiagen) and cloned as described earlier. For all cloned products, at least four clones were randomly picked and fully sequenced with the vector-specific primers M13F and M13R; for *aprBA* and *dsrAB*, we additionally used internal sequencing primers AprA-1-FW and AprB-5-RV (42) and DSR874F (10).

DGGE Analysis. DGGE analysis of 16S rRNA genes was performed as described by Meyer et al. (44). In every lane, only one band was observed, which was excised from the DGGE gel, and gel slices were stored in 50 mL MQ overnight at 4 °C. One microliter of this elution was used as a template for PCR reamplification using the forward primer (341f) without the GC clamp. Reamplifed DNA was purified and directly sequenced as described above.

rRNA Gene Based Phylogenetic Analyses. A 16S rRNA gene dataset for *Alphaproteobacteria* was constructed including 41 *Cand*. Riegeria sequences, three BLAST (45) hits from GenBank longer than 1,400 bp with sequence identities more than 89% to *Cand*. Riegeria galateiae (FJ152947, EU440696, and GQ402753), all *Alphaproteobacteria* with completely sequenced genomes used in a previous phylogenomic study (16), and sequences for landmark genera of cultivated *Rhodospirillales*. Table S1 provides details on the *Cand*. Riegeria 16S rRNA sequences used, including accession numbers. Table S2 provides accession numbers of sequences from reference *Alphaproteobacteria* and the deltaproteobacterial outgroup. The sequences were

aligned by using MAFFT Q-INS-i, which considers the secondary structure of RNA (46), and the alignments were trimmed at the 5′ and 3′ ends. We evaluated the optimal substitution model of sequence evolution with MrModeltest (47), and the general time-reversible (GTR) model with invariable sites (I) and a γ-correction for site-to-site rate variation (G) model was selected using the Akaike information criterion. No filters based on sequence conservation were used. We reconstructed the phylogenies using neighbor joining-, parsimony- (both MEGA 4 software) (48), maximum likelihood- (PHYML; phylogeny.fr Web service) (49, 50), and Bayesian inference-based (MrBayes) (51) algorithms. MrBayes was run for 5 million generations and trees were sampled every 1,000 generations after a burn-in of 40%. Node stability was evaluated using bootstrap (1,000× neighbor joining and parsimony), pps (Bayesian inference), and aLRT [maximum likelihood (52, 53)]. Bootstrap support of at least 70%, aLRT of at least 80%, and posterior probabilities of at least 0.80 were considered statistically significant. Strict consensus trees were constructed by collapsing all nodes conflicting in different phylogenetic methods up to the lowest node supported by all methods.

18S and 28S rRNA gene datasets were constructed from *Paracatenula* host sequences and from selected Catenulida sequences available in GenBank, with sequences of rhabditophoran flatworms (Macrostomida) as outgroup. Accession numbers of all sequences are shown in Fig. S7 and Table S1. The 18S and 28S rRNA gene datasets were separately aligned and trimmed as for the 16S gene analysis. Substitution models were evaluated for each gene, and the GTR+I+G model was selected for both. We concatenated the alignments and then reconstructed and evaluated the phylogenies as described earlier for 16S rRNA genes.

Phylogenetic Analyses of DsrB, AprA, and CbbM. Analyses of all genes were based on amino acid translations by using MAFFT alignments of full-length reference sequences obtained from available genomes and partial, PCR-amplified fragments. The optimal Wehlan and Goldman substitution model (WAG) for the DsrB alignment (500 aa positions; WAG+G), the AprA alignment (376 aa positions; WAG+G+I), and the CbbM alignment (478 aa positions; WAG+G+I) was evaluated with MrModeltest. Phylogenies were reconstructed for all genes using PHYML as well as MrBayes (3 million generations, 1 million burn-in). Node support in all gene trees is indicated for the ML analysis by using PHYML (aLRT) and Bayesian inference (pp). aLRT of at least 80% and posterior probabilities of at least 0.80 were considered statistically significant.

FISH. We designed oligonucleotide FISH probes by using the arb probe design tool included in the arb software package (54) (Table S3) and evaluated their specificity in silico by using the probe match tool probeCheck (55). Fluorescently labeled probes were purchased from Thermo, and FISH was performed according to Manz et al. (56) as adapted for LR-white resin (British BioCell International) sections described in Nussbaumer et al. (57). As a negative control, a nonsense probe (NON-338) was used. To determine stringent hybridization conditions for the PAR1151 probe, a formamide series was conducted by using *Cand*. Riegeria galateiae cell extractions. All FISH experiments were examined by using a Leica TCS-NT confocal laser-scanning microscope.

ACKNOWLEDGMENTS. We thank the Core facility for Cell Imaging and Ultrastructural Research at the University of Vienna and M. Stachowitsch. This work was supported by Austrian Science Fund Projects P17710 (to S.B. and N.R.H.), P20185 (to A.L.), P20394 (to H.R.G.-V., U.D., and J.O.), P20775 (to K.S.), and Y277-B03 (to M.H.) and is contribution 902 from the Carrie Bow Cay Laboratory, Caribbean Coral Reef Ecosystem Program, National Museum of Natural History, Washington, DC. Part of this work was carried out with the use of the resources of the Computational Biology Service Unit of Cornell University, which is partially funded by Microsoft Corporation.

1. Sterrer W, Rieger RM (1974) Retronectidae - a new cosmopolitan marine family of Catenulida (Turbellaria). *Biology of the Turbellaria*, eds Riser N, Morse M (McGraw-Hill, New York), pp 63–92.
2. Ott JA, Rieger G, Rieger R, Enderes F (1982) New mouthless interstitial worms from the sulfide system: Symbiosis with Prokaryotes. *Pubblicazioni Stazione Zoologica Napoli I. Mar Ecol (Berl)* 3:313–333.
3. Dirks U, Gruber-Vodicka HR, Leisch N, Sterrer WE, Ott JA (2011) A new species of symbiotic flatworms, *Paracatenula galateia* n. sp. (Platyhelminthes: Catenulida: Retronectidae) from Belize (Central America). *Mar Biol Res*, 10.1080/17451000.2011.574880.
4. Ott JA, et al. (1991) Tackling the sulfide gradient: A novel strategy involving marine nematodes and chemoautotrophic ectosymbionts. *Pubblicazioni Stazione Zoologica Napoli I. Mar Ecol (Berl)* 12:261–279.
5. Giere O, Conway N, Gastrock G, Schmidt C (1991) "Regulation" of gutless annelid ecology by endosymbiotic bacteria. *Mar Ecol Prog Ser* 68:287–299.
6. Muller F, Brissac T, Le Bris N, Felbeck H, Gros O (2010) First description of giant *Archaea* (*Thaumarchaeota*) associated with putative bacterial ectosymbionts in a sulfidic marine habitat. *Environ Microbiol* 12:2371–2383.
7. Dubilier N, Bergin C, Lott C (2008) Symbiotic diversity in marine animals: The art of harnessing chemosynthesis. *Nat Rev Microbiol* 6:725–740.
8. Bright M, Sorgo A (2003) Ultrastructural reinvestigation of the trophosome in adults of *Riftia pachyptila* (Annelida, Siboglinidae). *Invertebr Biol* 122:347–368.
9. Pasteris JD, Freeman JJ, Goffredi SK, Buck KR (2001) Raman spectroscopic and laser scanning confocal microscopic analysis of sulfur in living sulfur-precipitating marine bacteria. *Chem Geol* 180:3–18.
10. Loy A, et al. (2009) Reverse dissimilatory sulfite reductase as phylogenetic marker for a subgroup of sulfur-oxidizing prokaryotes. *Environ Microbiol* 11:289–299.
11. Meyer B, Kuever J (2007) Molecular analysis of the diversity of sulfate-reducing and sulfur-oxidizing prokaryotes in the environment, using *aprA* as functional marker gene. *Appl Environ Microbiol* 73:7664–7679.
12. Badger MR, Bek EJ (2008) Multiple Rubisco forms in proteobacteria: Their functional significance in relation to CO_2 acquisition by the CBB cycle. *J Exp Bot* 59:1525–1541.
13. Stackebrandt E, Ebers J (2006) Taxonomic parameters revisited: Tarnished gold standards. *Microbiol Today* 33:152–155.
14. Wang Q, Garrity GM, Tiedje JM, Cole JR (2007) Naive Bayesian classifier for rapid assignment of rRNA sequences into the new bacterial taxonomy. *Appl Environ Microbiol* 73:5261–5267.
15. Williams KP, Sobral BW, Dickerman AW (2007) A robust species tree for the *Alphaproteobacteria*. *J Bacteriol* 189:4578–4586.
16. Wu D, et al. (2009) A phylogeny-driven genomic encyclopaedia of Bacteria and Archaea. *Nature* 462:1056–1060.
17. Murray RGE, Stackebrandt E (1995) Taxonomic note: implementation of the provisional status Candidatus for incompletely described procaryotes. *Int J Syst Bacteriol* 45:186–187.
18. Kanokratana P, et al. (2011) Insights into the phylogeny and metabolic potential of a primary tropical peat swamp forest microbial community by metagenomic analysis. *Microb Ecol* 61:518–528.
19. Loy A, et al. (2005) 16S rRNA gene-based oligonucleotide microarray for environmental monitoring of the betaproteobacterial order "Rhodocyclales". *Appl Environ Microbiol* 71:1373–1386.
20. Larsson K, Jondelius U (2008) Phylogeny of Catenulida and support for Platyhelminthes. *Org Divers Evol* 8:378–387.
21. Albuquerque L, Rainey FA, Nobre MF, da Costa MS (2008) *Elioraea tepidiphila* gen. nov., sp. nov., a slightly thermophilic member of the Alphaproteobacteria. *Int J Syst Evol Microbiol* 58:773–778.
22. Bright M, Bulgheresi S (2010) A complex journey: transmission of microbial symbionts. *Nat Rev Microbiol* 8:218–230.
23. Hurtado LA, Mateos M, Lutz RA, Vrijenhoek RC (2003) Coupling of bacterial endosymbiont and host mitochondrial genomes in the hydrothermal vent clam Calyptogena magnifica. *Appl Environ Microbiol* 69:2058–2064.
24. Stewart FJ, Young CR, Cavanaugh CM (2008) Lateral symbiont acquisition in a maternally transmitted chemosynthetic clam endosymbiosis. *Mol Biol Evol* 25:673–687.
25. Stewart FJ, Young CR, Cavanaugh CM (2009) Evidence for homologous recombination in intracellular chemosynthetic clam symbionts. *Mol Biol Evol* 26:1391–1404.
26. Moran NA, McCutcheon JP, Nakabachi A (2008) Genomics and evolution of heritable bacterial symbionts. *Annu Rev Genet* 42:165–190.
27. Moran NA, McLaughlin HJ, Sorek R (2009) The dynamics and time scale of ongoing genomic erosion in symbiotic bacteria. *Science* 323:379–382.
28. Ochman H, Elwyn S, Moran NA (1999) Calibrating bacterial evolution. *Proc Natl Acad Sci USA* 96:12638–12643.
29. Kuo CH, Ochman H (2009) Inferring clocks when lacking rocks: The variable rates of molecular evolution in bacteria. *Biol Direct* 4:35.
30. Douzery EJP, Snell EA, Bapteste E, Delsuc F, Philippe H (2004) The timing of eukaryotic evolution: does a relaxed molecular clock reconcile proteins and fossils? *Proc Natl Acad Sci USA* 101:15386–15391.
31. Distel DL (1998) Evolution of chemoautotrophic endosymbioses in bivalves. *Bioscience* 48:277–286.
32. Moran NA (1996) Accelerated evolution and Muller's rachet in endosymbiotic bacteria. *Proc Natl Acad Sci USA* 93:2873–2878.
33. Dale C, Wang B, Moran N, Ochman H (2003) Loss of DNA recombinational repair enzymes in the initial stages of genome degeneration. *Mol Biol Evol* 20:1188–1194.
34. Kuwahara H, et al. (2008) Reductive genome evolution in chemoautotrophic intracellular symbionts of deep-sea *Calyptogena* clams. *Extremophiles* 12:365–374.
35. Scott KM, et al. (2006) The genome of deep-sea vent chemolithoautotroph *Thiomicrospira crunogena* XCL-2. *PLoS Biol* 4:e383.
36. Sachs JL, Essenberg CJ, Turcotte MM (2011) New paradigms for the evolution of beneficial infections. *Trends Ecol Evol* 26:202–209.
37. Krieger J, Giere O, Dubilier N (2000) Localization of RubisCO and sulfur in endosymbiotic bacteria of the gutless marine oligochaete *Inanidrilus leukodermatus* (Annelida). *Marine Biology (Berlin)* 137:239–244.
38. Juretschko S, et al. (1998) Combined molecular and conventional analyses of nitrifying bacterium diversity in activated sludge: *Nitrosococcus mobilis* and *Nitrospira*-like bacteria as dominant populations. *Appl Environ Microbiol* 64:3042–3051.
39. Kane MD, Poulsen LK, Stahl DA (1993) Monitoring the enrichment and isolation of sulfate-reducing bacteria by using oligonucleotide hybridization probes designed

from environmentally derived 16S rRNA sequences. *Appl Environ Microbiol* 59: 682–686.
40. Pradillon F, Schmidt A, Peplies J, Dubilier N (2007) Species identification of marine invertebrate early stages by whole-larvae in situ hybridisation of 18S ribosomal RNA. *Mar Ecol Prog Ser* 333:103–116.
41. von Reumont BM, et al. (2009) Can comprehensive background knowledge be incorporated into substitution models to improve phylogenetic analyses? A case study on major arthropod relationships. *BMC Evol Biol* 9:119.
42. Meyer B, Kuever J (2007) Molecular analysis of the distribution and phylogeny of dissimilatory adenosine-5′-phosphosulfate reductase-encoding genes (*aprBA*) among sulfur-oxidizing prokaryotes. *Microbiology* 153:3478–3498.
43. Blazejak A, Kuever J, Erséus C, Amann R, Dubilier N (2006) Phylogeny of 16S rRNA, ribulose 1,5-bisphosphate carboxylase/oxygenase, and adenosine 5′-phosphosulfate reductase genes from gamma- and alphaproteobacterial symbionts in gutless marine worms (oligochaeta) from Bermuda and the Bahamas. *Appl Environ Microbiol* 72: 5527–5536.
44. Meyer H, et al. (2006) Soil carbon and nitrogen dynamics along a latitudinal transect in Western Siberia, Russia. *Biogeochemistry* 81:239–252.
45. Altschul SF, Gish W, Miller W, Myers EW, Lipman DJ (1990) Basic local alignment search tool. *J Mol Biol* 215:403–410.
46. Katoh K, Kuma K-i, Toh H, Miyata T (2005) MAFFT version 5: Improvement in accuracy of multiple sequence alignment. *Nucleic Acids Res* 33:511–518.
47. Nylander JAA (2008) *MrModeltest v2.3 Program Distributed by the Author* (Uppsala Univ, Uppsala, Sweden).
48. Tamura K, Dudley J, Nei M, Kumar S (2007) MEGA4: Molecular Evolutionary Genetics Analysis (MEGA) software version 4.0. *Mol Biol Evol* 24:1596–1599.
49. Guindon S, Gascuel O (2003) A simple, fast, and accurate algorithm to estimate large phylogenies by maximum likelihood. *Syst Biol* 52:696–704.
50. Dereeper A, et al. (2008) Phylogeny.fr: Robust phylogenetic analysis for the non-specialist. *Nucleic Acids Res* 36(suppl 2):W465–W469.
51. Ronquist F, Huelsenbeck JP (2003) MrBayes 3: Bayesian phylogenetic inference under mixed models. *Bioinformatics* 19:1572–1574.
52. Anisimova M, Gascuel O (2006) Approximate likelihood-ratio test for branches: A fast, accurate, and powerful alternative. *Syst Biol* 55:539–552.
53. Guindon S, et al. (2010) New algorithms and methods to estimate maximum-likelihood phylogenies: Assessing the performance of PhyML 3.0. *Syst Biol* 59:307–321.
54. Ludwig W, et al. (2004) ARB: A software environment for sequence data. *Nucleic Acids Res* 32:1363–1371.
55. Loy A, et al. (2008) probeCheck—a central resource for evaluating oligonucleotide probe coverage and specificity. *Environ Microbiol* 10:2894–2898.
56. Manz W, Amann R, Ludwig W, Wagner M, Schleifer K-H (1992) Phylogenetic oligodeoxynucleotide probes for the major subclasses of proteobacteria: Problems and solutions. *Syst Appl Microbiol* 15:593–600.
57. Nussbaumer AD, Fisher CR, Bright M (2006) Horizontal endosymbiont transmission in hydrothermal vent tubeworms. *Nature* 441:345–348.

Supporting Information

Gruber-Vodicka et al. 10.1073/pnas.1105347108

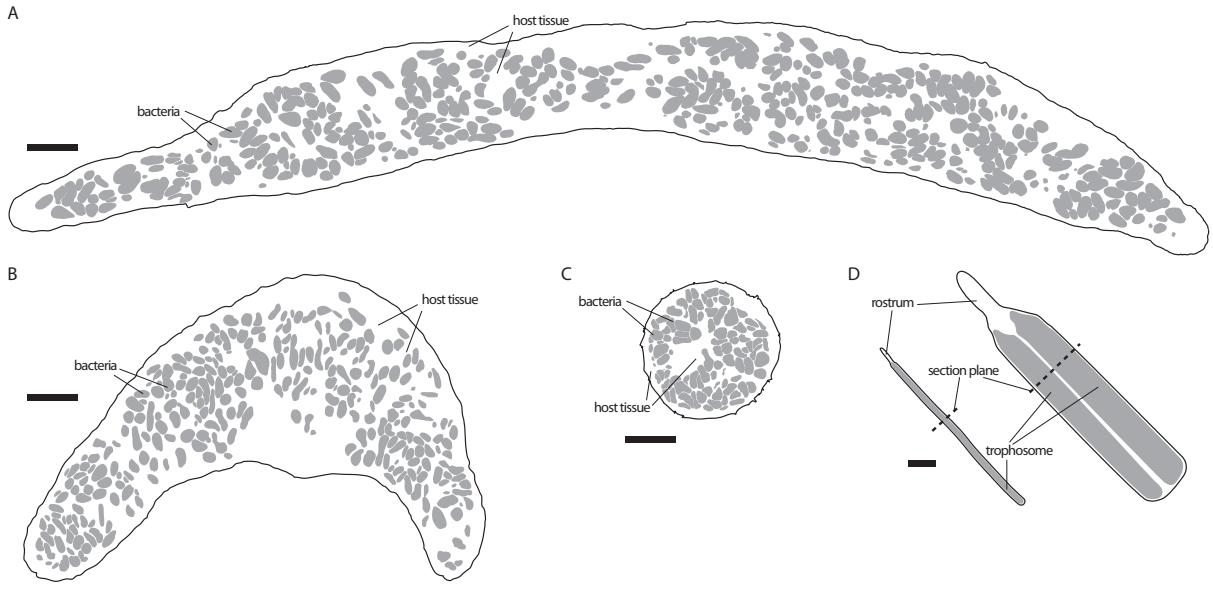

Fig. S1. Symbiont-to-host tissue ratio of three different *Paracatenula* species. (*A*–*C*) Vector trace images of TEM cross sections. Bacteria are indicated in gray; host epidermal outline indicated in black line. (Scale bars: 20 μm.) (*A*) Cross-section of *P.* cf. *galateia* from Dahab, Egypt: symbionts make up 41.2% of cross-section area. (*B*) Cross-section of *P. galateia* from Carrie Bow Cay, Belize: symbionts make up 36.7% of cross-section area. (*C*) Cross-section of *P.* cf. *polyhymnia*: symbionts make up 51.9% of cross-section area. (*D*) Schematic habitus of *P.* cf. *polyhymnia* (*Left*) and *P. galateia* (*Right*). Trophosome tissue with bacteria is indicated in gray, host outline indicated in black line, and dashed lines indicate positions of cross sections in *A*–*C*. (Scale bar: 200 μm.)

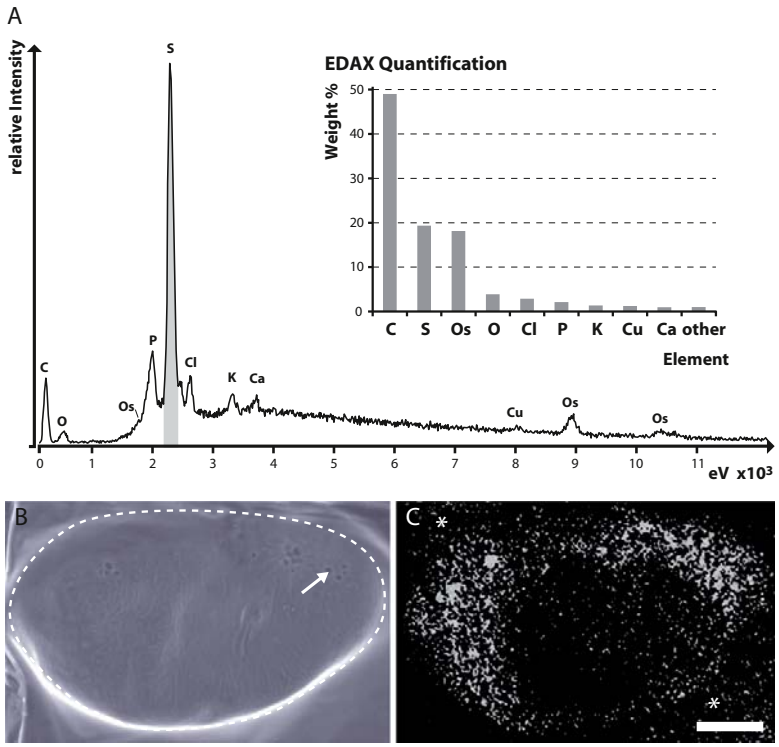

Fig. S2. Sulfur measurements of the trophosome material of *P. galateia*. (*A*) Energy dispersive X-ray spectrum of trophosome region. Measurement location marked with arrow in *B*; peaks of the nine most frequent elements are indicated above the peaks, and their weight (atomic mass) proportions are also shown (*Inset*). (*B*) Scanning EM image of partially dehydrated semithin cross-section of *P. galateia* embedded in Spurr resin; arrow indicates locality of spectrum in *A*. (*C*) Mapping of sulfur using the peak indicated with gray in spectrum (*A*) on the trophosome cross-section in *B*. *Regions of high sulfur content in resin outside of the worm caused by partial loss of sulfur in the embedding process. *B* and *C* are shown at the same scale. (Scale bar: 50 μm.)

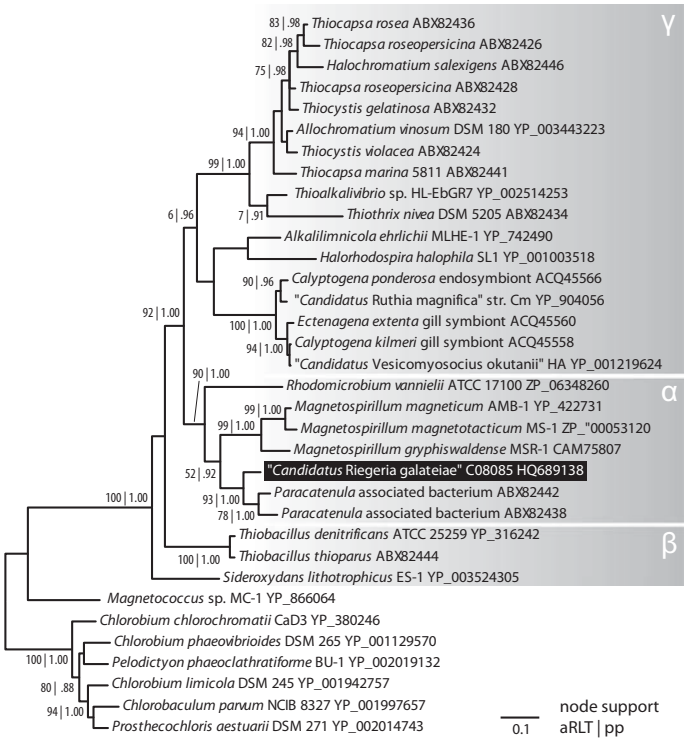

Fig. S3. Phylogenetic reconstruction of DsrB sequences from symbiotic and free-living SOB. *Alpha-*, *Beta-*, and *Gammaproteobacteria* are indicated with gray boxes, and the sequence from *Candidatus* Riegeria galateiae obtained in this study is marked in black. The analysis is based on a MAFFT amino acid alignment with 500 positions. The tree shown was estimated under the WAG+G model using PHYML and the tree was rooted with *Chlorobi*. Node support is indicated for ML analysis using PHYML (aRLT) as well as Bayesian inference (pp) with MrBayes (three Mio generations and one Mio burn-in). Accession numbers are given after the name and strain indicator. (Scale bar: 10% estimated sequence divergence.)

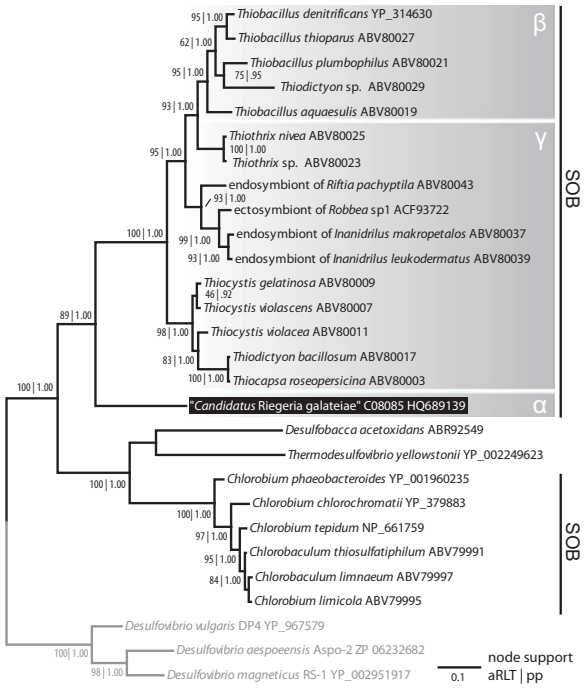

Fig. S4. Phylogenetic reconstruction of AprA lineage II sequences from SOB and sulfate-reducing bacteria. The different classes of *Proteobacteria* are indicated with Greek letters, the sequence from *Candidatus* Riegeria galateiae obtained in this study is marked in black, and bars mark SOB. *Desulfovibrio* sequences (*aprA* lineage I) were used as outgroup. The analysis is based on a MAFFT amino acid alignment with 376 positions, and the tree shown was estimated under the WAG+Gamma model using MrBayes with three Mio generations and one Mio burn-in; node support is indicated for ML analysis (PHYML; aRLT) and Bayesian inference (MrBayes; pp). Accession numbers are given after the name and strain indicator. (Scale bar: 10% estimated sequence divergence.)

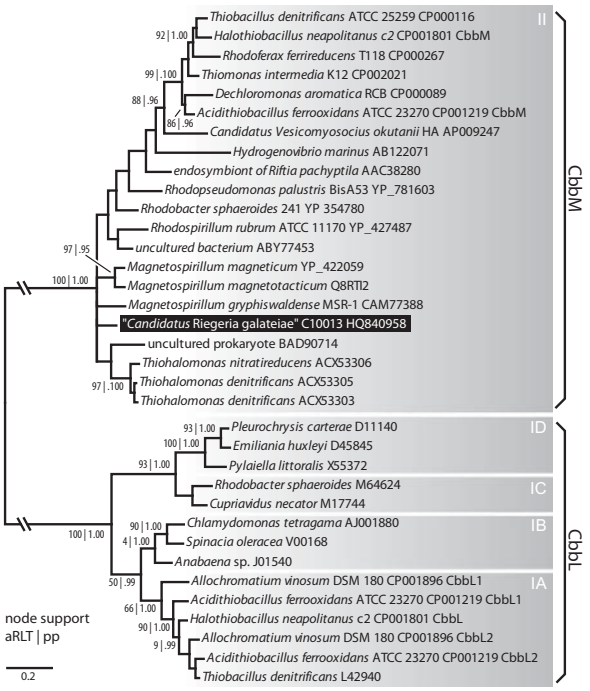

Fig. S5. Phylogenetic reconstruction of RubisCO (CbbM and CbbL) sequences. The different forms of RubisCO are indicated with gray boxes and the major lineages with black brackets, and the sequence from *Candidatus* Riegeria galateiae obtained in this study is marked in black. The analysis is based on a MAFFT amino acid alignment with 478 positions. The tree shown was estimated under the WAG+G+I model using MrBayes with one Mio generation and 0.2 Mio burn-in, rooted with the CbbL clade, and node support is indicated for ML analysis (PHYML; aRLT) and Bayesian inference (MrBayes; pp). (Scale bar: 20% estimated sequence divergence.)

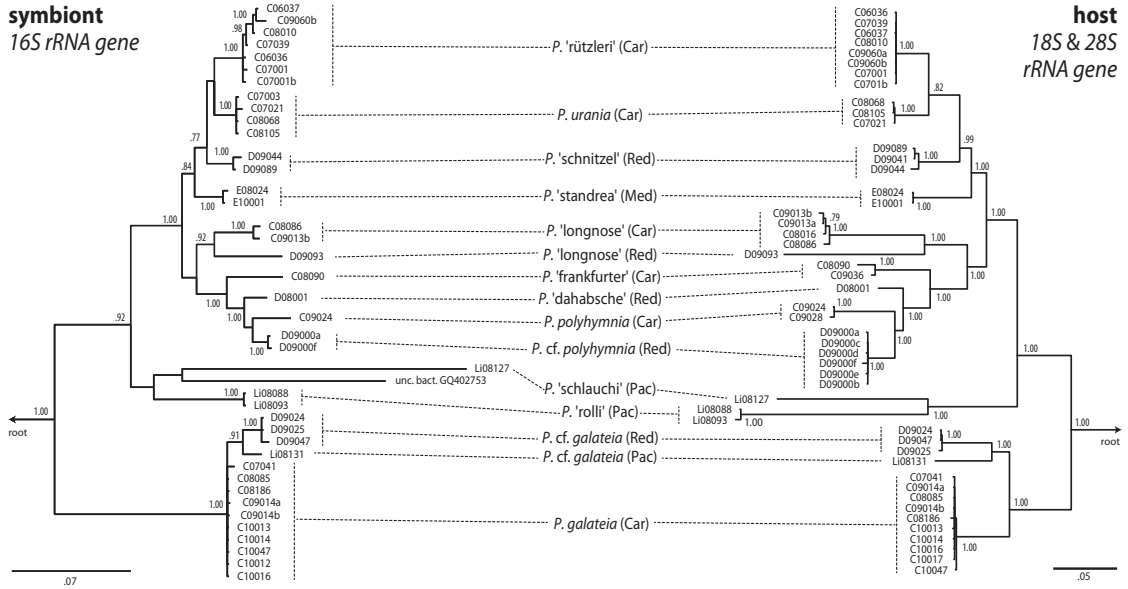

Fig. S6. Cocladogenesis between *Paracatenula* and *Candidatus* Riegeria. Tangle-gram of the trees of symbiont 16S rRNA (1,542 positions) and host concatenated 18S and 28S rRNA genes (3,492 positions) sequenced from worm sampled in the Caribbean Sea (Car), Mediterranean Sea (Med), Red Sea (Red), and Pacific Ocean (Pac). Both trees are based on MAFFT nucleotide alignments incorporating predicted secondary structure information and were estimated under the GTR+G+I model using MrBayes with five Mio generations and two Mio burn-in; node support in both trees is indicated (pp). The root part of the host phylogeny including other catenulids and the outgroup is shown in Fig. S7. The trees were calculated by using all available *Paracatenula* sequences (Table S2). Specimens where either host or symbiont data were lacking completely were pruned from the tree for clarity. Accession numbers for sequences from *Paracatenula* hosts and symbionts are given in Table S1. The accession numbers for the sequences used in the root part of the host tree are given in Fig. S7; for the symbiont tree, refer to Tables S1 and S2. [Scale bars: 7% (symbiont) and 5% (host) estimated sequence divergence.]

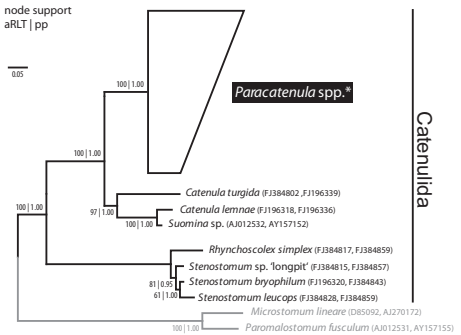

Fig. S7. Catenulid phylogeny based on concatenated 18S and 28S rRNA gene analysis. Root part of the tree presented in Fig. S6, indicating the position of the genus *Paracatenula* within Catenulida. Asterisks indicates the *Paracatenula* clade of this tree that is shown in Fig. S6 (host tree). The tree shown is based on a MAFFT nucleotide alignment incorporating predicted secondary structure information with 3,492 positions and was estimated under the GTR+G+I model using MrBayes with five Mio generations and two Mio burn-in; node support is indicated for maximum likelihood (PHYML; aRLT) as well as Bayesian inference (MrBayes; pp). The tree was rooted by using sequences of two rhabditophoran flatworms (Macrostomida) as outgroup (indicated in gray). Accession numbers are given after the organism name (18S and 28S rRNA gene, respectively) except for the *Paracatenula* spp. sequences, which are listed in Table S1. (Scale bar: 5% estimated sequence divergence.)

Table S1. Accession numbers of Paracatenula and "Cand. Riegeria" rRNA sequences used

Host name	Geographic origin	Sampling location	Specimen	"Cand. Riegeria" 16S	18S	28S
Paracatenula "rützleri"	Caribbean Sea	Belize, CBC	C06036	HQ68053*	HQ689068*	HQ689086*
Paracatenula "rützleri"	Caribbean Sea	Belize, CBC	C06037	HQ68052*	HQ689067*	HQ689085*
Paracatenula "rützleri"	Caribbean Sea	Belize, CBC	C07001	HQ68051*	—	HQ689084*
Paracatenula "rützleri"	Caribbean Sea	Belize, CBC	C07001b	HQ68050*	—	HQ689083*
Paracatenula urania	Caribbean Sea	Belize, CBC	C07003	HQ68049*	—	—
Paracatenula urania	Caribbean Sea	Belize, CBC	C07021	HQ68048*	HQ689066*	HQ689082*
Paracatenula "rützleri"	Caribbean Sea	Belize, CBC	C07039	HQ68047*	HQ689065*	HQ689081*
Paracatenula galateia	Caribbean Sea	Belize, CBC	C07041	HQ68046*	HQ231340	HQ231330
Paracatenula "rützleri"	Caribbean Sea	Belize, CBC	C08010	HQ68045*	HQ689064*	HQ689080*
Paracatenula "longnose"	Caribbean Sea	Belize, CBC	C08016	—	HQ689063*	HQ689079*
Paracatenula urania	Caribbean Sea	Belize, CBC	C08068	HQ68044*	HQ689062*	HQ689078*
Paracatenula galateia	Caribbean Sea	Belize, CBC	C08085	HQ68043*	HQ231341	HQ231331
Paracatenula "longnose"	Caribbean Sea	Belize, CBC	C08086	HQ68042*	HQ689061*	—
Paracatenula "frankfurter"	Caribbean Sea	Belize, CBC	C08090	HQ68041*	HQ689060*	HQ689077*
Paracatenula urania	Caribbean Sea	Belize, CBC	C08105	HQ68040*	—	HQ689076*
Paracatenula galateia	Caribbean Sea	Belize, CBC	C08186	HQ68039*	HQ231342	HQ231332
Paracatenula "longnose"	Caribbean Sea	Belize, CBC	C09013a	—	HQ689059*	HQ689075*
Paracatenula "longnose"	Caribbean Sea	Belize, CBC	C09013b	HQ68038*	HQ689058*	HQ689074*
Paracatenula galateia	Caribbean Sea	Belize, CBC	C09014a	HQ68037*	HQ231343	HQ231333
Paracatenula galateia	Caribbean Sea	Belize, CBC	C09014b	HQ68036*	HQ231344	HQ231334
Paracatenula polyhymnia	Caribbean Sea	Belize, CBC	C09024	HQ68035*	HQ689057*	HQ689073*
Paracatenula polyhymnia	Caribbean Sea	Belize, CBC	C09028	—	—	HQ689072*
Paracatenula "frankfurter"	Caribbean Sea	Belize, CBC	C09036	—	HQ689056*	—
Paracatenula "rützleri"	Caribbean Sea	Belize, CBC	C09060a	—	HQ689055*	HQ689071*
Paracatenula "rützleri"	Caribbean Sea	Belize, CBC	C09060b	HQ68034*	HQ689054*	HQ689070*
Paracatenula galateia	Caribbean Sea	Belize, CBC	C10012	HQ68033*	—	—
Paracatenula galateia	Caribbean Sea	Belize, CBC	C10013	HQ68032*	—	HQ231335
Paracatenula galateia	Caribbean Sea	Belize, CBC	C10014	HQ68031*	—	HQ231336
Paracatenula galateia	Caribbean Sea	Belize, CBC	C10016	HQ68030*	—	HQ231337
Paracatenula galateia	Caribbean Sea	Belize, CBC	C10017	—	—	HQ231338
Paracatenula galateia	Caribbean Sea	Belize, CBC	C10047	HQ68029*	—	HQ231339
Paracatenula "dahabsche"	Red Sea	Egypt, Dahab	D08001	HQ69095*	HQ689108*	HQ689122*
Paracatenula cf polyhymnia	Red Sea	Egypt, Dahab	D09000a	HQ69094*	HQ689107*	HQ689121*
Paracatenula cf polyhymnia	Red Sea	Egypt, Dahab	D09000b	—	–	HQ689120*
Paracatenula cf polyhymnia	Red Sea	Egypt, Dahab	D09000c	—	HQ689106*	HQ689119*
Paracatenula cf polyhymnia	Red Sea	Egypt, Dahab	D09000d	—	HQ689105*	HQ689118*
Paracatenula cf polyhymnia	Red Sea	Egypt, Dahab	D09000e	—	HQ689104*	HQ689117*
Paracatenula cf polyhymnia	Red Sea	Egypt, Dahab	D09000f	HQ69093*	HQ689103*	—
Paracatenula "spaghetti"	Red Sea	Egypt, Dahab	D09003	—	—	HQ689116*
Paracatenula cf galateia	Red Sea	Egypt, Dahab	D09024	HQ69092*	HQ689102*	HQ689115*
Paracatenula cf galateia	Red Sea	Egypt, Dahab	D09025	HQ69091*	—	HQ689114*
Paracatenula "schnitzerl"	Red Sea	Egypt, Dahab	D09031	—	—	HQ689113*
Paracatenula "schnitzel"	Red Sea	Egypt, Dahab	D09041	—	HQ689101*	HQ689112*
Paracatenula "schnitzel"	Red Sea	Egypt, Dahab	D09044	HQ69090*	HQ689100*	—
Paracatenula cf galateia	Red Sea	Egypt, Dahab	D09047	HQ69089*	HQ689099*	HQ689111*
Paracatenula "schnitzel"	Red Sea	Egypt, Dahab	D09089	HQ69088*	HQ689098*	HQ689110*
Paracatenula "speedy"	Red Sea	Egypt, Dahab	D09091	—	HQ689097*	—
Paracatenula "longnose"	Red Sea	Egypt, Dahab	D09093	HQ69087*	HQ689096*	HQ689109*
Paracatenula "stanadrea"	Mediterranean Sea	Italy, Elba	E08024	HQ69124*	HQ689125*	HQ689127*
Paracatenula "stanadrea"	Mediterranean Sea	Italy, Elba	E10001	HQ69123*	—	HQ689126*
Paracatenula "rolli"	Pacific Ocean	Australia, LI	Li08088	HQ69129*	HQ689133*	HQ689137*
Paracatenula "rolli"	Pacific Ocean	Australia, LI	Li08093	HQ69128*	HQ689132*	HQ689136*
Paracatenula cf urania	Pacific Ocean	Australia, LI	Li08098	HQ845108*	—	—
Paracatenula "schlauchi"	Pacific Ocean	Australia, LI	Li08127	HQ845109*	HQ689131*	HQ689135*
Paracatenula cf galateia	Pacific Ocean	Australia, LI	Li08131	HQ845110*	HQ689130*	HQ689134*

—, no PCR product obtained. CBC, Carrie Bow Cay; LI, Lizard Island.
*Sequence generated in the present study.

Table S2. Accession numbers of alphaprotebacterial and deltaproteobacterial 16S rRNA sequences used

Bacteria	Sequence
Alphaproteobacteria	
Rhizobiales	
Bartonella bacilliformis KC583	NC_008783
Bartonella quintana Toulouse	NC_005955
Beijerinckia indica subsp. indica 9039	NC_010581
Bradyrhizobium sp. ORS278	NC_009445
Brucella melitensis 16M	NC_003317, NC_003318
Mesorhizobium loti MAFF303099	NC_002678
Mesorhizobium sp. BNC1	NC_008254
Methylobacterium radiotolerans JCM 2831	NC_010505
Methylobacterium sp. 4–46	NC_010511
Nitrobacter winogradskyi Nb-255	NC_007406
Rhizobium leguminosarum bv. viciae 3841	NC_008380
Rhodopseudomonas palustris BisB18	NC_007925
Xanthobacter autotrophicus Py2	NC_009720
Sphingomonadales	
Erythrobacter litoralis HTCC2594	NC_007722
Novosphingobium aromaticivorans DSM 12444	NC_007794
Sphingomonas wittichii RW1	NC_009511
Sphingopyxis alaskensis RB2256	NC_008048
Zymomonas mobilis subsp. mobilis ZM4	NC_006526
Hyphomonadales	
Hyphomonas neptunium ATCC 15444	NC_008358
Maricaulis maris MCS10	NC_008347
Rhodobacteraceae	
Paracoccus denitrificans PD1222	NC_008686, NC_008687
Dinoroseobacter shibae DFL 12	NC_009952
Jannaschia sp. CCS1	NC_007802
Roseobacter denitrificans OCh 114	NC_008209
Silicibacter pomeroyi DSS-3	NC_003911
Rhodobacter sphaeroides 2.4.1	NC_007494, NC_007493
Rhodospirillaceae	
Azospirillum lipoferum	Z29619
Insolitispirillum peregrinum LMG 4340	EF612767
Magnetospirillum magneticum AMB-1	NC_007626
Novispirillum itersonii IAM 14945	AB074520
Rhodocista pekingensis 3-p	AF523824
Rhodospirillum rubrum ATCC 11170	NC_007643
Roseospira marina CE2105	AJ298879
Acetobacteraceae	
Acidiphilium cryptum JF-5	NC_009484
Elioraea tepidiphila TU-7	EF519867
Gluconacetobacter diazotrophicus PAl 5	NC_010125
Gluconobacter oxydans 621H	NC_006677
Granulibacter bethesdensis CGDNIH1	NC_008343
Rickettsiales	
Anaplasma marginale str. St. Maries	NC_004842
Anaplasma phagocytophilum HZ	NC_007797
Ehrlichia canis str. Jake	NC_007354
Ehrlichia ruminantium str. Welgevonden	NC_005295
Neorickettsia sennetsu Miyayama	NC_007798
Orientia tsutsugamushi Boryong	NC_009488
Rickettsia bellii RML369-C	NC_007940
Rickettsia typhi Wilmington	NC_006142
Wolbachia endosymbiont TRS of *Brugia malayi*	NC_006833
Wolbachia pipientis symbiont of *Dipetalonema gracile*	AJ548802
Incertae sedis	
"*Candidatus* Pelagibacter ubique" HTCC1062	NC_007205
Caulobacter sp. K31	NC_010338
Geminicoccus roseus 18922	AM403172
Magnetococcus sp. MC-1	NC_008576
Parvibaculum lavamentivorans DS-1	NC_009719

Table S2. Cont.

Bacteria	Sequence
Deltaproteobacteria (outgroup)	
Geobacter sulfurreducens PCA	U13928
Geobacter uraniireducens Rf4	EF527427
Pelobacter propionicus DSM 2379	NC_008609

For 16S rRNA genes extracted from genomes, the genome accession numbers are given.

Table S3. Probes used for FISH

Probe	Standard probe name[†]	Specificity	Sequence 5′ modification	Target RNA	Position[‡]	Formamide, %/hybridization time, h/probe concentration, ng/μL	Reference
EUB338	S-*-BactV-0338-a-A-18	Most bacteria	5′-GCT GCC TCC CGT AGG AGT-3′ FLUOS	16S	338–355	40%/3/4.6	1
ALF968	L-C-gProt-1027-a-A-17	*Alphaproteobacteria*, except for *Rickettsiales* no mismatch to "*Cand*. Riegeria galateiae"	5′-GCC TTC CCA CAT CGT TT-3′ Cy5	16S	968–985	40%/3/2.7	2
Par1151	S-*-CRg-1151-a-A-21	"*Cand*. Riegeria galateiae" [§]	5′-CTT GTC ACC GGC AGT TCC CTC-3′ Cy3	16S	1,151–1,171	40%/3/2.7	Present study
NON338	Not named	Antisense	5′-ACT CCT ACG GGA GGC AGC-3′ Cy3	16S	338–355	40%/3/2.7	3

[†]According to Alm et al. (4).
[‡]16S rRNA position, *E. coli* numbering (5).
[§]The probe as 4/2231/9474 bacterial non target hits in the RDP database with 0/1/2 mismatches (6).

1. Amann RI, Krumholz L, Stahl DA (1990) Fluorescent-oligonucleotide probing of whole cells for determinative, phylogenetic, and environmental studies in microbiology. *J Bacteriol* 172: 762–770.
2. Neef A (1997) Anwendung der in situ-Einzelzell-Identifizierung von Bakterien zur Populationsanalyse in komplexen mikrobiellen Biozönosen [Application of in-situ single cell Identification of bacteria in population analysis of complex microbial communities]. PhD thesis (Technische Universität München, Munich).
3. Wallner G, Amann R, Beisker W (1993) Optimizing fluorescent in situ hybridization with rRNA-targeted oligonucleotide probes for flow cytometric identification of microorganisms. *Cytometry* 14:136–143.
4. Alm EW, Oerther DB, Larsen N, Stahl DA, Raskin L (1996) The oligonucleotide probe database. *Appl Environ Microbiol* 62:3557–3559.
5. Brosius J, Palmer ML, Kennedy PJ, Noller HF (1978) Complete nucleotide sequence of a 16S ribosomal RNA gene from *Escherichia coli*. *Proc Natl Acad Sci USA* 75:4801–4805.
6. Cole JR, et al. (2009) The Ribosomal Database Project: Improved alignments and new tools for rRNA analysis. *Nucleic Acids Res* 37(suppl 1):D141–D145.

Chapter 3

Continued *de novo* formation and asexual transmission of bacteriocytes in the symbiotic flatworm *Paracatenula galateia*

Authors: Ulrich Dirks*, Harald R. Gruber-Vodicka, Nikolaus Leisch, Silvia Bulgheresi, Bernhard Egger, Peter Ladurner and Jörg A. Ott

Keywords: bacteriocyte, symbiont transmission, neoblast, regeneration, asexual reproduction, paratomy

Publication status: Manuscript since 2011-07-25 under review in the Journal of the International Society for Microbial Ecology (ISME); Topic: Host-Microbe Interactions.

Detailed description of UD´s contribution: UD designed major parts of the study, established the protocols and performed all experiments and most of the fieldwork, analyzed data and wrote the manuscript.

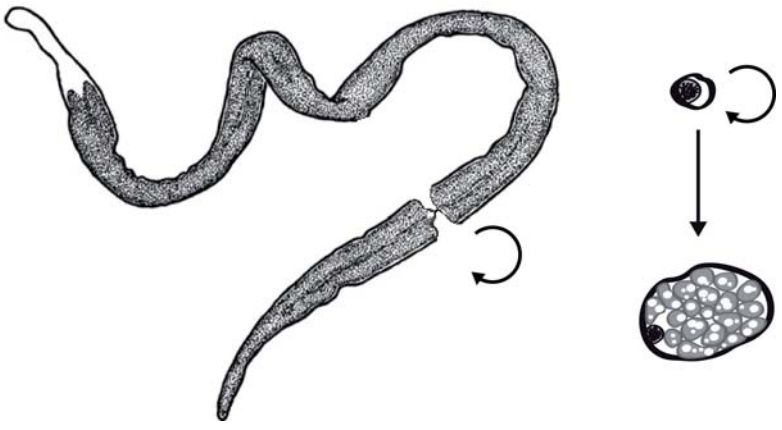

Abstract

Animals which harbour symbiotic bacteria in special cells (bacteriocytes) are important models for studying interactions between cells of different organisms. In all systems studied so far, *de novo* formation of bacteriocytes occurs only once when the symbiosis is established in early host development. During vertical transmission to the next host generation intracellular symbionts are exposed to population-bottlenecks and other stress factors since they must exit the parental bacteriocytes and re-enter those of the progeny. Here, we present the free-living symbiotic flatworm *Paracatenula galateia* and its intracellular, sulfur-oxidizing bacteria as a system which has novel strategies of bacteriocyte formation and vertical symbiont transmission. Using thymidine analogue S-phase labelling and immunohistochemistry we show that all cells in adult worms – including bacteriocytes – originate exclusively from continuously proliferating aposymbiotic stem cells (neoblasts). This unique feature makes *P. galateia* an excellent system to study bacteriocyte determination and differentiation. We also provide morphological and immunohistochemical evidence that *P. galateia* reproduces by a mode of asexual fragmentation and regeneration termed paratomy and thus transmits numerous symbiont-containing bacteriocytes to its asexual progeny. The transmission of complete bacteriocytes is the most direct and secure mechanism of vertical symbiont transmission known so far and it guarantees the inheritance of high symbiont numbers, reducing population bottleneck-effects. Moreover, it results in a permanently intracellular liaison between host and symbionts, helping to explain their tight codiversification. Both, bacteriocyte production from aposymbiotic stem cells throughout the life cycle and their transmission to the asexual offspring are novel mechanisms of symbiosis maintenance and reflect the sophisticated symbiont integration into host development.

Introduction

Beneficial symbiosis between two organisms (mutualism) with different metabolic or mechanical abilities increases the fitness of both partners and can extend their range of suitable habitats significantly (Boucher et al. 1982). Intracellular symbiosis is a special kind of symbiosis in which a microbe (symbiont) lives inside a cell of another organism (host). The latter were so far mostly found in the eukaryotes and diverse examples for unicellular and multicellular hosts species are known (Cavanaugh et al. 1981, Keyser et al. 1982, Bianciotto et al. 1996, Dubilier et al. 2008, Horn, 2008).

A major challenge in symbiosis research is to identify the mechanisms that allow symbiotic partners to selectively establish and maintain symbiotic associations, in particular those of bacteria inside animal host cells - the bacteriocytes. This involves differentiation and maintenance of bacteriocytes throughout the symbiotic part of the life cycle and the transmission of symbionts through host generations.

Many animal hosts, especially those in obligate symbiotic relationships, show high levels of morphological adaptations which reflect the integration of their symbiotic life style into the developmental program. Intracellular symbionts are in most cases restricted to specialized tissues or organs such as the bacteriome found in different insects (Denlinger & Ma 1975, Douglas & Dixon 1987) or the trophosome of the mouth- and gutless deep sea tube worms (Siboglinidae) (van der Land & Norrevang 1975). Bacteriome and trophosome are functionally analogue tissues and mainly consist of symbiont housing bacteriocytes. In both, insects and tubeworms, bacteriocyte *de novo* formation (infection of aposymbiotic cells with symbiotic bacteria) was found to be restricted to the embryonic/larval development of the animals (Braendle et al. 2003, Miura et al. 2003, Nussbaumer et al. 2006, Harmer et al. 2008). Later, during postembryonic development the bacteriocytes themselves proliferate and it is assumed that neither infection nor differentiation of host cells producing new bacteriocytes any longer happens (Douglas & Dixon 1987, Lambiase et al. 1997, Pflugfelder et al. 2009). The bacteriocyte is the essential unit where interaction between host and symbiont takes place. However, it is still unknown what the crucial changes are that turn aposymbiotic cells into bacteriocytes. Since in all systems studied so far *de novo* bacteriocyte formation is restricted to early developmental stages of the host, the investigation of this essential process remains difficult.

To transmit beneficial symbionts to the offspring animals use a variety of strategies. In most known cases the symbionts have to leave the parental symbiont housing tissue/cells to be either inherited directly to the offspring (vertical transmission) or released to an environmental pool from which the aposymbiotic offspring selectively takes up its symbionts (horizontal transmission). In many symbiotic associations, however, both vertical and horizontal modes seem to be mixed (Bright & Bulgheresi 2010). Strictly vertical transmission strategies are typically reflected in a tight codiversification of the partners (Sachs et al. 2011).

The flatworm order termed Catenulida are the bilateria with the most simple bauplan (Rieger, 1981). Mouth- and gutless catenulids of the genus *Paracatenula* are members of the meiofauna in marine shallow water sediments. They harbor intracellular chemosynthetic alphaproteobacterial symbionts, "*Candidatus* Riegeria" which can equal the hosts´ biomass (Sterrer & Rieger 1974, Ott et al. 1982, Gruber-Vodicka et al. 2011). The most intensively studied species of the genus, *Paracatenula galateia* Dirks et al. 2011, is dorso-ventrally flattened, about 300 µm wide and extremely variable in length (1-6 mm) (Figure 1A). The body consists of two parts: (1) the rostrum anterior to the brain which is narrow and symbiont free and (2) the posterior "trophosome region" mainly consistsing of the symbiont housing bacteriocytes (Figure 1A, 1D). Collectively all bacteriocytes constitute a tissue termed "trophosome" in functional analogy to the trophosome of siboglinid tubeworms (van der Land & Norrevang, 1975). A recent study by Gruber-Vodicka et al. (2011) reports a tight codiversification between species of the genus *Paracatenula* and their specific symbionts possibly dating back up to 500 MY. This points to a strict vertical symbiont transmission in the genus, however, the reproduction strategies were unknown by the time we started this study.

Platyhelminthes possess pluripotent (maybe totipotent) stem cells - the so-called neoblasts - during their whole lifespan (Baguna et al. 1989, Ladurner et al. 2000, Newmark & Sanchez Alvarado 2000, Bode et al. 2006). Neoblasts are self-renewing and the sole source of all differentiated cell types including the germ cells (reviewed in Peter et al. 2004). Morphologically they are characterized by some typical features which are chromatoid bodies (secretions from the nucleus which contain proteins and RNA and disappear progressively when neoblasts enter differentiation), a small size and very high nuclear to cytoplasmic ratio and a characteristic heterochromatin pattern (Hori 1982, Auladell et al. 1993, Kotaja & Sassone-Corsi 2007, Fernandéz-Taboada et al. 2010). In addition to their function in cell renewal neoblasts provide

exceptional regenerative power to many flatworm taxa (reviewed in Reddien & Sanchez Alvarado 2004 and Egger et al. 2007). Since the genus *Paracatenula* is part of the Platyhelminthes one can assume that also bacteriocytes derive from aposymbiotic neoblasts by repeated infection and the animals may possess high regenerative capabilities.

A high diversity of sexual and asexual reproduction modes are found among the Platyhelminthes. Most members of the order Catenulida, to which the genus *Paracatenula* belongs, predominantly reproduce by a type of asexual fission called paratomy (Ehlers 1985). During paratomy new clonal worms are growing from the posterior end of the animal, thus generating a chain of zooids (the latin word "Catenula" means "small chain"). The zooids subsequently develop into separate individuals and detach from the mother zooid. Sexual reproduction is rarely observed in catenulids (Ehlers 1985). Sterrer & Rieger, however, could not clarify the reproduction strategies of *Paracatenula* in their initial study on this genus (1974).

In this study we investigated the formation of new bacteriocytes and the mechanism of symbiont transmission to the offspring in *P. galateia*. Tracking the origin of different cells using S-phase pulse and pulse-chase labeling with thymidine analogoues we can show that bacteriocytes and all other somatic cell types derive from aposymbiotic neoblast stem cells. Furthermore, we present evidence that asexual fragmentation is a possible and most likely the prevailing mode of reproduction and a straightforward way to transmit symbiont-containing bacteriocytes to the asexual offspring.

Material & Methods

Sampling

Since none of the *Paracatenula* species can be grown in culture, all experiments which required live animals were performed immediately after sampling in the field laboratories of Carrie Bow Cay, Belize (16°48'11 N, 88°04'55 W) and Dahab, Egypt (28°28'13.83"N, 34°30'32.51"E). Sediments were collected in shallow water in the vicinity of Carrie Bow Cay (February 2009 and 2010) or in the "Napoleon Reef" in Dahab (June 2010). The worms were extracted by gently shaking the sand with ample amounts of filtered sea water (FSW) followed by pouring the supernatant through a 63 µm pore-size mesh that retains

the animals. Animals were then immediately washed from the mesh into petri dishes and picked by hand with *Pasteur* pipettes under a dissecting microscope. Then they were either fixed immediately (see below) or kept alive for different experiments for up to 16 days in 2 ml glass vials containing FSW and a small amount of sediment from the sampling area.

Transmission Electron Microscopy (TEM)

Freshly collected animals were immediately relaxed in $MgCl_2$ solution isotonic to SW for 5 min and fixed in 2.5% glutaraldehyde in a 0.1 M sodium cacodylate buffer, post fixed for 2 h with 1% osmium tetroxide in 0.1 M sodium cacodylate buffer (pH 7.3) and, after dehydration, embedded in Low Viscosity Resin (Agar Scientific). Complete ultra-thin cross-sections mounted on formvar-coated slot grids were post stained with 0.5% uranyl acetate for 20 min and lead citrate for 6 min. Sections were viewed on a Zeiss EM-902 and images were recorded with an Olympus SharpEye camera system using the AnalySIS 5.0 software. Single images were merged and further processed with the Adobe Photoshop CS5 software.

Thymidine analogue and nocodazole incubations

For labeling of S-phase cells the thymidine analogues EdU (5-ethynyl-2'-deoxyuridine, Click-it EdU Kit, Invitrogen) or BrdU (5′-Bromo-2′-deoxyuridine, Sigma) were dissolved in FSW to a concentration of 2.5 mM. Animals were incubated for the length of the labeling pulse (always 30 min) in one of these solutions. Each pulse was followed by five washes in FSW and eventually a chase in FSW (ranging from 12 h up to 148 h, $n \geq 5$ for each chase). Incubations (including chase incubations) in FSW containing 1 µg/ml nocodazole (Sigma) for 12 h were used to arrest cells in mitosis. Afterwards the animals were immediately relaxed in $MgCl_2$ solution isotonic to SW for 5 min followed by fixation in 4% formaldehyde in phosphate buffered saline (PBS) for 12 h at 4°C. Fixed animals were stored in PBS for up to three weeks at 4°C or in pure methanol at -20°C for longer periods.

Click-chemistry and immunocytochemistry

Alexa fluor 488-azide fluorescent dye was covalently connected to the EdU label in fixed specimens of *P. galateia* performing the "click reaction" following the protocol of the EdU click-iT Kit (Invitrogen). Stainings with antibodies against BrdU (Becton & Dickinson), serotonin (staining serotonergic nerves) (Sigma) and phosphorylated histone 3 (staining mitotic cells) (Millipore) were performed according to the

immunostaining protocols established by Ladurner et al. (1997, 2000) except for the protease treatment. We used Proteinase K (Sigma) at a final concentration of 0.1 mg/ml for up to 10 min at room temperature. Fluorescencently stained whole animals were mounted on slides and scanned with a confocal laser-scanning microscope (Zeiss LSM 510).

For permanent non-fluorescent labeling we used a horseradish peroxidase (HRP) catalyzed deposition staining approach (see Egger, et al. 2009) except that we used secondary antibodies directly conjugated to HRP (GE Healthcare). Pre-stained whole animals were embedded in LR-white resin (London Resin Company) and 2 µm thin cross sections of the trophosome region were produced and counterstained with 1% methylene blue. The sections were examined under a bright field microscope (Zeiss Axio Imager).

For both EdU-click-iT and antibody stainings negative controls were conducted.

Further analysis and processing of the images was done with the Zeiss LSM Image Browser and the Adobe Photoshop CS5 software. Illustrations were produced with Adobe Illustrator CS5 software.

Rostrum amputation

Freshly collected *P. galateia* and *P.* c.f. *polyhymnia* were reversibly anesthetized with $MgCl_2$ solution isotonic to FSW (see above). Using a clean razor blade the worms (n = 50 for each species) were cut transversally posterior to the brain region (dashed line in Figure 7) or further posterior in the trophosome region. Fragments were kept in glass vials as described above and regeneration was observed and photographically documented in 12 h intervals using a dissecting microscope with a camera device.

Calculation of the symbiont quantity in the trophosome region

When squeezed out of the worm´s body, *P. galateia* symbionts are of a spherical shape and have a diameter of 8.26 ± 0.63 µm. Trophosome region cross sections contain 325 ± 26 symbiont cells (15 sections from 3 specimens). One millimeter of trophosome therefore contains approximately 36000 – 42000 symbionts.

Results

Tissue composition of the trophosome region

We analyzed the tissue composition of the trophosome region using TEM cross sections of *P. galateia*. Three prominent cell and tissue types were identified: (1) a thin epidermis (Figure 1B), (2) neoblasts stem cells (Figure 1B, 1C) and (3) the trophosome consisting of large bacteriocytes (Figure 1B, 1E and S1 showing a dividing symbiont). Rarely other differentiated cell types like e.g. dorso-ventral muscles

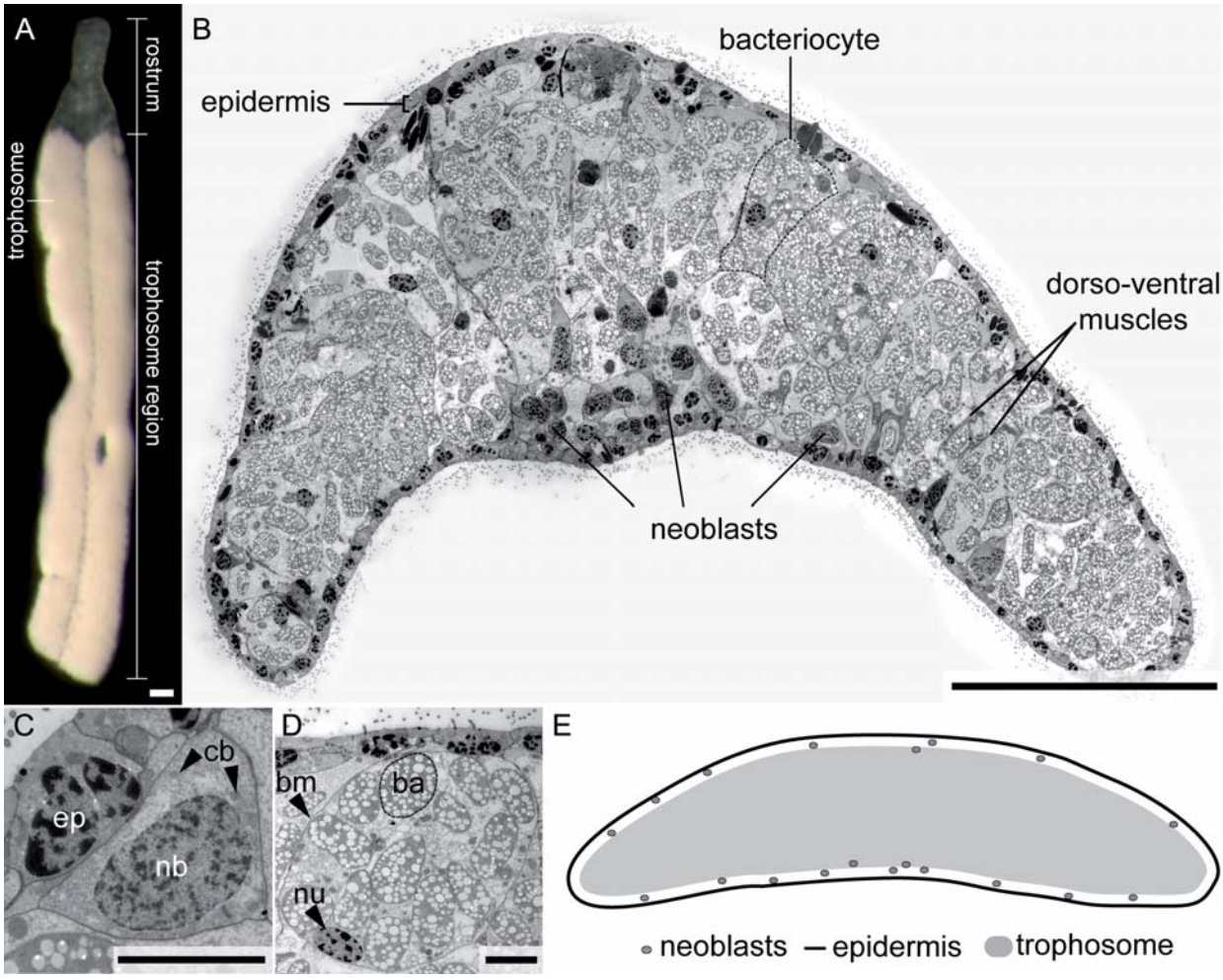

Figure 1: The habitus of *P. galateia* and the ultrastructure of the trophosome region**.** (A) Micrograph of a life *P. galateia* under incident light showing the smooth, silky appearance of trophosome and the transparency of the rostrum. (B) TEM trophosome region cross section. One bacteriocyte (surrounded by a dashed line), the thin epidermis, neoblasts stem cells and dorso-ventral muscles are labeled. (C) TEM section of a neoblast (nb) proximal to the epidermis (ep); the cell possesses highly active chromatin in the nucleus, chromatoid bodies (cb, arrowheads) and a high nucleo-cytoplasmatic ratio. (D) TEM section of a bacteriocyte with the delicate bacteriocyte membrane (bm, arrowhead); it contains the eukaryotic nucleus (nu, arrowhead) and numerous symbiotic bacteria (ba) which in turn contain bright refractive granules. (E) Schematic drawing of the trophosome region cross section reduced to the three cell- and tissue types most important for this study. Scale bars in (A) and (B) 50 µm, in (C) and (D) 5 µm.

were found to permeate the trophosome between the bacteriocytes (Figure 1B). The neoblasts were identified based on their characteristic pattern of heterochromatin, the high nucleo-cytoplasmatic ratio and the presence of chromatoid bodies in the cytoplasm (Figure 1C arrowheads). They were mostly found proximal and adjacent to the epidermis of the dorsal and ventral side. A simplified scheme of a trophosome region cross section is shown in Figure 1E.

Neoblasts are restricted to the trophosome region

We studied which cell types in *P. galateia* are actively passing through the cell cycle by using thymidine analogue pulse-labeling. In whole mounts of specimens pulse-labeled with EdU (or BrdU) (pulse length always 30 min) we detected S-phase cells exclusively in the posterior body region (trophosome region) (n=10). In EdU-labeled specimens in which also serotonergic nerves were stained, the S-phase cells appeared to be evenly distributed posterior to the brain (Figure 2A). On semithin sections through the trophosome region pulse-labeled specimens we found the labeled cells proximal to the epidermis on both

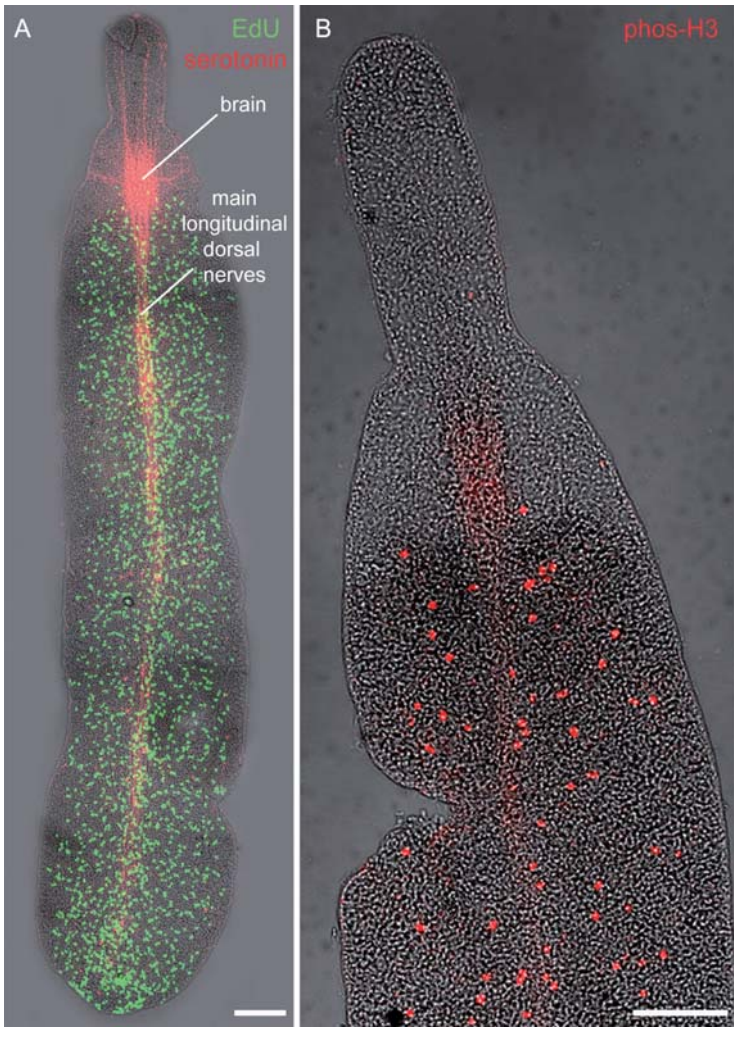

Figure 2: Distribution of S-phase and mitotic cells. (A) Confocal fluorescence projections of 30 min EdU pulse-labeled S-phase cells (green) and serotonergic nerves (red) superimposed with interference-contrast images of *P. galateia* whole mounts. S-phase cells are restricted to the body region posterior to the brain. Longitudinal dorsal nerves extend from the brain continuously until the posterior end of the body. (B) Superimposition of interference-contrast and confocal fluorescence projections of mitotic cells (red) in the anterior body region of a 12 h nocodazole treated *P. galateia*. Mitotic cells are restricted to the body region posterior to the brain. Scale bars in (A) and (B) 100 µm.

the dorsal and ventral side (n=30 from three specimens) (Figure 3A, B). This distribution is congruent with that described above for neoblasts on TEM sections. No label was observed in already differentiated cells types like epidermal- or muscle cells, nor in nuclei of bacteriocytes or in the bacterial symbionts themselves.

The number of mitotic cells, which were detected with an antibody against phosphorylated histone 3, was always low and highly variable between different individuals. We used nocodazole (an inhibitor of microtubule polymerization) to arrest and accumulate cells in mitosis. In whole mounts of nocodazole treated worms mitotic cells were found to be evenly distributed in the trophosome region while they were absent from the rostrum (n=10) (Figure 2B). This mirrors the distribution of the S-phase neoblasts (Figure 2A). On stained sections we always found mitotic cells proximal to the epidermal cells, the same position described for S-phase neoblasts on sections (n=30 from three specimens) (Figure 3C). We did not find any mitotic cells in the epidermis or inside the trophosome. In whole mounts of EdU pulse-labeled

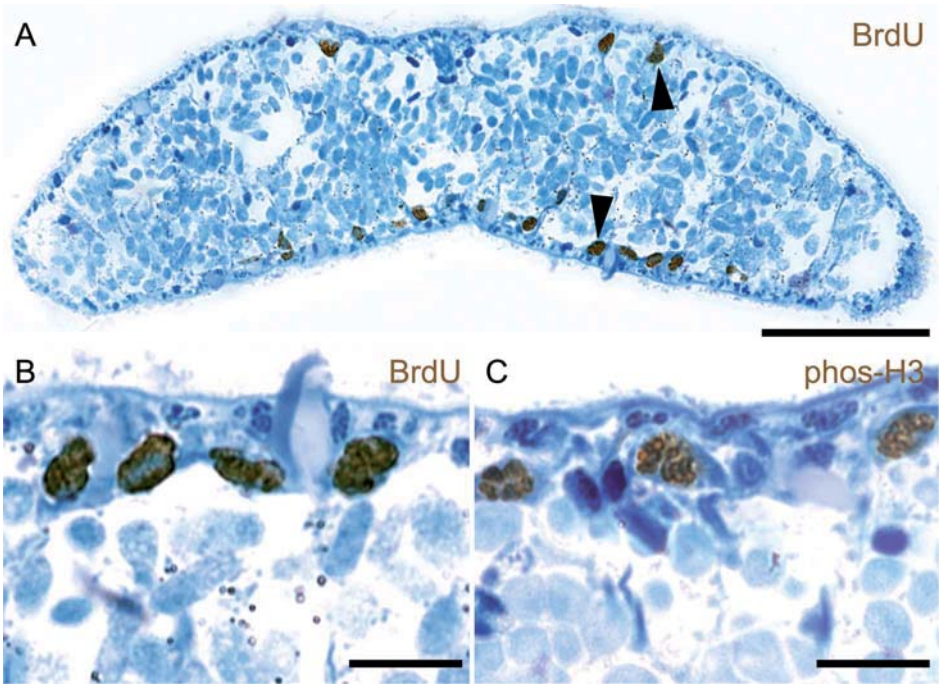

Figure 3: S-phase and mitotic cells are found in subepidermal positions. Bright field micrographs of immuno-stained trophosome region sections. All sections were counterstained with methylene blue (blue). (A) 30 min BrdU pulse-labeled S-phase cells (brown) in subepidermal positions on the dorsal and ventral side of the trophosome region (arrows). (B) Detailed micrograph of BrdU-labeled cells in sub epidermal positions. (C) Detailed micrograph of mitotic cells (brown) in sub epidermal positions of trophosome region cross sections. Mitotic cells were accumulated by 12 h nocodazole treatment. Scale bars in (A) 50 µm, (B) and (C) 10 µm.

worms subjected to a 12 h nocodazole chase the majority of mitosis label was overlapping with the EdU signals (Figure S2) indicating that mitotic cells are derived from previously labeled S-phase cells.

Neoblasts are the source of bacteriocytes and all other cell types

To study cell migration and differentiation into bacteriocytes and other cells types we performed EdU and BrdU pulse-chase incubations. Pulse-labeled worms were subjected to increasing chase length to determine the time when cell migration and differentiation starts. The first cell migrations were detected after 72 h chase when three out of five specimens showed clusters of EdU-labeled cells entering the rostrum (arrowhead in Figure 4A). After 96 h chase all specimens showed labeled cells distributed over the whole length of the rostrum (n=5) which indicates ongoing migration and differentiation. In these whole mounts we identified labeled cells in the epidermis (arrowhead in Figure 4B) and in the brain (double arrowhead in Figure 4B). In semithin sections of specimens with BrdU pulse and 120 h chase (n=60 from three specimens) and 148 h chase (n=40 from two specimens) we observed labeled cells in the epidermis, in subepidermal positions and in the trophosome (Figure 5A and B). In the trophosome nuclei of bacteriocytes were labeled (dotted line in Figure 5B) as well as those of cells between bacteriocytes which probably belong to dorsoventral-muscles, nerves or mesenchymal cells (Figure 5C). No label was detected in the symbionts.

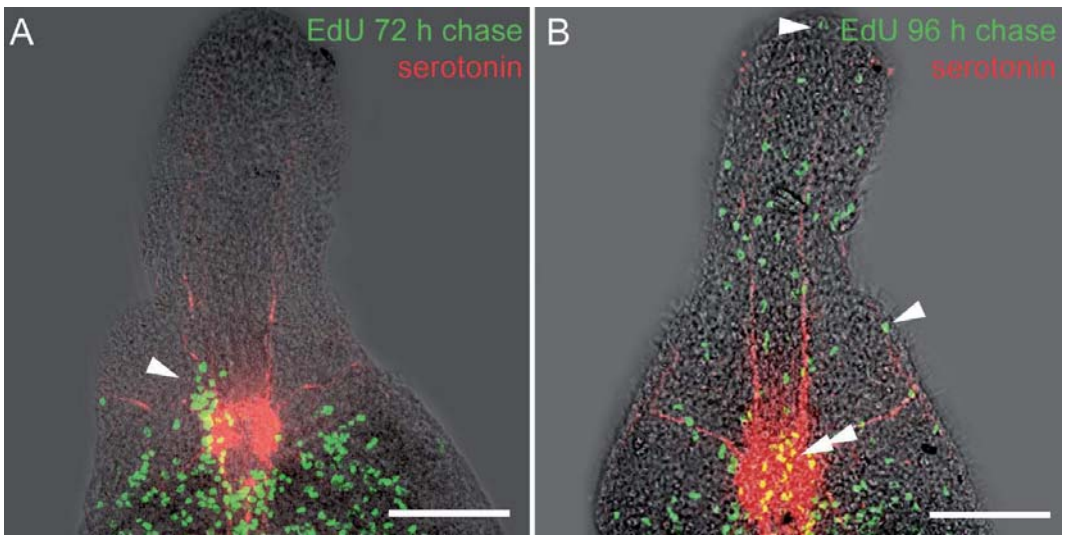

Figure 4: Pulse-chase labeled cells migrate into the rostrum. Confocal projections of EdU pulse-chase-labeled cells (green) and serotonergic nerves (red) superimposed with interference-contrast images of *P. galateia* whole mounts. Only the anterior parts of the worms are shown. (A) Worms with EdU-pulse and 72 h-chase showing labeled cells in the moment of entering the rostrum (arrowhead). (B) After 96 h chase the labeled cells are distributed over the whole length of the rostrum. Label can be detected in the epidermis and in nerve cells of the brain (yellow double label, arrows). Scale bars in (A) and (B) 100 µm.

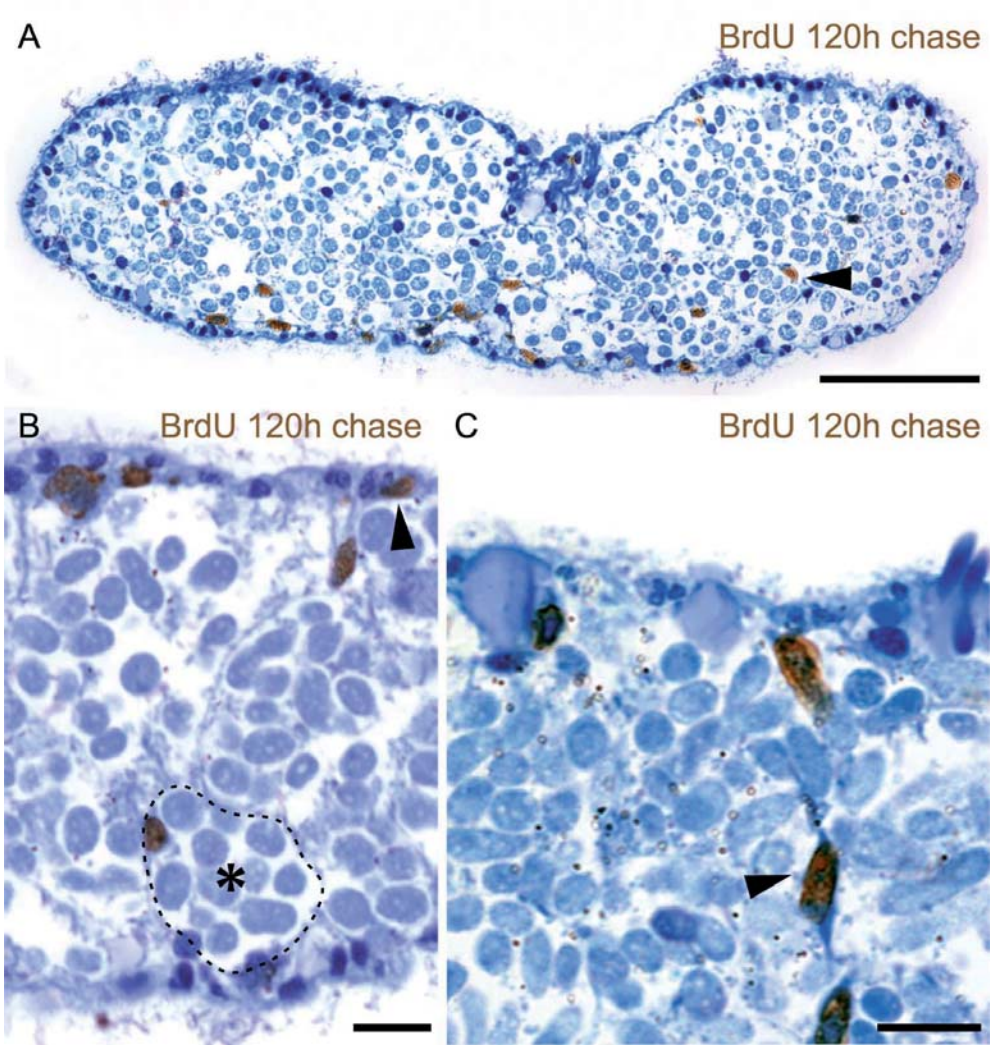

Figure 5: Pulse-chase labeled S-phase cells in trophosome region cross sections. Bright field micrographs of 30 min BrdU pulse 120 h chase immuno-labeled *P. galateia* trophosome region cross sections. All sections were counterstained with methylene blue (blue). (A) BrdU-labeled cells (brown) were distributed in all regions of the section including the trophosome (arrowhead). (B) Detailed micrograph of BrdU-labeled bacteriocyte (asterisk, surrounded by a dashed line) and labeled epidermal cells (arrowhead). (C) Other BrdU-labeled cell types between the bacteriocytes. Scale bars in (A) 50 µm, (B) and (C) 10 µm.

P. galateia can reproduce by paratomy and is capable to regenerate from small fragments

Fission planes (FPs) are constrictions perpendicular to the anterior-posterior axis correlated to asexual fission in flatworms. Frequently FPs were observed in freshly collected *P. galateia* and other species of the genus (arrowheads in Figure 6A and S3). They were found most frequently in long specimens (≥3 mm) and were confined to the trophosome region. Specimens possessing FPs and stained with anti-serotonin antiserum had the main longitudinal serotonergic nerves interrupted and well separated into nerve fractions anterior and posterior to the FP (arrowhead in Figure 6B). A prominent commissure in the

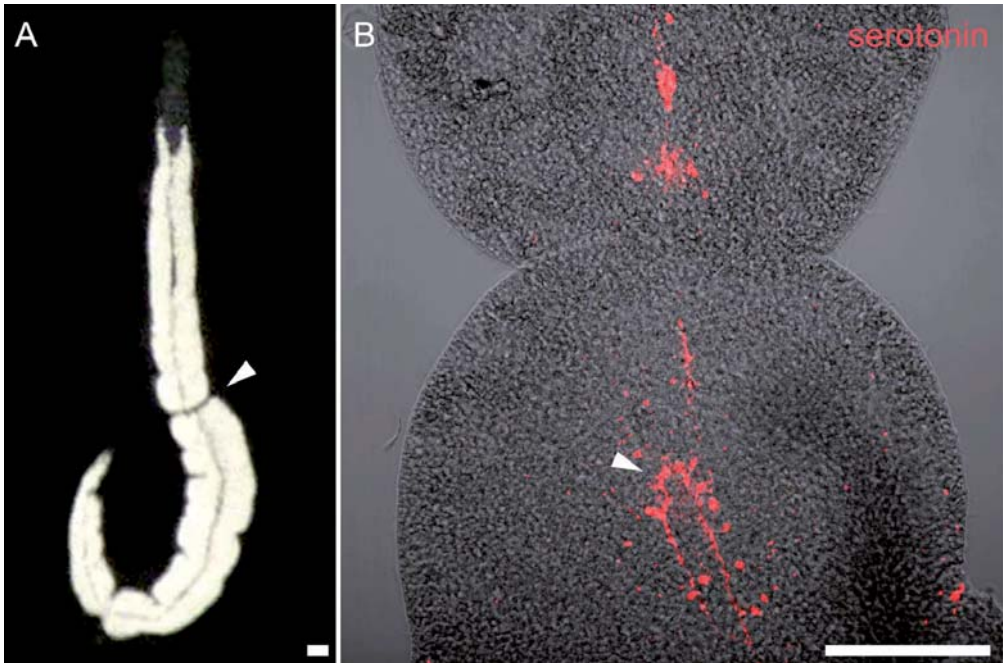

Figure 6: Rearranging of nerves in a fission plane area. (A) *In vivo* squeeze preparation of *P. galateia* under incident light. The animal possesses a fission plane (arrowhead) in the trophosome region. (B) Confocal fluorescent projection of a serotonin staining (red) superimposed with an interference-contrast image of a fission plane area. The longitudinal nerves (red) are separated into an anterior and posterior fraction. A commissure (arrowhead) in the posterior fraction indicates the reorganization of the nerves. Scale bars in (A) and (B) 100 µm.

posterior nerve fraction shows the reorganization of the central nervous system before fragment separation (arrow in Figure 6B). This indicates that the FPs are not due to mechanical stress but are signs of paratomy (transverse fission during which differentiation of new organs occurs prior to separation from the parental animal; see introduction). Under culture conditions, however, FPs did not progress and no detachment of fragments could be observed within the limited observation period of 16 days.

To investigate the fate of headless *P. galateia* trophosome region fragments which are most probably produced in the natural environment we tested their ability to regenerate a rostrum. Intact worms were decapitated posterior to the brain (dashed line in Figure 7A) and subsequently four stages in the rostrum regeneration process could be observed. Decapitation resulted in a trophosome region fragment of varying length (≥1 mm) with a wound at its anterior end (stage 0) (Figure 7B). Within the following two days the wound surface was minimized and closed before a symbiont-free anterior region appeared (stage 1) (Figure 7C). Then the outgrowth of the tip of the rostrum followed (stage 2) (Figure 7D) leading to the formation of the typical shoulder-shaped transition between rostrum and trophosome region (stage 3) (Figure 7E). The time to complete rostrum regeneration varied between 12 and 16 days (n=10 for each

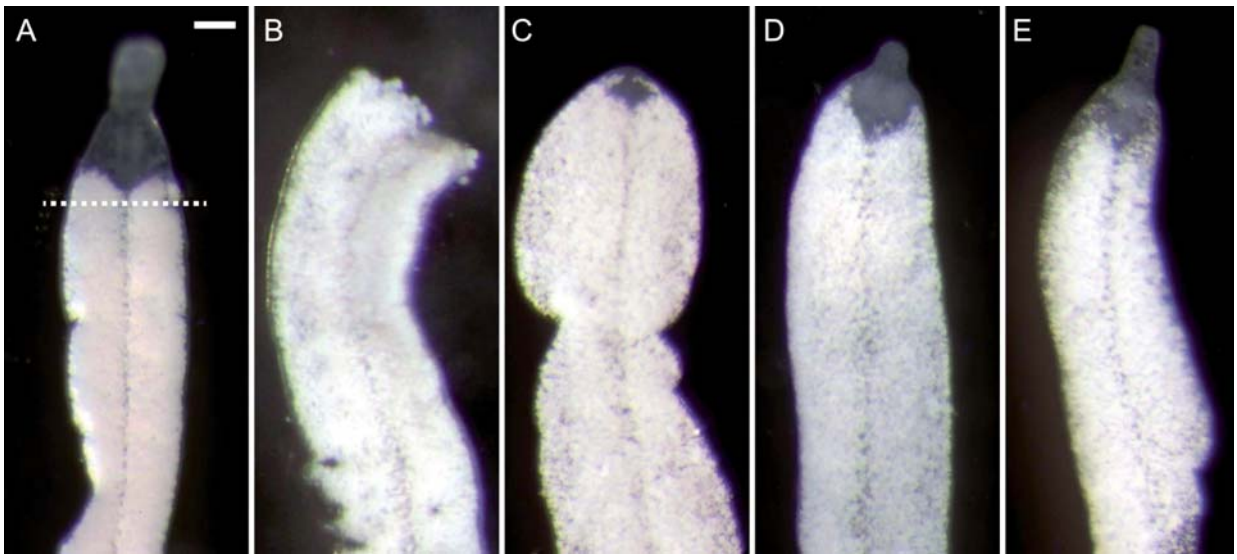

Figure 7: Trophosome region fragments can regenerate the rostrum. Squeeze preparations of live *P. galateia* under incident light. (A) Intact *P. galateia* prior to rostrum amputation. The dashed line indicates the level of cutting. (B) *P. galateia* right after rostrum amputation (stage 0). Small shreds of injured bacteriocytes leak out the cutting wound. (C) Regeneration stage 1: the cutting-wound is closed and a symbiont free area on the anterior tip indicates ongoing rostrum regeneration. (D) Regeneration stage 2: a small outgrowing rostrum is visible on the anterior tip. (E) Regeneration stage 3: the new rostrum has its final characteristic shape and has almost grown to its full size. Scale bar in A 100 µm, all images are at the same scale.

stage). In addition, rostrum regeneration after decapitation was studied in another species, *P.* c.f. *polyhymnia* with comparable results (Figure S4) except that rostrum regeneration was completed within only 48-72 h. We also cut *P. galateia* with long trophosome regions twice or three times. These fragments (length ≥0.5 mm) were also capable of rostrum regeneration, regardless if they were cut on only one or on both sides (Figure S5) (n=20).

In the rostrum fragments resulting from the decapitation the wound also closed within the first days. Although all of these fragments retained a small piece of trophosome after cutting (Figure 7A, dashed line indicates the cutting plane) a regrowth was not seen (n≥40), probably due to the small number of neoblasts remaining in this piece (compare Figure 2A). All rostrum fragments died within the 16 days of observation.

In order to find out how many symbionts may be transmitted to the asexual offspring during paratomy or inside accidently produced fragments we assessed their quantity per millimeter trophosome region based on the mean dimensions of their cells and their number on cross sections. Our estimates suggest that each millimeter contains 36000 – 42000 symbionts.

Discussion

The bacterial symbionts are integrated into the ancient cell-renewal machinery of the flatworm host

Platyhelminthes are exceptional model systems in stem cell and regenerative biology (Baguna et al. 1989, Palmberg 1990, Ladurner et al. 2000, Newmark & Sanchez Alvarado 2000, Wagner et al. 2011). Their simple neoblast stem cell system in which all differentiated cells constantly derive from undetermined stem cells provides a unique opportunity to investigate the development of specific cell types (Peter et al. 2004). In this study we identified neoblast stem cells as the source of bacteriocytes and other somatic cell types in *Paracatenula*. With a combined approach using ultrastructure, incubations with thymidine analogues and immunostainings we provide several lines of evidence for this finding: (1) the detection of cells with typical flatworm-neoblast features (see introduction) in *P. galateia;* (2) the restriction of neoblasts (S-phase and mitotic cells) to the posterior body region which is comparable with that found in many other flatworm species (Palmberg 1990, Ladurner et al. 2000, Newmark & Sanchez Alvarado 2000); (3) migration of pulse-chase labeled S-phase cells and their differentiation into various cell types known from many other flatworm models (Ladurner et al. 2000, Newmark & Sanchez Alvarado 2000, Wagner et al. 2011). All our results strongly support our hypothesis that adult *P. galateia* continuously derive bacteriocytes and all other cell types exclusively from aposymbiotic neoblasts.

In other animal phyla *de novo* bacteriocyte formation through infection of aposymbiotic cells was found to be restricted to early developmental stages, while later in development no infection of aposymbiotic cells could be observed. In adults of siboglinid tubeworms (*Lamellibrachia luymesi* and *Riftia pachyptila*) unipotent bacteriocyte stem cells proliferate and produce new bacteriocytes. During their division the symbionts are transferred to both daughter cells, one of which retains the status of an unipotent stem cell and the other one terminally differentiates and loses the capability to divide (Pflugfelder et al. 2009). This agrees with the general mode of tissue renewal of annelids which is covered by proliferating multi- and unipotent tissue specific stem cells (Myohara et al. 1999, and reviewed in Yoshida-Noro & Tochinai 2010). In insect hosts various, slightly different strategies of bacteriocyte infection and maintenance were described. In the aphids *Acyrtosiphon pisum* and *Megoura viciae* as well as the cockroach *Periplaneta americana de novo* bacteriocyte formation from aposymbiotic cells is restricted to early developmental stages (Douglas & Dixon, 1987, Lambiase et al. 1997, Braendle et al. 2003, Miura et al. 2003). In adults the bacteriocytes

of *A. pisum* themselves divide while those of *M. viciae* do not divide anymore and are progressively reduced due to repeated transfer of symbionts to the offspring. Post-reproductive *M. viciae* completely lose their symbionts. In *P. americana* mitotic bacteriocytes were found (Brooks & Richards, 1955). All these variations follow the common cell renewal strategies in insects: Totipotency is restricted to germ cells and all other stem cell types get progressively more and more restricted from pluripotent to tissue specific multipotent or unipotent stem cells during insect development (reviewed in Corley & Lavine, 2006). To summarize, in both insects and tubeworms aposymbiotic cells are infected with symbionts only in early developmental stages and bacteriocytes are formed *de novo* only once for every individual. In adults either all bacteriocytes or tissue specific bacteriocyte stem cells divide and thus contribute to growth and maintenance of the symbiotic tissue (Figure 8A). In contrast adult *P. galateia* continuously generate new bacteriocytes from aposymbiotic stem cells in order to maintain the trophosome and increase its size (Figure 8B). All these hosts belonging to three animal phyla have integrated bacteriocyte production into their conventional cell renewal systems. In general cell renewal strategies of an animal taxon should be indicative for bacteriocyte formation and maintenance in their respective symbiotic tissues. Besides the Platyhelminthes also Acoela, which probably are deuterostomes (Philippe et al. 2011), have a pluripotent (maybe totipotent) stem cell system with comparable features (Gschwentner et al. 2001, De Mulder et al. 2009, Egger et al. 2009). Therefore it would be interesting to study the formation process of the symbiont housing cells in the acoels *Symsagittifera roscoffensis* (formerly called *Convoluta roscoffensis*) Graff 1891 (Doonan & Dooday 1982, Douglas 1985) or *Convolutriloba longifissura* Bartolomaeus & Balzer 1997 (Akesson et al. 2001).

In this study we could not clarify how symbionts get inside newly formed pre-bacteriocytes (cells which are determined to become a bacteriocyte) of *P. galateia*. There are several possibilities: (1) bacteriocytes release symbionts to the extracellular space which then get phagocytized by pre-bacteriocytes, (2) bacteriocytes transiently fuse with the pre-bacteriocytes building a syncytium and transfer symbionts or (3) bacteriocytes pinch off symbiont containing vesicles which subsequently fuse with pre-bacteriocytes. Inside the bacteriocytes each symbiont is encapsulated by a host derived membrane (Ott et al. 1982). This should simplify symbiont transfer across the host´s cell membranes.

We never detected BrdU or EdU label inside the symbionts although they apparently proliferate in the

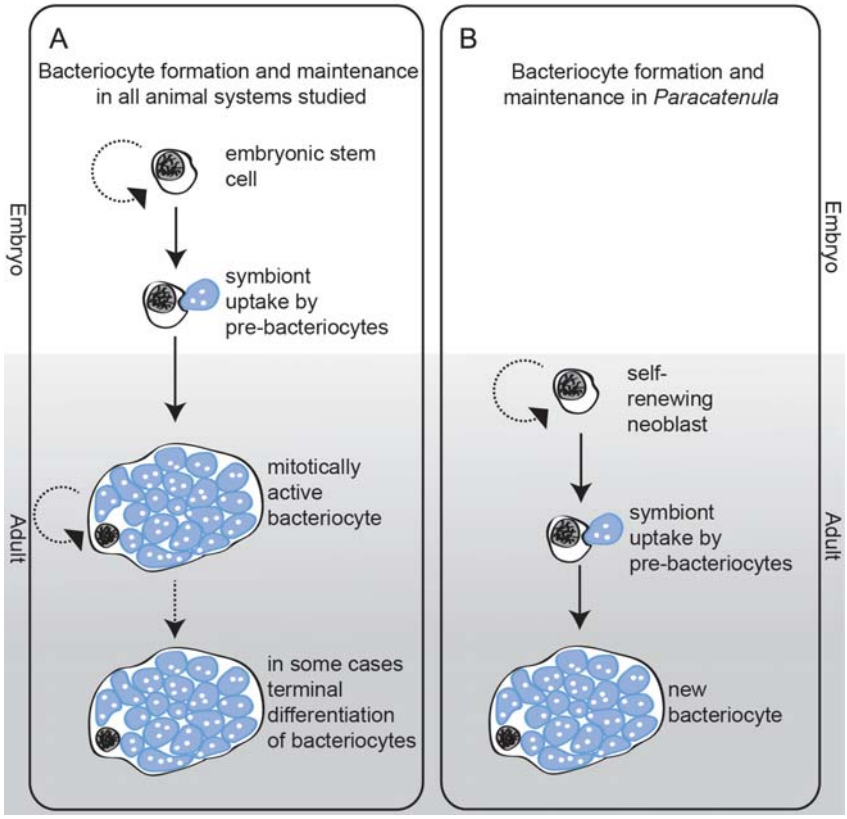

Figure 8: Different strategies of bacteriocyte production. Schematic drawing of the developmental origin and maintenance of bacteriocytes in different animal systems. (A) Bacteriocyte production in all animal systems systems studied. In early developmental stages bacteriocytes are formed *de novo* by infection of aposymbiotic cells with symbionts. Postembryonic no *de novo* formation happens anymore. In some systems all bacteriocytes are capable to divide and in other systems unipotent bacteriocyte stem cells proliferate, self-renew and produce terminal differentiating bacteriocytes which do not divide anymore. (B) Bacteriocyte production in *Paracatenula*. Since early developmental stages of the worms were never found this part is missing. In adults proliferating self-renewing neoblasts constantly produce new pre-bacteriocytes which get infected by the symbionts and thus become bacteriocytes. The bacteriocytes itself cannot divide.

bacteriocytes (Figure S1). This is in accordance with other studies of animal-associated microbes where also no BrdU incorporation into the bacterial DNA could be found (Kloiber et al. 2009, Pflugfelder et al. 2009). Fuhrman & Azam (1982) found evidence that some autotrophic bacteria do not incorporate thymidine analogues. Since the alphaproteobacterial *Paracatenula*-symbionts are chemoautotrophic this might be a possible explanation (Gruber-Vodicka et al. 2011).

P. galateia reproduces asexually and regenerates

Many catenulids like e.g. members of the genera *Catenula* and *Stenostomum* reproduce predominantly by paratomy (Moraczewski 1977, Ehlers 1985, Palmberg 1990). In the same genera also high regenerative

powers were observed. Our results indicate that *P. galateia*, *P.* cf. *polyhymnia* and probably all other species of the genus (own unpublished observation) are capable of paratomy and can regenerate the rostrum. Natural disturbances such as wave action and bioturbation by macrofauna may cause accidental fragmentation in these fragile animals (Sterrer & Rieger 1974, Dirks et al. 2011). The frequent finding of fragments or battered individuals in our extractions suggests the importance of regeneration in nature. In amputation experiments we prove the regenerative potential of different *Paracatenula* species to regrow the rostrum even in small body fragments. Under good growth conditions repeated paratomy and fragmentation/regeneration can lead to an exponential growth of the population which may explain the extremely patchy distribution of the worms (own unpublished observation). A drawing of the hypothetical reproduction of *Paracatenula* by paratomy is presented in Figure 9. Since sexual reproduction has never been observed in *Paracatenula* species asexual fragmentation is most likely the predominant maybe the only mode of reproduction (Sterrer & Rieger 1974, Dirks et al. 2011).

Bacteriocyte transmission: straightforward transmission of intracellular symbionts

The diversity of strategies regarding symbiont transmission through host generations was recently reviewed by Bright & Bulgheresi (2010). Horizontal and vertical transmission are the two fundamentally different modes described (see introduction). Trophosome region fragments of *P. galateia* always contain many

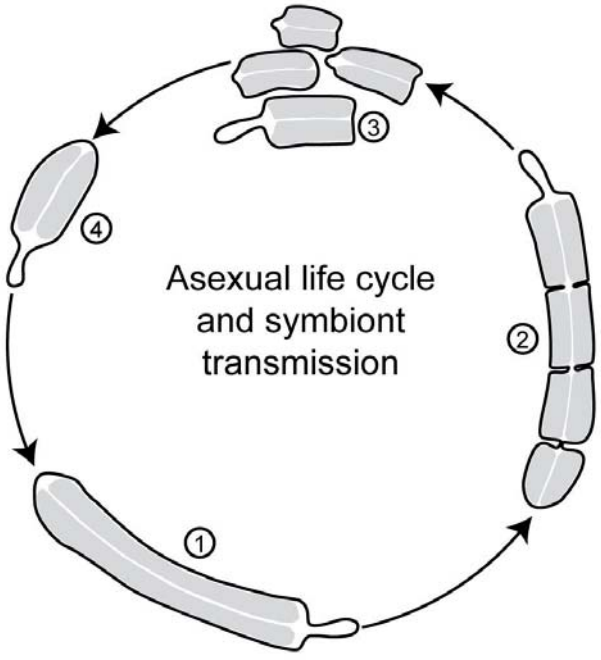

Figure 9: Scheme of the hypothetical asexual reproduction by paratomy**.** Drawing of *P. galateia* reproducing by paratomy (grey = trophosome). Paratomy starts when the worm (the trophosome region in particular) extends a certain length (1). Progressively constrictions appear perpendicular to the anterior-posterior axis and zooids develop (2) which finally detach from the mother zooid (3). Then each of the zooids grows up to a complete worm (4) whereas the trophosome region continuously growths until it extends a certain size and the process of paratomy starts again.

hundreds to thousands of bacteriocytes. As a consequence the worm transmits high numbers of symbionts (36000-42000 per mm trophosome region) to the asexual offspring. This "bacteriocyte transmission" is the safest and simplest solution for symbiont transmission bearing no risk for host and symbiont to lose contact. The permanent liaison resulting from this may explain the tight codiversification reported for hosts and symbionts in the genus *Paracatenula*. In most other systems intracellular symbionts have to undergo a complex journey during vertical transmission. They have to translocate from the parental symbiont housing tissue into either germ cells or the developing progeny. In both cases the symbionts experience environmental changes especially if they have to pass an extracellular space and take the risk to loose contact with the host (reviewed in Bright & Bulgheresi 2010). Although asexual reproduction by fragmentation or budding is common in many lower metazoans like e.g. sponges, cnidarians, acoels, flatworms and some annelids, the transmission of whole symbiont housing cells has been described only for *Hydra viridis* and *C. longifissura*. During budding of *H. viridis* the algal and bacterial symbionts are transmitted directly through dividing gastrodermal cells to the developing bud. In contrast sexually produced offspring has to take up both kinds of symbionts from the environment which shows this intracellular association is not unlimited in time (Thorington & Margulis 1979). For this reason no codiversification can be observed between this hydroid and the symbionts. The acoel *C. longifissura* also transmits its intracellular algal symbionts during asexual fission, however, a detailed investigation is pending (Akesson et al. 2001).

The strict vertical transmission of a limited number of symbionts to the offspring bears the risk of accumulating slightly deleterious mutations through genetic drift (Moran 1996, Peek et al. 1998, Rispe & Moran 2000, Mira & Moran 2002). This problem was termed "transmission bottleneck". When reproducing by paratomy or accidental fragmentation *P. galateia* minimizes such a "bottleneck effect" due to the large numbers of symbiont containing bacteriocytes inside of the fragments. For comparison Buchner observed that fewer than 200 bacteria are transmitted to each offspring of the louse *Pediculus* (1965). In different aphid-species the number of symbiont cells transmitted ranged from 800 to 8000 (Mira & Moran 2002).

The symbionts' tight integration into *P. galateia*'s machinery of cell renewal and reproduction opens up new avenues for symbiosis research. Prospective investigation will reveal if the asexual transmission of complete bacteriocytes avoiding host-symbiont decoupling and the vertical transmission of large numbers of symbionts reducing the "bottleneck effect" are the mechanisms which guarantee continuity and thereby

the tight codiversification between *Paracatenula*-species and symbionts. Moreover, this system offers a starting point to bridge a major gap in the understanding of bacteriocyte formation and the advanced evolution of an intracellular symbiotic bacterium becoming an organelle of the eukaryotic cell.

Acknowledgments

We gratefully acknowledge Wolfgang Sterrer and Renate Ott for supporting the fieldwork, Monika Bright for many improving suggestions on the manuscript and Michael Stachowitsch for language editing the manuscript. We thank the Core facility for Cell Imaging and Ultrastructural research and the department of microbial ecology at the University of Vienna for providing facilities.

Funding

This work was supported by the Austrian Science Fund (FWF) project P20394 (HRG, UD, JAO), and is contribution (XXXX) from the Carrie Bow Cay Laboratory, Caribbean Coral Reef Ecosystem Program, NMNH, Washington, D.C.. Furthermore this work was partly funded by the graduate school initiative "Symbiotic Interactions" at the University of Vienna and a Sparkling Science grant from the Austrian Ministry of Science and Research and a Leverhulme grant (F/07 134/DA).

Abbreviations

BrdU, 5′-Bromo-2′-deoxyuridine; EdU, 5-ethynyl-2'-deoxyuridine; FP, fission plane (constrictions perpendicular to the anterior-posterior axis correlated to asexual fission in flatworms); FSW, filtered sea water; HRP, horseradish peroxidase; TEM, transmission electron microscopy; PBS, phosphate buffered saline; $MgCl_2$, magnesium chloride; MY, million years

Supplementary figures

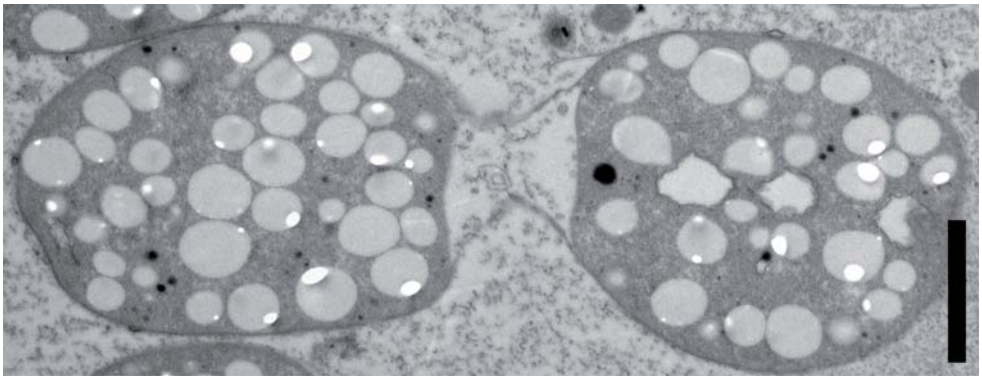

Figure S1: The symbionts proliferate inside the bacteriocytes. Detailed TEM-micrograph of a dividing bacterial symbiont. In the bacterial cells sulfur storage granules (white inclusions) are visible.

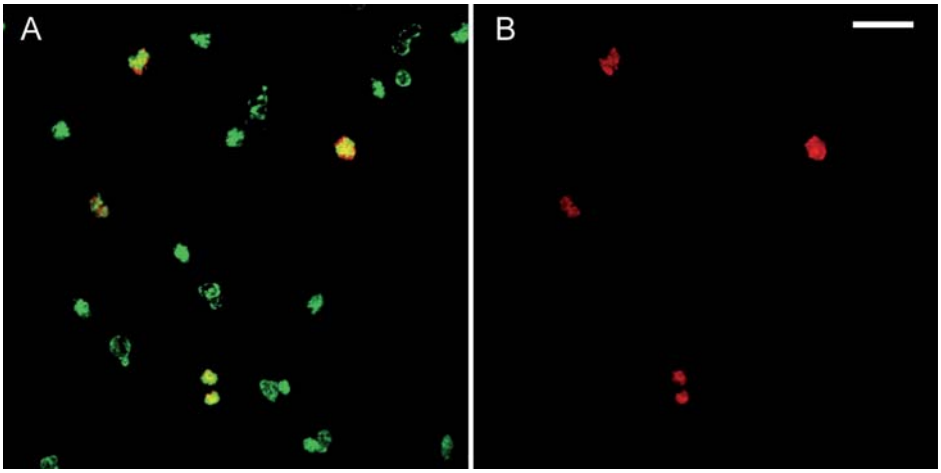

Figure S2: The pulse-labeled cells enter mitosis after a certain chase time. Confocal fluorescence projections of EdU labeled S-phase cells (green) and mitotic cells (red) in the *P. galateia* trophosome region. The worm was subjected to a 30 min EdU pulse followed by a 12 h nocodazole chase. (A) Double label of EdU and mitosis. All mitotic cells do also show EdU S-phase label (yellow). (B) Same image section showing only the red mitosis label. Scale bar in (A) and (B) 10 µm.

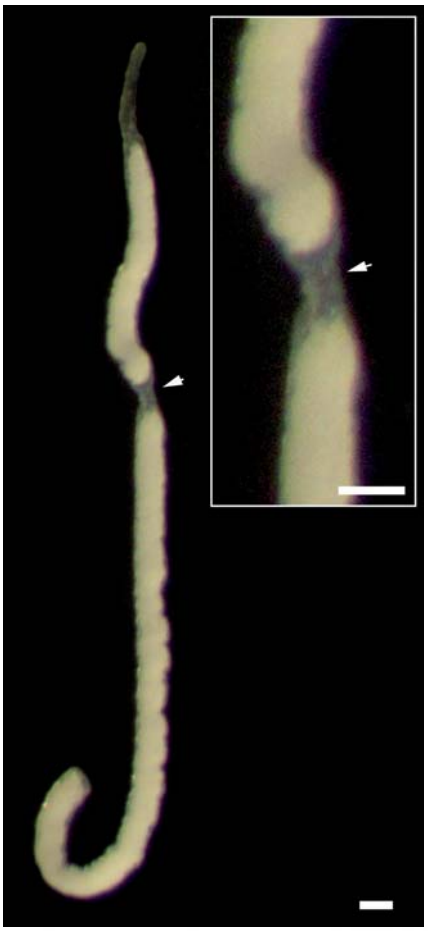

Figure S3: Fission plane in the trophosome region of *P.* cf *polyhymnia***.** *In vivo* squeeze preparation of *P.* cf *polyhymnia* under incident light. (A) The animal possesses a fission plane (arrowhead) in the trophosome region. The inset shows a higher magnification of the fission plane. Scale bar 50 µm in both.

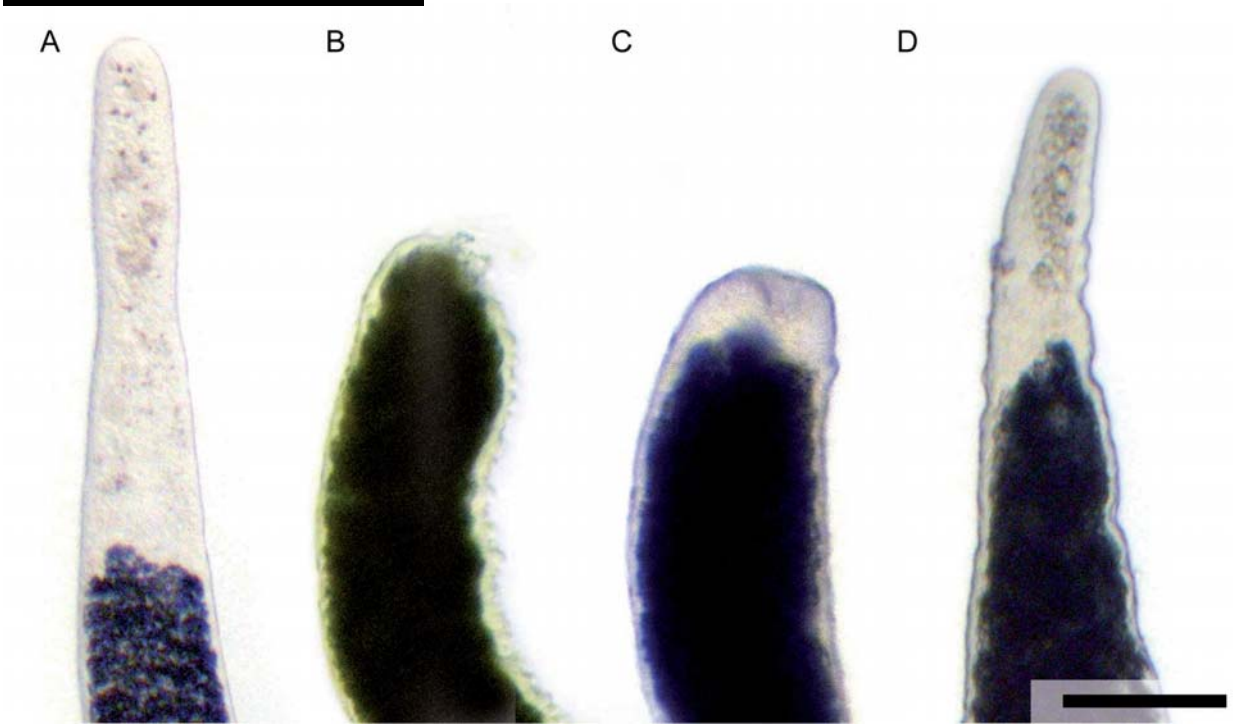

Figure S4: Regeneration after rostrum amputation of *P.* cf *polyhymnia***.** Micrographs of regenerating *P.* cf *polyhymnia.* Live worms before (A) and directly after rostrum amputation (B). Rostrum regeneration 24 h (C) and 48 h (D) after amputation. Scale bar in (A-D) 50 µm.

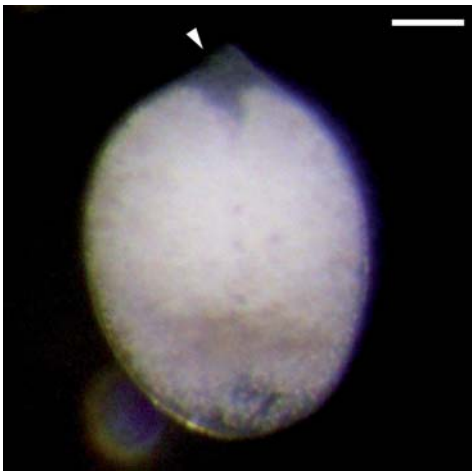

Figure S5: Regeneration of tiny trophosome region fragments of *P. galateia.* Micrograph of a 0.5 mm long regenerating trophosome region fragment 14 days after rostrum amputation. A small rostrum is visible on one side (arrowhead). Scale bar 100 µm.

References

Akesson B, Gschwentner R, Hendelberg J, Ladurner P, Muller J, Rieger R (2001). Fission in *Convolutriloba longifissura*: asexual reproduction in acoelous turbellarians revisited. Acta Zoologica 82: 231-239.

Auladell C, Garcia-Valero J, Baguñà J (1993). Ultrastructural localization of RNA in the chromatoid bodies of undifferentiated cells (neoblasts) in planarians by the RNase–gold complex technique. *Journal of Morphology* 216: 319-326.

Baguna J, Salo E, Auladell C (1989). Regeneration and pattern formation in planarians. III. Evidence that neoblasts are totipotent stem cells and the source of blastema cells. *Development* 107: 77-86.

Bianciotto V, Bandi C, Minerdi D, Sironi M, Tichy H, Bonfante P (1996). An obligately endosymbiotic mycorrhizal fungus itself harbors obligately intracellular bacteria. *Appl Environ Microbiol* 62: 3005-3010.

Bode A, Salvenmoser W, Nimeth K, Mahlknecht M, Adamski Z, Rieger RM et al. (2006). Immunogold-labeled S-phase neoblasts, total neoblast number, their distribution, and evidence for arrested neoblasts in *Macrostomum lignano* (Platyhelminthes, Rhabditophora). *Cell Tissue Res* **325:** 577-587.

Boucher DH, James S, Keeler KH (1982). The Ecology of Mutualism. *Annual Review of Ecology and Systematics* 13: 315-347.

Braendle C, Miura T, Bickel R, Shingleton AW, Kambhampati S, Stern DL (2003). Developmental origin and evolution of bacteriocytes in the aphid-Buchnera symbiosis. *PLoS Biol* 1: 70-76.

Bright M, Bulgheresi S (2010). A complex journey: transmission of microbial symbionts. *Nat Rev Micro* 8: 218-230.

Brooks MA, Richards AG (1955). Intracellular Symbiosis in Cockroaches: II. Mitotic Division of Mycetocytes. *Science* 122: 242.

Buchner P (1965). Endosymbiosis of Animals with Plant Microorganisms. Interscience Publishers. New York.

Cavanaugh CM, Gardiner SL, Jones ML, Jannasch HW, Waterbury JB (1981). Prokaryotic Cells in the Hydrothermal Vent Tube Worm *Riftia pachyptila* Jones: Possible Chemoautotrophic Symbionts. *Science* 213: 340-342.

Corley LS, Lavine MD (2006). A review of insect stem cell types. *Seminars in Cell & Developmental Biology* 17: 510-517.

De Mulder K, Kuales G, Pfister D, Willems M, Egger B, Salvenmoser W et al.(2009). Characterization of the stem cell system of the acoel *Isodiametra pulchra*. *BMC Developmental Biology* 9: 69.

Denlinger DL, Ma W-C (1975). Maternal nutritive secretions as possible channels for vertical transmission of microorganisms in insects: The Tsetse fly example. *Ann N Y Acad Sci* 266: 162-165.

Dirks U, Gruber-Vodicka H, Leisch N, Sterrer W, Ott J (2011). A new species of symbiotic flatworms, *Paracatenula galateia* sp. nov. (Platyhelminthes: Catenulida: Retronectidae) from Belize (Central America). *Marine Biology Research*: in press.

Doonan SA, Dooday GW (1982). Ecological studies of symbiosis in *Convoluta roscoffensis*. *Marine Ecology* 8: 69-73.

Douglas AE (1985). Growth and Reproduction of *Convoluta Roscoffensis* Containing Different Naturally Occurring Algal Symbionts. *Journal of the Marine Biological Association of the United Kingdom* 65: 871-879.

Douglas AE, Dixon AFG (1987). The mycetocyte symbiosis of aphids: Variation with age and morph in virginoparae of *Megoura viciae* and *Acyrthosiphon pisum*. *Journal of Insect Physiology* 33: 109-113.

Egger B, Gschwentner R, Rieger R (2007). Free-living flatworms under the knife: past and present. *Development Genes and Evolution* 217: 89-104.

Egger B, Gschwentner R, Hess M, Nimeth K, Adamski Z, Willems M et al.(2009a). The caudal regeneration blastema is an accumulation of rapidly proliferating stem cells in the flatworm *Macrostomum lignano*. *BMC Developmental Biology* 9: 41.

Egger B, Steinke D, Tarui H, De Mulder K, Arendt D, Borgonie G et al.(2009b). To be or not to be a flatworm: the acoel controversy. *PloS one* 4: e5502.

Ehlers U (1985). "Das Phylogenetische System der Plathelminthes.". Stuttgart: Gustav Fisher.

Fernandéz-Taboada E, Moritz S, Zeuschner D, Stehling M, Schöler HR, Saló E et al.(2010). Smed-SmB, a member of the LSm protein superfamily, is essential for chromatoid body organization and planarian stem cell proliferation. *Development* 137: 1055-1065.

Fuhrman JA, Azam F (1982). Thymidine incorporation as a measure of heterotrophic bacterioplankton production in marine surface waters: Evaluation and field results. *Marine Biology* 66: 109-120.

Gruber-Vodicka HR, Dirks U, Leisch N, Baranyi C, Stoecker K, Bulgheresi S et al.(in press). *Paracatenula*, an ancient symbiosis between thiotrophic *Alphaproteobacteria* and catenulid flatworms. *PNAS*: in press.

Gschwentner R, Ladurner P, Nimeth K, Rieger R (2001). Stem cells in a basal bilaterian: S-phase and mitotic cells in *Convolutriloba longifissura* (Acoela, Platyhelminthes). *Cell Tissue Res* 304: 401-408.

Harmer TL, Rotjan RD, Nussbaumer AD, Bright M, Ng AW, DeChaine EG et al.(2008). Free-Living Tube Worm Endosymbionts Found at Deep-Sea Vents. Appl Environ Microbiol 74: 3895-3898.

Hori I (1982). An ultrastructural study of the chromatoid body in planarian regenerative cells. *Journal of Electron Microscopy* 31: 63-72.

Horn M (2008). Chlamydiae as Symbionts in Eukaryotes. *Annual Review of Microbiology* 62: 113-131.

Keyser HH, Bohlool B, Hu TS, Weber DF (1982). Fast-Growing Rhizobia Isolated from Root Nodules of Soybean. *Science* 215: 1631-1632.

Kloiber U, Pflugfelder B, Rinke C, Bright M (2009). Cell proliferation and growth in *Zoothamnium niveum* (Oligohymenophora, Peritrichida) - thiotrophic bacteria symbiosis. *Symbiosis* 47: 43-50.

Kotaja N, Sassone-Corsi P (2007). The chromatoid body: a germ-cell-specific RNA-processing centre. *Nat Rev Mol Cell Biol* 8: 85-90.

Ladurner P, Mair GR, Reiter D, Salvenmoser W, Rieger RM (1997). Serotonergic Nervous System of Two Macrostomid Species: Recent or Ancient Divergence? *Invertebr Biol* 116: 178-191.

Ladurner P, Rieger R, Baguna J (2000). Spatial distribution and differentiation potential of stem cells in hatchlings and adults in the marine platyhelminth *Macrostomum* sp.: a bromodeoxyuridine analysis. *Dev Biol* 226: 231-241.

Lambiase S, Grigolo A, Laudani U, Sacchi L, Baccetti B (1997). Pattern of bacteriocyte formation in *Periplaneta americana* (L.) (Blattaria: Blattidae). *International Journal of Insect Morphology and Embryology* 26: 9-19.

Mira A, Moran NA (2002). Estimating Population Size and Transmission Bottlenecks in Maternally Transmitted Endosymbiotic Bacteria. *Microbial Ecology* 44: 137-143.

Miura T, Braendle C, Shingleton A, Sisk G, Kambhampati S, Stern DL (2003). A comparison of parthenogenetic and sexual embryogenesis of the pea aphid *Acyrthosiphon pisum* (Hemiptera: Aphidoidea). *J Exp Zool B Mol Dev Evol* 295: 59-81.

Moraczewski J (1977). Asexual reproduction and regeneration of Catenula (Turbellaria, Archoophora). *Zoomorph* 88: 65 - 80.

Moran NA (1996). Accelerated evolution and Muller's rachet in endosymbiotic bacteria. *Proceedings of the National Academy of Sciences* 93: 2873-2878.

Myohara M, Yoshida-Noro C, Kobari F, Tochinai S (1999). Fragmenting oligochaete *Enchytraeus japonensis*: A new material for regeneration study. *Development, Growth & Differentiation* 41: 549-555.

Newmark PA, Sanchez Alvarado A (2000). Bromodeoxyuridine specifically labels the regenerative stem cells of planarians. *Dev Biol* 220: 142-153.

Nussbaumer AD, Fisher CR, Bright M (2006). Horizontal endosymbiont transmission in hydrothermal vent tubeworms. *Nature* 441: 345-348.

Ott JA, Rieger G, Rieger R, Enderes F (1982). New mouthless interstitial worms from the sulfide system: Symbiosis with Prokaryotes. PSZN I: *Mar Ecol* 3: 313-333.

Palmberg I (1990). Stem cells in microturbellarians - an autoradiographic and immunocytochemical study. *Protoplasma* 158: 109 - 120.

Peek AS, Vrijenhoek RC, Gaut BS (1998). Accelerated evolutionary rate in sulfur-oxidizing endosymbiotic bacteria associated with the mode of symbiont transmission. *Molecular Biology and Evolution* 15: 1514-1523.

Peter R, Gschwentner R, Schürmann W, Rieger R, Ladurner P (2004). The significance of stem cells in free-living flatworms: one common source for all cells in the adult. *Journal of Applied Biomedicine* 2: 21-35.

Pflugfelder B, Cary SC, Bright M (2009). Dynamics of cell proliferation and apoptosis reflect different life strategies in hydrothermal vent and cold seep vestimentiferan tubeworms. *Cell Tissue Res* 337: 149-165.

Philippe H, Brinkmann H, Copley RR, Moroz LL, Nakano H, Poustka AJ et al. (2011). Acoelomorph flatworms are deuterostomes related to *Xenoturbella*. *Nature* 470: 255-258.

Reddien PW, Sanchez Alvarado A (2004). Fundamentals of planarian regeneration. *Annu Rev Cell Dev Biol* 20: 725-757.

Rieger RM (1981). Morphology of the Turbellaria at the ultrastructural level. *Hydrobiologia* 81: 213-229.

Rispe C, Moran NA (2000). Accumulation of Deleterious Mutations in Endosymbionts: Muller's Ratchet with Two Levels of Selection. *The American Naturalist* 156: 425-441.

Sachs JL, Essenberg CJ, Turcotte MM (2011). New paradigms for the evolution of beneficial infections. *Trends in Ecology & Evolution* 26: 202-209.

Sterrer W, Rieger R (1974). Retronectidae - a new cosmopolitan marine family of Catenulida (Turbellaria). In: Riser N, Morse M (eds). *Biology of the Turbellaria*. McGraw-Hill: New York. pp 63-92.

Thorington G, Margulis L (1979). Transmission of symbionts through the sexual cycle of *Hydra viridis*. I. Observations on living organisms. *Transactions of the American Microscopical Society* 98: 401-413.

van der Land J, Norrevang A (1975). The systematic position of *Larnellibrachia* (Annelida, Vestimentifera). *Zool Syst Evolutionsforsch Sonderheft* 1: 86-101.

Wagner DE, Wang IE, Reddien PW (2011). Clonogenic Neoblasts Are Pluripotent Adult Stem Cells That Underlie Planarian Regeneration. Science 332: 811-816.

Yoshida-Noro C, Tochinai S (2010). Stem cell system in asexual and sexual reproduction of *Enchytraeus japonensis* (Oligochaeta, Annelida). *Development, Growth & Differentiation* 52: 43-55.

CHAPTER 4

Proliferation pattern during rostrum regeneration of the symbiotic flatworm *Paracatenula galateia* – a pulse-chase-pulse analysis

Authors: Ulrich Dirks, Harald R. Gruber-Vodicka, Bernhard Egger and Jörg A. Ott

Keywords: morphallaxis, epimorphosis, bacteriocyte, paratomy, blastema, neoblast

Publication status: Manuscript ready for submission to Cell and Tissue Research.

Detailed description of UD´s contribution: UD designed major parts of the study, performed all experiments and most of the fieldwork, analyzed the data and wrote the manuscript.

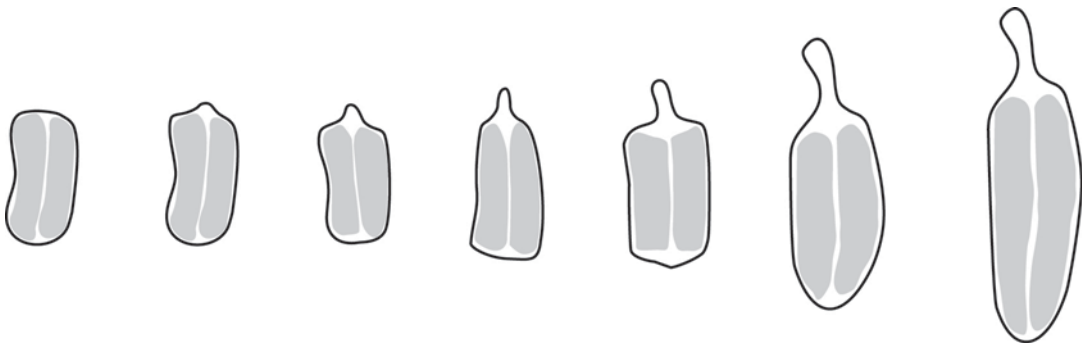

Abstract

Their remarkable regeneration capacities and pluripotent stem cells - termed neoblasts - have brought Platyhelminthes into the focus of research. While selected groups (e.g. tricalds) are among the best studied invertebrates, our data provides new insights into regenerative processes in the most basal group of the Platyhelminthes, the Catenulida. We decapitated specimens of the mouth- and gutless free-living catenulid *Paracatenula galateia* which harbors intracellular bacterial symbionts in its posterior body region, the trophosome region, counting for up to 50% of the volume. Afterwards we analyzed the behavior of the amputated fragments and the anterior and posterior regeneration. Using an EdU-chase-BrdU thymidine analogue double-labeling approach combined with immunohistochemistry, we show that neoblasts are the main drivers of the regeneration processes. During anterior regeneration (rostrum regeneration) EdU pulse-chase-labeled cells aggregate inside the regenerating rostrum while BrdU pulse-labeling before fixation indicates clusters of S-phase neoblasts at the same position. In parallel serotonergic nerves reorganize and the brain regenerates. In completely regenerated animals the original condition with S-phase neoblasts restricted to the body region posterior to the brain is restored. In contrast the posterior regeneration or growth of the trophosome region in anterior fragments was not observed. The data we present here provide interesting insights into the cellular processes underlying regeneration of the emerging catenulid bacteria symbiosis model *P. galateia* and suggests that the neoblast stem cell systems is indeed a plesiomorphic feature of basal platyhelminthes.

Introduction

From the human point of view the capability to regenerate lost body parts is a fascinating phenomenon. Among many invertebrates, however, regeneration is a common feature which is often also connected with asexual reproduction. For more than 100 years Platyhelminthes have been famous model systems to study the principles underlying the regeneration of lost body parts. Owing to their extraordinary regeneration capacity, some flatworms have been called ‘‘almost immortal under the edge of the knife’’ (Dalyell 1814). Today it is known that there is a huge variety among the regenerative powers of different flatworm taxa and researchers have tried to categorize and find a pattern explaining why some species can regenerate lost body parts and others cannot (reviewed in Egger et al. 2007). Comparative data suggest a link between asexual reproduction and regenerative capabilities as these processes co-occur and show strong parallels in their progression pattern (Moraczewski 1977). Therefore it has been suggested to use the term “pregeneration” alternatively for those modes of asexual reproduction where differentiation of tissues occurs before the fragmentation (e.g. paratomy or budding). An essential feature for the regeneration processes shared by all Platyhelminthes is their remarkable system of pluripotent stem cells – the neoblast (Bode et al. 2006 and literture therein, Newmark and Sanchez Alvarado 2000). In all studied taxa neoblasts are the only proliferating cells in adult flatworms and hence they are the sole source of differentiated cell types during the continued cell-turnover, but also during regeneration of lost body parts.

In previous studies we investigated the way mouth and gutless catenulid flatworms of the genus *Paracatenula* reproduce asexually by paratomy and thus vertically transmit their intracellular bacterial symbionts to the asexual offspring. We described first details about *Paracatenula*’s neoblast system and the capability of these worms to regenerate the rostrum after head amputation. Since indications for sexual reproduction in this genus are rare and a proof is still missing it was speculated that *Paracatenula*-species predominantly use paratomy and a fragmentation-regeneration strategy to reproduce asexually and thus maintain a permanent stock of to their obligate intracellular symbionts (Dirks et al. in review). Gruber et al. (2011) showed a tight codiversification between the different hosts in the genus and their specific symbionts which further suggests strict vertical symbiont transmission.

In this present study we characterize morphological details and the role of neoblast stem cells during rostrum regeneration of *P. galateia* Dirks et al. 2011. Using an EdU and BrdU-pulse-chase-pulse approach

we selectively labeled and traced stem cells previous to experimental decapitation and in the following regeneration process. This study is the first detailed investigation into cell proliferation patterns in regenerative processes of an obligate symbiotic Platyhelminth (sensu strictu).

Material & Methods

Sampling

Since none of the *Paracatenula* species can be grown in culture, all experiments which required live animals were performed immediately after sampling in the field laboratories of Carrie Bow Cay, Belize (16°48'11 N, 88°04'55 W) and Dahab, Egypt (28°28'13.83"N, 34°30'32.51"E). Sediments were collected in shallow water in the vicinity of Carrie Bow Cay (February 2009 and 2010) or in the "Napoleon Reef" in Dahab (June 2010). The worms were extracted by gently shaking the sand with ample amounts of filtered sea water (FSW) followed by pouring the supernatant through a 63 µm pore-size mesh that retains the animals. Animals were then immediately washed from the mesh into petri dishes and picked by hand with *Pasteur* pipettes under a dissecting microscope. Then they were either fixed (see below) or kept alive for different experiments for up to 16 days in 2 ml glass vials containing FSW and a small amount of sediment from the sampling area.

Decapitation and pulse-chase-pulse incubations

For labeling of S-phase cells the thymidine analogues EdU (5-ethynyl-2'-deoxyuridine, Click-it EdU Kit, Invitrogen) or BrdU (5′-Bromo-2′-deoxyuridine, Sigma) were dissolved in FSW to a concentration of 2.5 mM. Animals were incubated for 30 min in EdU containing FSW followed by five washes in FSW. After that they were reversibly anesthetized with $MgCl_2$ solution isotonic to FSW and a razor blade was used to decapitate the animals transversally posterior to the brain region (Figure 1B). The fragments were carefully put into the prepared glas culture tubes and kept there for different chase times at room temperature (~25°C) on a dimmed place. In 24 h intervals animals were observed for up to 384 h in total. At different stages of regeneration (chase times of 48 h, 120 h, 172 h, 264 h and 384 h; n=5 for each chase time) animals were subjected to a 30 min BrdU-pulse. Afterwards the worms were washed five times in FSW and briefly anesthetized with $MgCl_2$ and fixed in 4% formaldehyde in phosphate buffered saline

(PBS) for 12h at 4°C. Fixed animals were stored in pure methanol at -20°C for longer periods.

Click-chemistry and immunocytochemistry

Alexa fluor 488-azide fluorescent dye was covalently connected to the EdU-label in fixed specimens of *P. galateia* performing the "click reaction" following the protocol of the EdU click-iT Kit (Invitrogen). Stainings with antibodies against BrdU (B&D) and serotonin (staining serotonergic nerves) (Sigma) were performed according to the immunostaining protocol established by Ladurner et al. (1997, 2000) except for the protease treatment. We used Proteinase K (Sigma) at a final concentration of 0.1 mg/ml for up to 10 min at room temperature. For both EdU-click-iT and all antibody stainings negative controls were conducted. Fluorescently stained whole animals were mounted on slides and scanned with a confocal laser-scanning microscope (Zeiss LSM 510).

Further analysis and processing of the images was done with the Zeiss LSM Image Browser and the Adobe Photoshop CS5 software. Illustrations were produced with Adobe Illustrator CS5 software.

Light microscopy

In the field laboratory live animals were carefully squeezed under a coverslip on a microscope slide and observed with phase contrast microscope (Zeiss, Germany). Live animals were transferred back to their culture dishes after observation, so the same specimen could be observed at different time intervals.

Results

In intact *P. galateia* subjected to a 30 min EdU-pulse (no chase) S-phase neoblasts are detected exclusively in the body region posterior to the brain. The rostrum is always devoid of S-phase neoblasts (Figure 1A) (compare also Dirks et al. 2011). In this study freshly collected specimens were subjected to a 30 min EdU-pulse before the rostrum was transversally amputated (cutting plane is shown in Figure 1B). The fate of neoblasts which had incorporated EdU during their S-phase was traced later. Additionally a 30 min pulse with BrdU was applied after different chase/regeneration times shortly before the experiment was stopped and the animals were fixed. This BrdU-pulse after different time intervals was used to detect proliferating cells during later stages of the regeneration process. Afterwards EdU, BrdU as well as serotonergic nerves were fluorescently labeled and visualized using a confocal laser scanning microscope.

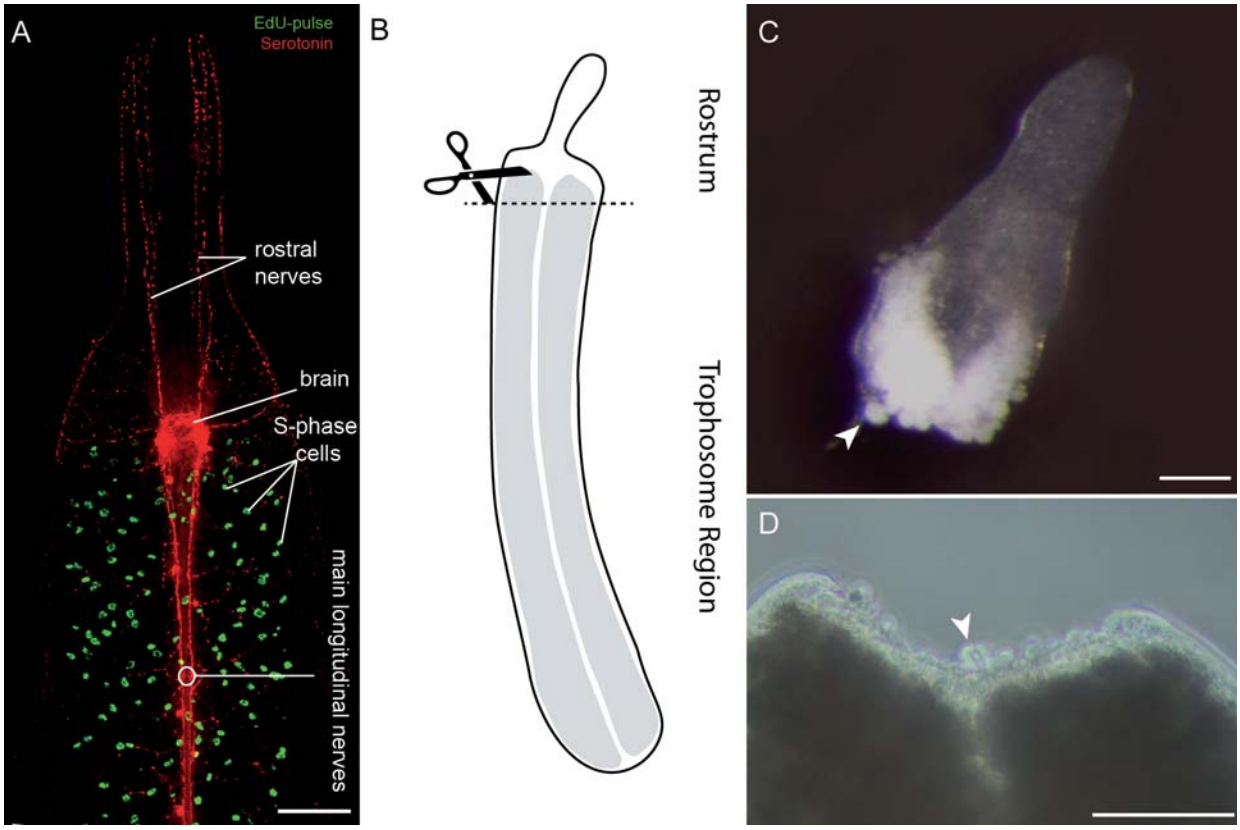

Figure 1: (A) Fluorescently stained EdU-pulse-labeled *P. galateia* specimen. EdU-labeled S-phase cells and antibody-stained serotonergic nerves are seen in red. Structures like brain, S-phase cells and nerves, which are of special importance for this study, are labeled within the picture. (B) Schematic drawing of a *P. galateia*. The scissors and the dashed line indicate the position of amputation. (C) Rostrum fragment under incident light directly after amputation. Note the single bacteriocytes leaking out of the open wound (arrowhead). (D) Interference contrast (IC) image of a trophosome region fragment directly after amputation. The arrowhead indicates spherical cells leaking out of the wound. Scale bars 100 µm in A,C and D.

The amputation resulted in an anterior fragment (rostrum fragment) (Figure 1C) and a posterior fragment (trophosome fragment) (Figure 1D). Immediately after cutting we often found single bacteriocytes emerging from the cutting wound of both fragments (arrowheads in Figure 1C and D). Within the following 16 days we documented the processes of rostrum regeneration of the anteriorly regenerating trophosome fragments. A trophosome regrowth of the posteriorly regenerating rostrum fragments was never observed within the limited observation period. Here we first describe a number of steps in the rostrum regeneration process including proliferation and migration patterns of neoblasts, blastema formation and the behavior of the worms.

Rostrum regeneration of trophosome region fragments

While intact *P. galateia* show directed forward and backward movement, the freshly decapitated trophosome region fragments temporarily rolled up. After a few seconds they slowly relaxed and started an idly forward movement. Sometimes peristaltic contractions of the fragments were observed. Similar behavior has been observed from intact worms as a sign of stress e.g. after magnesium chloride treatment or freshwater shock. After about 6-12 h the decapitated fragments became immobile ($n \geq 30$). The cutting wound was initially reduced in size likely by the constriction of circular muscles and closed within 48 h by the flattening of surrounding epidermis cells (Figure 2A). In this stage the bacteriocytes were distributed up to the anterior tip of the worms. EdU and also BrdU label was evenly distributed in the fragments and almost 60% of the cells showed both labels (Figure 2B,C,E) (n=5). This indicates that either the S-phase of the EdU-pulse-labeled neoblasts was still progressing after the 48 h chase, or that some EdU-labeled cells had already completed their cell cycle and reached a second S-phase in which they were labeled with BrdU. Serotonin staining of the 48 h anterior regenerates showed longitudinal nerves ending blindly in the wound area and a network of fine subepidermal nerves (Figure 2D,E) (n=5).

Five days (120 h) after the amputation the trophosome region fragments slowly started to move in a forward direction. The bacteriocytes did not reach the anterior end and rostrum regeneration had started (Figure 2F). A strong aggregation of EdU pulse-chase labeled cells was found in the symbiont free regenerating area and in addition labeled cells were found to be almost evenly distributed in the remainder of the trophosome region, albeit with a far lower density than at the beginning of the experiment (Figure 2G) (n=3). In the area of regeneration we also detected a massive cluster of BrdU-labeled S-phase cells indicating proliferation within this tissue (Figure 2H) (n=3). These proliferating S-phase cells are most probably neoblasts forming a regeneration blastema (accumulation of undifferentiated cells at the wound site covered by an epithelium). A further clustering of BrdU-labeled cells was found along the major longitudinal nerve cords while the rest of the body showed a lower density and an even distribution (Figure 2H,J). The major longitudinal nerves were still found to end blindly but did not reach the anterior end due to the epigrowth of the blastema (Figure 2I). After 120 h chase EdU/BrdU double-labeled cells were more difficult to detect since the EdU signal intensity was weakened probably due to dilution of the label in recent mitoses. Nevertheless many cells, especially those aggregated in the blastema (site of

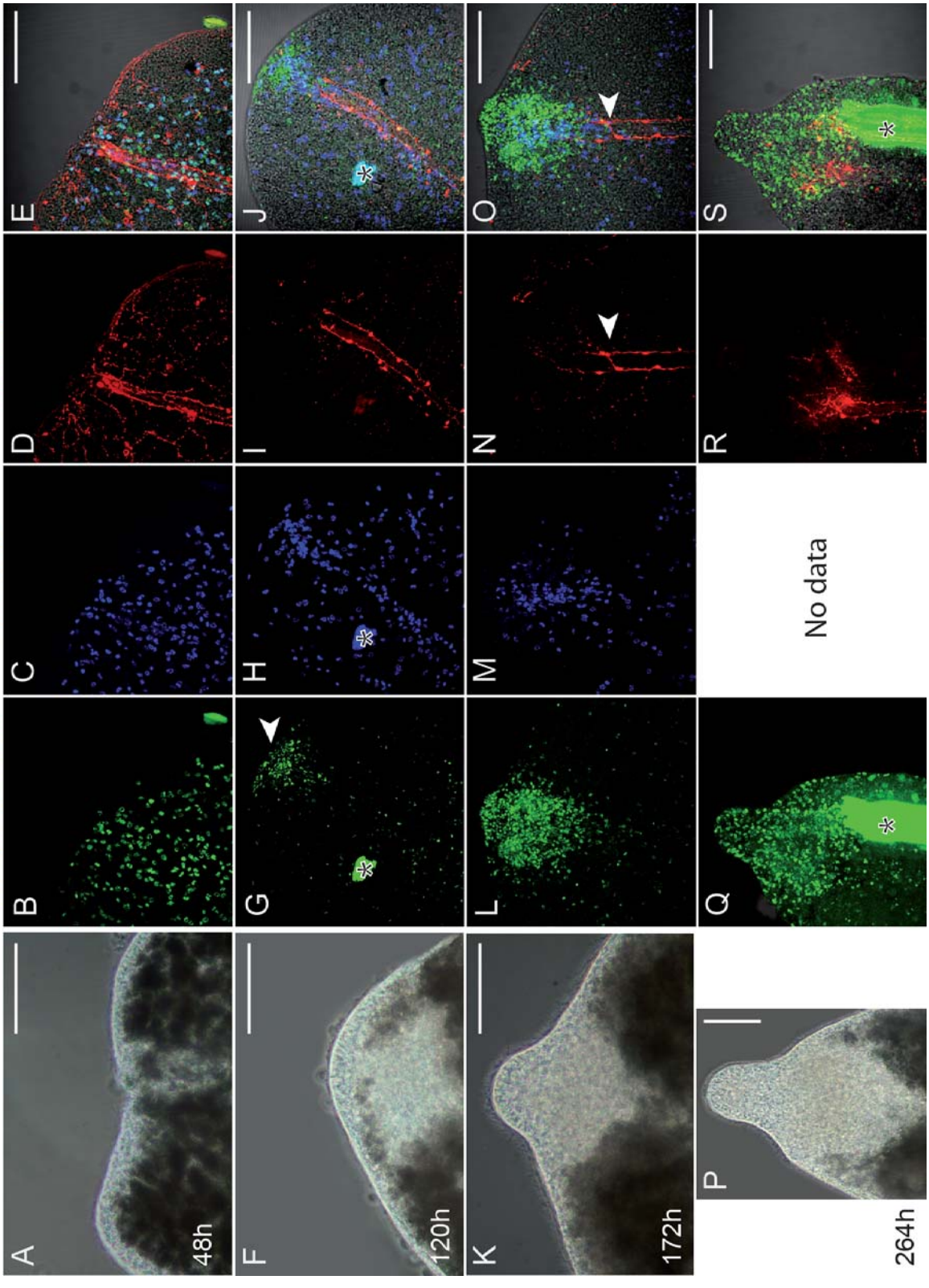

Figure 2: Interference contrast (IC) and fluorescence micrographs of different stages of rostrum regeneration of *P. galateia*. Each horizontal column of images belongs to the same stage. The time of regeneration (48 h, 120 h, 172 h and 264 h) is indicated in the IC-images on the far left. On top of each vertical column the type of image, incubation or staining is shown. As it is indicated by the color of the font, EdU label is seen in green, BrdU label in blue and serotonin in red. The rightmost column shows overlays of the three fluorescence images on the left plus an IC image. Arrowheads point on important events in the regeneration process to which also is referred in the results. Asterisks (*) indicate image artifacts. The scale bars for all images are 100 µm.

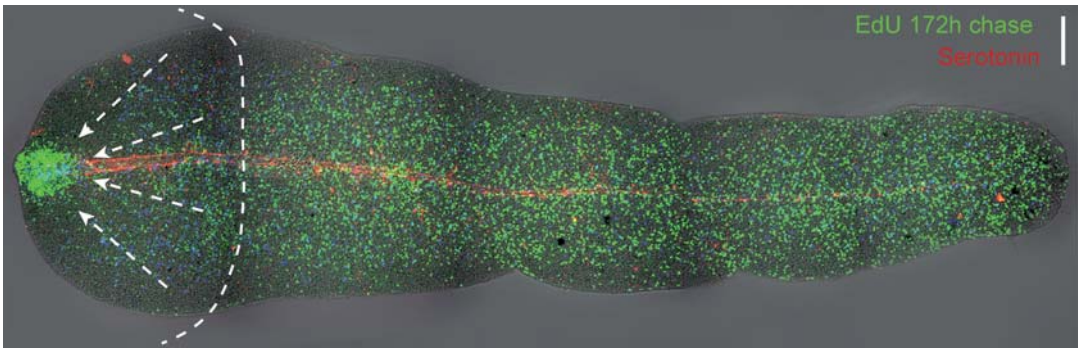

Figure 3: *P. galateia* trophosome region fragment 172 h after decapitation. EdU pulse-chase-labeled cells (green) are strongly aggregated in the regenerating rostrum (left). The labeled cells in the anterior region of the worm have been recruited to the wound area to contribute to the regeneration process (arrows and the dashed lines roughly indicate the sphere of influence). In the posterior region the EdU labeled cells show an even distribution. A staining of serotonergic nerves is seen in red. Scale bar 100 µm.

rostrum regeneration) showed the light blue staining indicating EdU/BrdU double-label (Figure 2J)(n=3).

The next step in the regeneration process around 172 h after decapitation was the outgrowth of the tip of the rostrum (Figure 2K). By that time all worms had restored their normal locomotion. The regenerating rostrum was completely free of symbionts and EdU-labeled cells were found to be considerably more aggregated in the blastema (Figure 2L) (n=5). In the anteriormost 500-600 µm of the trophosome worms showed a clearly lowered density of EdU-labeled cells which reflects the recruitment of the EdU pulse-chase labeled cells into the site of regeneration (Figure 3). In the same worms also the density of BrdU-labeled cells in the blastema was increased compared to the remainder of the worm's body which showed an even distribution of BrdU-labeled S-phase cells (Figure 2M)(n=5). Double-labeled cells are found in the center of the blastema (Figure 2O). By that time the nerves show first clear indications of reorganization. A prominent commissure is visible at the anterior end of the major longitudinal nerves and tiny nerve branches extend further into the anterior direction (arrowheads, Figure 2N,O), possibly representing the rostral nerves found in the rostrum of intact *P. galateia* (compare Figure 1A).

After around 264 h of regeneration the rostrum had regained the typical shoulder-shaped transition between rostrum and trophosome region (Figure 2P). A large proportion of the cells constituting the newly formed rostrum showed EdU labeling (Figure 2Q) (n=3). The staining of the BrdU-labeled S-phase cells did not work in any of the specimens we observed[1]. On the boundary of trophosome and rostrum the major

1 The missing results were traced to a faulty batch of BrdU.

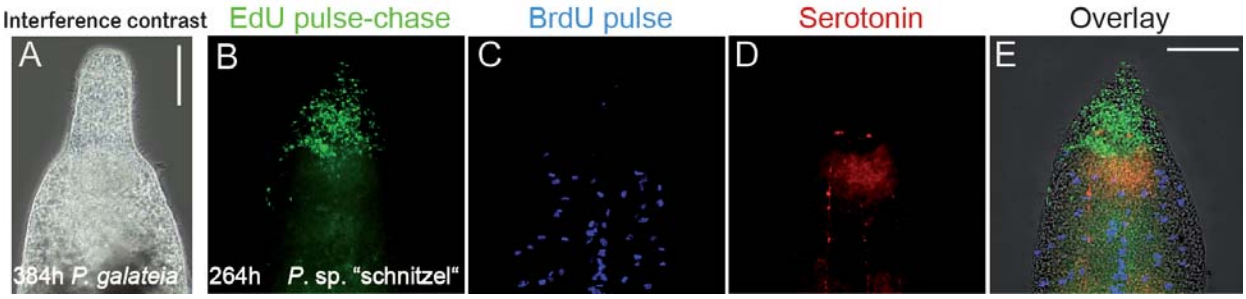

Figure 4: (A) IC image of *P. galateia* after 384 h of rostrum regeneration; (B-E) Fluorescent images of *P.* sp."schnitzel" after 264h of rostrum regeneration. (B) EdU-pulse-264 h-chase seen in green; (C) BrdU pulse-staining; (D) staining of serotonergic nerves in red; (E) an overlay of all pictures. The scale bar for A and B-E is 100µm.

longitudinal nerves ended up in a commissure with an intense accumulation of serotonergic nerves which indicates an advanced state of brain regeneration (Figure 2R,S) (n=3).

In *P. galateia* rostrum regeneration appeared to be complete after about 384h (Figure 4A). No difference in the behavior of these regenerates compared to the non-amputated control animal could be observed (n=4). For technical reasons the contribution and fate of neoblasts in the final step of rostrum regeneration could not be analyzed in *P. galateia*[2]. Alternatively we studied this final step in another, not yet described species of the genus called *Paracatenula* sp. "schnitzel". The regeneration process followed the same pattern as described for *P. galateia* but was completed slightly faster after around 264 h. The pulse-chase EdU label in *P.* "schnitzel" was highly aggregated in the regenerated rostrum (Figure 4B) (n=3) comparable to the label observed in *P. galateia*. The BrdU-labeled S-phase cells were restricted to the region posterior to the brain and no signals were detected in the rostrum (Figure 4C,E) (n=3). This indicates the disappearance of the blastema and the restoration of the original condition where neoblasts are restricted to the body region posterior to the brain. Besides the regenerated brain at the boundary of the trophosome the serotonin stainings showed longitudinal nerves (Figure 4D,E) (n=3) which are more delicate than those seen in *P. galateia* (compare Figure 1A).

Pattern of neoblast proliferation and migration in amputated rostrum fragments

Compared to intact worms the freshly amputated rostrum fragments did not show an obvious change in their behavior besides increased speed and agility. Posterior regeneration of rostrum fragments, just

2 None of the *Paracatenula* species can be cultured so far. All experiments have been done with freshly collected *P. galateia*. In the limited time frame of 20 days on Carrie Bow Cay Island (Belize), the long-term (chase ≥10 days) regeneration experiments including the pulse-chase-pulse labeling were not successful.

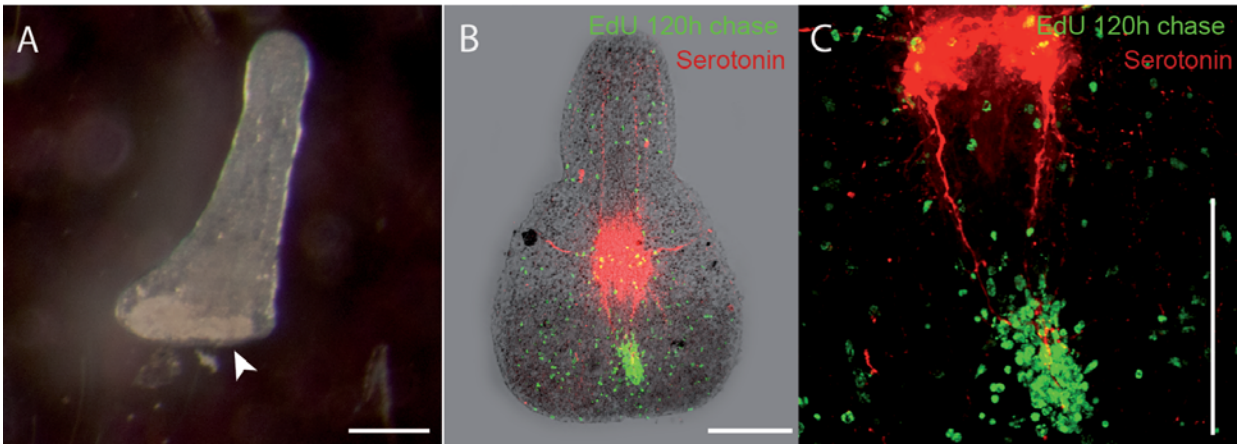

Figure 5: Posterior regenerating rostrum fragments. (A) Rostrum fragment 48 h after amputation under incident light. The wound on the posterior end is almost closed due to the flattening of surrounding epidermal cells. (B) EdU-pulse-120h-chase labeled rostrum fragment. The EdU labeled cells (green) are evenly distributed in in all areas of the fragment, but a massive aggregation of cells encapsulating the posterior tip of the longitudinal main nerves (red) is seen. (C) This image shows a higher magnification of the labeled cells encapsulation the tip of the nerves. Scale bar 100µm in all images.

like regeneration of the anterior trophosome fragments started with the reduction of the wound size by constriction of the ring musculature and wound closure within 48 h, including a flattening of surrounding epidermal cells (arrowhead in Figure 5A). Within the following 16 days all rostrum fragments died without showing any further signs of posterior growth/regeneration. Two EdU pulse-120 h-chase labeled rostrum fragments could be fixed and analyzed. In both the EdU-labeld cells had migrated into the rostrum and several EdU-labeled cells showed overlapping serotonin staining. While one of the rostrum fragments showed an aggregation of cells encapsulating the posterior tip of the longitudinal main nerves (Figure 5B,C), in the other one an even distribution of EdU label was observed (Figure S1).

Discussion

Morphallaxis and behavior

In *P. galateia*, a predominantly asexually reproducing catenulid, rostrum amputation always was followed by morphallactic processes leading to wound closure. This is probably a plesiomorphy feature of flatworms since the same pattern was observed in various taxa (Egger et al. 2006, and reviewed in Egger et al. 2007, Moraczewski 1977). Also the behavior that both fragment types (anterior and posterior fragments) showed after amputation and during regeneration is similar to that described from other flatworms. The first reaction to decapitation is always an escape reaction like moving backwards or coiling up. After the first "shock effect" fragments containing the brain often continue moving rapidly while brainless fragments remain relatively stationary during regeneration until the brain is restored (Moraczewski 1977, Reddien and Sanchez Alvarado 2004).

Slow regeneration

In the species *Paracatenula* cf. *polyhymnia* the rostrum regeneration process takes only 48-72 h (Dirks et al. in review). Moraczewski (1977) described that a *Catenula* sp. needed about 60h for rostrum regeneration and Palmberg (1991) showed that *Microstomum lineare* regenerated its rostrum completely in only 45h. The time of about two weeks *P. galateia* needs to regenerate the complete rostrum is quite long in comparison with the above mentioned species. Additionally the EdU-chase-BrdU experiments indicate that the cell cycle (S-phase in particular) may take more than 48h in total. Preliminary experiments with non-amputated *P. galateia* in which we used nocodazole to accumulate pulse-labeled cells in mitosis point to the length of S-phase and G2-phase in the frame of 48-72h (own unpublished data). This would be exceptionally slow compared to other flatworms like e.g. *Macrostomum lignano* passing through both S-phase and G2-phase within maximal 24h (probably even faster) (Nimeth et al. 2004). It has been shown in different animal systems that in addition to the known checkpoints, at which the eukaryotic cell cycle can be arrested, certain conditions like the lack of nutrients can slow down the progress of different parts of the cell cycle including the S-phase (Alexiades and Cepko 1996, Paulovich and Hartwell 1995, Steinemann 1980). Besides *P. galateia* possibly being traumatized due to the loss of its head it is also likely that it is starving under the culture conditions. The worms do not have a mouth or a gut and thus totally depend on the bacterial symbionts for nutrition (Gruber-Vodicka et al. 2011). So far it is not possible to

cultivate any of the known *Paracatenula* species likely because host and symbiont starve to death after a while. Therefore a starvation-induced "slow-down" of the cell cycle may be possible. Until a cultivation of the symbiosis is possible it will be difficult to prove whether this is the case.

No posterior regeneration

Within 16 days observing the *P. galateia* rostrum fragments neither growth of the symbiont-housing trophosome tissue nor of a symbiont free "tail" (which is present in other *Paracatenula* species; see Dirks et al. 2011) occurred. It is hard to believe that these worms are incapable to regenerate posteriorly since there is no other example of animals that can regenerate anteriorly but not posteriorly (reviewed in Egger et al. 2007). Here we provide four hypothetical explanations for the absence of posterior regeneration from rostrum fragments under the experimental conditions: (1) The number of neoblasts in the rostrum fragments is too small to accomplish posterior regeneration. The rostrum is devoid of neoblasts (see Figure 1A), thus anterior fragments contained just a rather small number. Since neoblasts are the major drivers of regeneration their almost absence may lead to a slow down or even to an incapability to regenerate. (2) In flatworm species from various taxa it was observed that regeneration of any body part requires certain parts of the digestive system (Egger et al. 2006, Egger et al. 2007) which is lacking in *Paracatenula* and has been functionally replaced by the trophosome. So far it is not known from which germ layer the trophosome derives. If it originates from the endoderm and is a modification of the pharynx or gut, the inability of *P. galateia* to regenerate posteriorly may have its cause in the lack of this organ. (3) The loss of almost the whole trophosome should results in insufficient host nutrition by the symbionts. This starvation may lead to a slow down or even arrest in the neoblast cell cycle preventing regeneration and growth of the eukaryotic tissue. In other flatworms it has been shown that starvation can even lead to shrinkage and degeneration of certain organs (Baguna 1976, Baguna and Romero 1981, Nimeth et al. 2004). The fact that no cultivation attempt of any *Paracatenula* species was successful so far may point to inappropriate nutrition (culture conditions) of one or both symbiotic partners. (4) Finally the trophosome region consists almost solely of the symbiont housing bacteriocytes surrounded by an epidermis. If the bacterial symbionts do not grow (proliferate), regeneration and growth of the trophosome region would be a waste of energy and resources for the host. All these reasons may lead to the incapability of *P. galateia* rostrum fragments to regenerate posterior parts under laboratory conditions. It is, however, extremely

likely that under natural nutrition/conditions the animals can alo regenerate posteriorly.

Regeneration of a symbiotic metazoan

Since the studies of Thomas Hunt Morgan (1905) it was speculated and today it is well known that a gradient of morphogens is important to reestablish axes and the identities of tissues in regenerating flatworms. To form a gradient along an axis a minimal tissue size (or cell number) is required (Adell et al. 2010 reviewed regeneration gradients in planarians). For *P. galateia* we did not study which is the smallest trophosome region fragments capable to regenerate a rostrum, but we showed in this and a previous study (Dirks et al. in review) that small 0.5mm fragments do regrow a rostrum on only the anterior side. It has to be considered that almost 40% of *P. galateia´*s trophosome region is made up by the bacterial symbionts (Gruber-Vodicka et al. 2011). Apparently this high symbiont/host ratio does not negatively influence the morphogenic gradients necessary to establish axis formation in regenerating *P. galateia*. Future studies will reveal further details on gradient formation during regeneration of lost body parts in *P. galateia*.

With the exception of the peritrich ciliate *Zoothamnium niveum,* no chemosynthetic symbiosis or the isolated symbionts has been successfully cultivated (Dubilier et al. 2008, Rinke et al. 2007). Although we have made a good progress in keeping *P. galateia* alive, a permanent cultivation is not possible at the moment. Nevertheless the understanding of developmental processes and host-symbiont interactions in this exceptional tight animal-bacteria symbiosis model *P. galateia* is of great importance for the field of symbiosis research.

Supplementary figure

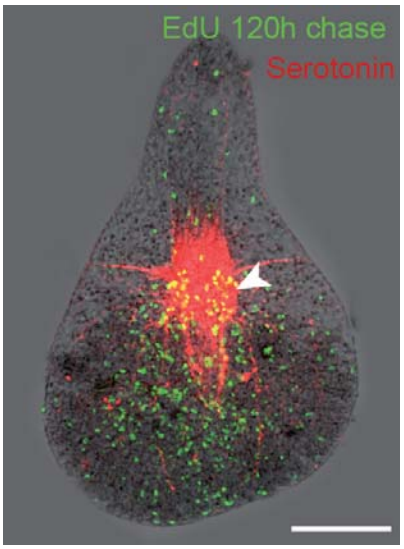

Figure S1: EdU pulse-120h-chase-labeled rostrum fragment of *P. galateia*. Most EdU labeled cells (green) are evenly distributed in the posterior region of the fragment while a few labeled cells are also found in the rostrum. Note the double label of EdU and serotonin (yellow) in the brain area. Scale bar 100 μm.

References

Adell T, Cebrià F, Saló E (2010). Gradients in Planarian Regeneration and Homeostasis. *Cold Spring Harbor Perspectives in Biology* **2:** a000505.

Alexiades M, Cepko C (1996). Quantitative Analysis of Proliferation and Cell Cycle Length During Development of the Rat Retina. *Developmental Dynamics* **205:** 293 - 307.

Baguna J (1976). Mitosis in the intact and regenerating planarian *Dugesia mediterranea* n.sp. I. Mitotic studies during growth, feeding and starvation. *J Exp Zool* **195:** 53 - 64.

Baguna J, Romero R (1981). Quantitative analysis of cell types during growth, degrowth and regeneration in the planarians *Dugesia mediterranea* and *Dugesia tigrina*. *Hydrobiologia* **84:** 181 - 194.

Bode A, Salvenmoser W, Nimeth K, Mahlknecht M, Adamski Z, Rieger RM et al. (2006). Immunogold-labeled S-phase neoblasts, total neoblast number, their distribution, and evidence for arrested neoblasts in *Macrostomum lignano* (Platyhelminthes, Rhabditophora). *Cell Tissue Res* **325:** 577-587.

Dalyell J (1814). *Observations on some interesting phenomena in animal physiology exhibited by several species of planariae.* London, UK: Edinburgh House.

Dirks U, Gruber-Vodicka H, Leisch N, Sterrer W, Ott J (2011). A new species of symbiotic flatworms, *Paracatenula galateia* sp. nov. (Platyhelminthes: Catenulida: Retronectidae) from Belize (Central America). *Marine Biology Research***:** in press.

Dirks U, Gruber H, Leisch N, Bulgheresi S, Egger B, Ladurner P et al. (in review). Continued De Novo Formation and Asexual Transmission of Bacteriocytes in the Symbiotic Flatworm *Paracatenula galateia*. *ISME Journal*.

Dubilier N, Bergin C, Lott C (2008). Symbiotic diversity in marine animals: the art of harnessing chemosynthesis. *Nature reviews* **6:** 725-740.

Egger B, Ladurner P, Nimeth K, Gschwentner R, Rieger R (2006). The regeneration capacity of the flatworm *Macrostomum lignano* - on repeated regeneration, rejuvenation, and the minimal size needed for regeneration. *Dev Genes Evol* **216:** 565-577.

Egger B, Gschwentner R, Rieger R (2007). Free-living flatworms under the knife: past and present. *Development Genes and Evolution* **217:** 89-104.

Gruber-Vodicka HR, Dirks U, Leisch N, Baranyi C, Stoecker K, Bulgheresi S et al. (2011). *Paracatenula*, an ancient symbiosis between thiotrophic *Alphaproteobacteria* and catenulid flatworms. *Proceedings of the National Academy of Sciences*.

Ladurner P, Rieger R, Baguna J (2000). Spatial distribution and differentiation potential of stem cells in hatchlings and adults in the marine platyhelminth Macrostomum sp.: a bromodeoxyuridine analysis. Dev Biol 226: 231-241.

Ladurner P, Mair GR, Reiter D, Salvenmoser W, Rieger RM (1997). Serotonergic Nervous System of Two Macrostomid Species: Recent or Ancient Divergence? Invertebr Biol 116: 178-191.

Moraczewski J (1977). Asexual reproduction and regeneration of *Catenula* (Turbellaria, Archoophora). *Zoomorph* **88:** 65 - 80.

Morgan TH (1905). "Polarity" considered as a phenomenon of gradation of materials. *J Exp Zool* **2:** 495-506.

Newmark PA, Sanchez Alvarado A (2000). Bromodeoxyuridine specifically labels the regenerative stem cells of planarians. *Dev Biol* **220:** 142-153.

Nimeth KT, Mahlknecht M, Mezzanato A, Peter R, Rieger R, Ladurner P (2004). Stem cell dynamics during growth, feeding, and starvation in the basal flatworm *Macrostomum sp.* (Platyhelminthes). *Dev Dyn* **230:** 91-99.

Palmberg I (1991). Differentiation during asexual reproduction and regeneration in a microturbellarian. *Hydrobiologia*.

Paulovich AG, Hartwell LH (1995). A checkpoint regulates the rate of progression through S phase in *S. cerevisiae* in Response to DNA damage. *Cell* **82:** 841-847.

Reddien PW, Sanchez Alvarado A (2004). Fundamentals of planarian regeneration. *Annu Rev Cell Dev Biol* **20:** 725-757.

Rinke C, Lee R, Katz S, Bright M (2007). The effects of sulphide on growth and behaviour of the thiotrophic *Zoothamnium niveum* symbiosis. *Proceedings Biological sciences / The Royal Society* **274:** 2259-2269.

Steinemann M (1980). Chromosomal replication in *Drosophila virilis*. *Chromosoma* **78:** 211-223.

Conclusive Discussion

The results presented in this thesis shed light on *Paracatenula* (especially the newly described species *P. galateia*) as a candidate model system to study symbiotic interactions between an animal host and intracellular bacterial symbionts. The major goal was to investigate the mechanisms which *Paracatenula*-flatworms use to maintain their symbiotic association during growth and development (ontogenesis) and to transmit or reestablish the association during reproduction. The four chapters included in this thesis answer these questions and provide further interesting insights into this fascinating animal/bacteria symbiosis. The first two chapters are the detailed zoological and microbiological description of the symbiotic partners including the molecular analysis of their phylogenies. Chapter 3 and 4 resolve the developmental, regenerative and reproductive mechanisms used by the hosts to continuously maintain the symbiotic association. Each chapter contains a discussion of its respective results and methods. Accordingly this conclusive discussion does not recapitulate those but it includes some general afterthoughts on outcome of this thesis and questions which remained open. In the end an outlook on the future potential of *Paracatenula* as a model system in symbiosis research is provided.

The adaptation to the habitat

Paracatenula-species inhabit the upper few centimeters of sheltered marine soft bottom sediments in warm temperate to tropical regions. Usually the oxidized layer in these sediments is restricted to the upper few millimeters to centimeters while deeper, anoxic layers are sulfidic due to microbial sulfate reduction. Sulfide (H_2S) is extremely toxic for animals, because it poisons the nervous system and irreversibly blocks mitochondrial respiration. This is why eukaryotes avoid migrating into heavily sulfidic sediment layers. However, depending on water movements and the sediment grain size, there is a transition layer – the RDP (redox potential discontinuity) – between the sulfidic and the oxidized layer in which both, oxygen and sulfide concentrations are low or even zero (Ott et al. 1991, Ott 1993). For nearly all microbes it is

impossible to bridge this distance in order to gain energy by aerobic oxidation of reduced sulfur compounds. In contrast most animals can pass this distance and access both layers. Therefore it is not astonishing that many sulfur oxidizing microbes in this habitat are engaged in mutualistic symbiotic associations with animals. These microbes serve not only as a renewable food/energy source on or inside the animals body, but they also protect their hosts from the harmful effects of hydrogen sulfide by metabolizing it (Dubilier *et al.* 2008, Ott et al. 2004, Ott and Novak 1989, Ott et al. 1991).

Meiofauna in marine soft bottom sediments is often worm-shaped being able to wiggle and move between the grains (e.g. Annelida, Nematoda, Platyhelminthes, Acoela…). According to the general body plan of the Platyhelminthes also *Paracatenula*-species possess cilia on their surface which allow them to glide forwards and backwards. Due to an extremely soft body they can pass fairly narrow holes (e.g. *P. galateia* with a maximum width of 270 µm can pass through a sieve of 65µm mesh size (own observation)). In case of getting stuck (see Figure 1), the animals often break in two, because a "cost" for being so soft is fragility. All known species of the genus also tend to break or even burst open in response to environmental changes like strong microscope light or minor osmotic changes. Despite of the difficulty to handle the worms, their fragility is not adverse in every aspect. In the chapters 3 and 4 it is shown that fragmentation is followed by regeneration of the lost body parts and thus it can lead to an exponential growth of a clonal population.

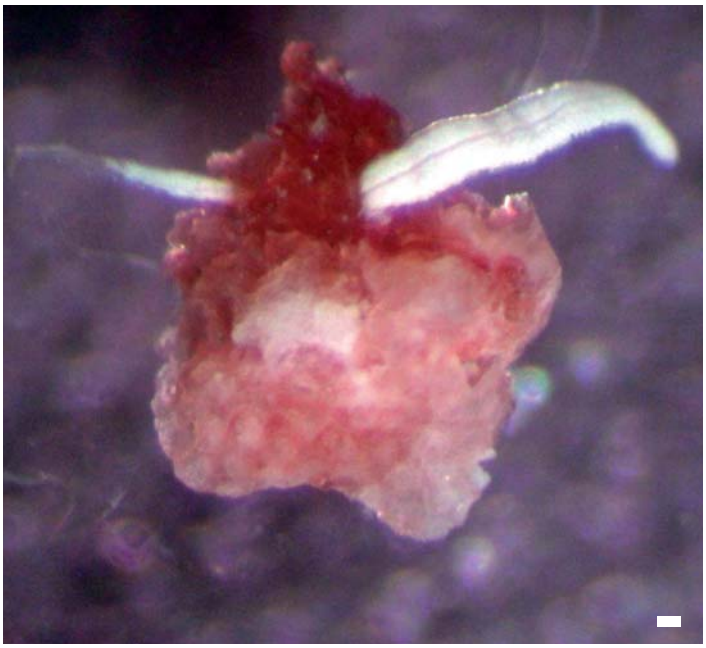

Figure 1: *Paracatenula galateia* got stuck in a fairly narrow hole of a coral skeleton. Scale bar 100µm.

Symbiont transmission during sexual and asexual reproduction

Within this thesis it is described how *P. galateia* and other species of the genus reproduce asexually by paratomy and thereby vertically transmit symbionts. However, it remains unclear if *Paracatenula* also

reproduce sexually and how the symbionts are transmitted if doing so. Here we discuss several general and specific arguments why there might be sexual reproduction in *Paracatenula* and why it was not observed yet. Finally we speculate how symbiont transmission during sexual reproduction might be accomplished:

Is the soma subjected to senescence? Most likely not only sexual, but also asexual metazoans undergo senescence (accumulation of deleterious mutations, telomere shortening,…) (Martínez and Levinton 1992). Studies on different predominantly asexually reproducing animals showed that their soma ages while the germ line does not. This finding, however, implies an unequivocal distinction between germ line and soma. If soma and germ-line do not segregate, then it would follow that any cell can become part of the germ line and senescence should not evolve (Martínez and Levinton 1992). In the case of P*aracatenula* clear proof for the existence of the germ line are still pending. Sterrer and Rieger (1974) found different types of inclusions in *Paracatenula*-species which they interpreted as spermatozoa. Leisch et al. (2011) found spicule shaped structures with unknown function in the species *P.* cf. *polyhymnia* and in chapter one of this thesis we describe peculiar inclusions in *P. galateia* which in the end also could not be assigned to any function. Sperm are the most diverse of all animal cell types (see Schärer et al. 2011 and references therein). The diversity in sperm design is thought to reflect adaptations to the highly variable conditions under which sperm function and compete to achieve fertilization. The peculiar inclusions in the different *Paracatenula* species may resemble such adaptations of sperm to „unusual“ conditions, but a proof remains open. Hence, nothing is known about soma and germ line segregation in these worms. As long as we do not unequivocally identify germ cells, trace and compare their origin with that of somatic cells, none of the two variants (senescence of the soma or not) can be excluded. Recent research on different rhabditophoran flatworm species indicates that probably a specific subpopulation of neoblast, expressing a *nanos*-like marker gene, is involved in germ cell production (Handberg-Thorsager and Saló 2007, Kuales et al. 2011). The data in this thesis provide a first characterization of the stem cells in *P. galateia*. A further investigation (e.g. the search for *nanos*like genes) will doubtless help to better understand processes like the hypothetical germ cell formation in *Paracatenula*. However, as long as a cultivation of these obligate symbiotic animals is not possible, the experimental access (especially experiments involving senescence) is strongly limited.

Is there a universal need of multicellular organisms to have sex? For a long time it was widely believed that sex is universal among multicellular organisms due to at least two reasons: asexual linages adapt too slow to environmental changes and the above discussed senescence of soma. Apart from this, sex is an evolutionary paradox because it consumes much more resources than asexual reproduction (Butlin 2002). In consequence it is not astonishing that different animals (e.g. various rotifers but also most catenulids) reproduce exclusively asexually under good (stable), but switch to sexual reproduction under problematic conditions, likely to accelerate recombination (Buchner 1937, Ehlers 1985, Falush 1999, Larsson 2007 and references therein). However, recent findings revealed that there are obviously also rotifers that live abstinent of sex since tens of millions of years. Welch & Meselson (2000) investigated Bdelloid rotifers and neither males or hermaphrodites, nor meiosis could be detected. Detailed sequence analysis of several genes from different species suggests that Bdelloid rotifers have been asexual for about 80 million years ($>10^8$generations). Based on genetic and fossil data also some species of the ostracod family *Darwinulidae* appear to abandon sex since at least 100 million years (Martens et al. 2003). For both, the rotifers and the ostracods it is not well understood how the expectable adaptation and senescence problems are overcome. A study by Gladyshev et al. (2008) revealed massive horizontal gene transfer (HGT) in Bdelloid rotifers, which may resemble a genetic exchange comparable to that in sexual populations. This accumulation of HGT has so far only been documented in combination with endosymbionts or endoparasites, which are both not found in the rotifers. For the *Paracatenula*-symbiosis a solely asexual reproduction can also not be excluded. The tight codiversification between host and symbiont indicate a strict vertical symbiont transmission like it was described in case of the asexual reproduction in chapter 3. Since the bacterial symbionts are intracellular and therefore could be involved in HGT-events replacing the recombination due to sexual reproduction, it is possible that sexual reproduction has been reduced or even lost like in the Bdelloid rotifers. From most other catenulid flatworms it is known, however, that asexual reproduction is the preferred way of reproduction under favorable conditions. Sexual catenulids have not often been observed and described in detail since during the asexual periods all sexual features vanish (Larsson 2007 and references therein). It is possible that *Paracatenula*-species follow similar patterns switching between sexual and asexual reproduction with a strong dominance on the asexual side. But also the "completely new mode of reproduction – such as parthenogenesis from sperm", which was suggested by Sterrer and Rieger (1974) along the transformation of male cells into oocytes described by Borkott (1970) for the

freshwater catenulid *Stenostomum* has not turned out to be wrong, yet. Sexual reproduction maybe is used as "the last resort" under unfavorable environmental conditions. In case of the species *P. galateia* we extremely seldom found animals which were slightly smaller than the average and might be juveniles (see Figure 3D in chapter 1). Future studies focusing on the detection of sperm, eggs or developmental stages of *Paracatenula* should involve sampling in different seasons with less favorable (stable) environmental conditions in order to increase the chance of detecting animals with features indicative for sexual reproduction.

Is the statocyst a feature of sexually produced *P. galateia*? The above mentioned smaller, possibly juvenile *P. galateia* animals, always possessed a statocyst, a feature most average sized animals do not have (own unpublished observation). A hypothesis is that only the sexually reproduced worms develop a statocyst while the asexually produced offspring does not regenerate it with the rostrum. This would explain why most "average sized" worms lack statocysts (see Figure 2).

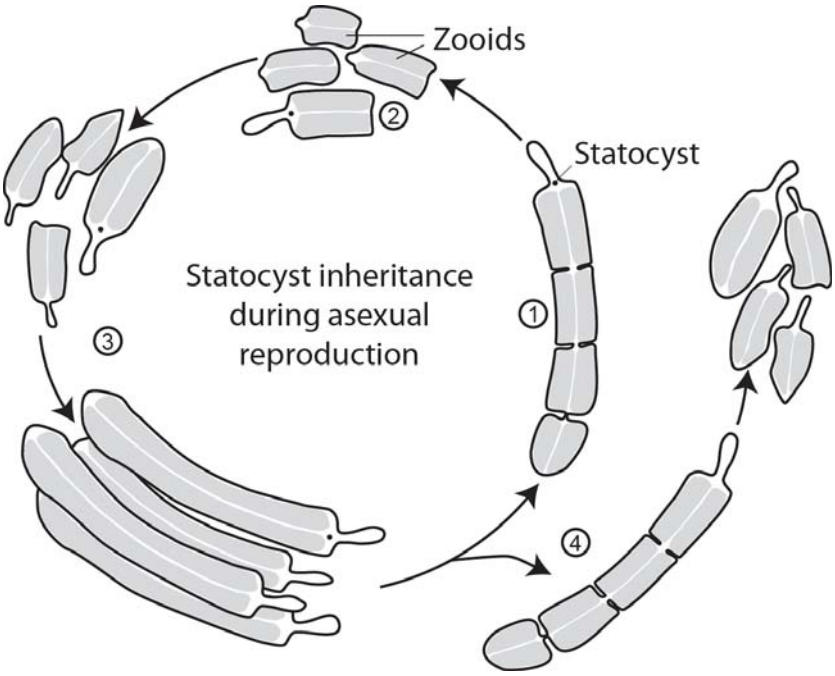

Figure 2: Hypothesis of the progressive depletion of animals with a statocyst in an asexual *Paracatenula* population. (compare figure 9 in chapter 3) 1: *Paracatenula* with statocyst reproducing by paratomy. 2: One zooid inherits the statocyst inside the parental rostrum, the others lack statocysts. 3: The zooids grow and regenerate everything except the statocyst. The worm with statocyst proceeds with step 1. 4: The statocyst-lacking worms produce further asexual offspring without statocyst.

A prediction of symbiont transmission during sexual reproduction: Since all known *Paracatenula*-species lack mouth and gut, it is fairly obvious that they rely on the nourishment provided by their symbiotic bacteria to survive. To guarantee the continuity of the species, the parental generation has either to transmit symbionts to the offspring in a perfectly safe way, or the aposymbiotic offspring has to take

up the symbiont selectively from an environmental symbiont population. In chapter 2 the long lasting codiversification between host and symbiont species is described, which strongly points to a vertical mode of symbiont transmission which we have already shown for asexual reproduction. The likelihood is extremely high, that during sexual reproduction the symbionts are also vertically transmitted from the parents to the offspring. In other symbioses this is for example ensured by symbiont integration into the germ cells or by direct transfer from the parent to the fertilized egg or embryo (reviewed in Bright and Bulgheresi 2010).

Establishing a new model system

Since the discovery in 1974 by Sterrer and Rieger and the reinvestigation by Ott et al. (1982) the genus *Paracatenula* remained relatively unexplored. This is mainly because of the sensitivity of these symbiotic animals to all kinds of handling procedures which causes that most researchers sampling sediments containing *Paracatenula* rarely find intact worms, but mostly battered fragments. In this thesis it is shown that it is possible to efficiently sample and even incubate intact worms for weeks. A first analysis of the ultrastructure and the investigation of the stem cells unmasked these worms as one of the most simple metazoan symbiosis systems known, which strictly consist of only two partners, one *Paracatenula* host-species and its specific *Candidatus* Riegeria bacterial symbiont. *Paracatenula* have a fairly simple body plan with a comprehensible number of cell types. In most known species the tissue (including the epidermis) is translucent and whole mount stainings do not require any bleaching step. The neoblast system, which was successfully detected by applying S-phase labeling with thymidine analogoues, allows tracing the origin and fate of all differentiated cell types, including the bacteriocytes. In no other bacteriocyte possessing symbiosis such a simple cell renewal strategy (all cell types derive from one source) has been observed, yet. Since the animals lack mouth and gut they (most probably) rely on their symbiotic bacteria as an energy source – the symbiosis is obligate. This enclosed two-partner system enables to study cellular and molecular interactions between host and symbiont without disturbance of external factors like e.g. ingested food.

The *Paracatenula*-symbiosis represents a highly evolved mutualistic partnership between a multicellular animal hosts and intracellular bacteria. Recent research showed that the strategies which symbionts and

hosts use to circumvent their mutual immune systems are in many ways similar to those in pathogenic interactions. In this thesis it is shown that the *Paracatenula* symbiosis is in many aspects unique among the known model systems and especially the neoblast stem cell system allows exceptional experimantal access. The understanding of this lasting intracellular association will reveal new insights in animal-bacteria interactions and thus may help to identify new drug targets in deleterious host-microbe interactions.

References

Bright M, Bulgheresi S (2010). A complex journey: transmission of microbial symbionts. *Nat Rev Micro* 8: 218-230.

Buchner H (1937). Experimentelle Untersuchungen über den Generationswechsel der Rädertiere. *Molecular and General Genetics* MGG 72: 1-49.

Butlin R (2002). The costs and benefits of sex: new insights from old asexual lineages. *Nat Rev Genet* 3:11-317.

Dubilier N, Bergin C, Lott C (2008). Symbiotic diversity in marine animals: the art of harnessing chemosynthesis. *Nature reviews* 6: 725-740.

Ehlers U (1985). "*Das Phylogenetische System der Plathelminthes*.". Gustav Fisher: Stuttgart.

Falush (1999). Measuring the benefits of sex. *Journal of Evolutionary Biology* 12: 1026-1028.

Gladyshev EA, Meselson M, Arkhipova IR (2008). Massive Horizontal Gene Transfer in Bdelloid Rotifers. *Science* 320: 1210-1213.

Handberg-Thorsager M, Saló E (2007). The planarian *nanos*-like gene Smednos is expressed in germline and eye precursor cells during development and regeneration. *Development Genes and Evolution* 217: 403-411.

Kuales G, De Mulder K, Glashauser J, Salvenmoser W, Takashima S, Hartenstein V et al. (2011). Boule-like genes regulate male and female gametogenesis in the flatworm *Macrostomum lignano*. *Dev Biol* In Press, Corrected Proof.

Larsson K (2007). Taxonomy and Phylogeny of Catenulida (Platyhelminthes) with Emphasis on the Swedish Fauna. Ph.D. thesis, Uppsala University.

Leisch N, Dirks U, Gruber-Vodicka HR, Sterrer W, Schmid M, Ott JA (in press). Microanatomy of the trophosome region of *Paracatenula* cf. *polyhymnia*, a catenulid flatworm with symbiotic bacteria. *Zoomorph*.

Mark Welch D, Meselson M (2000). Evidence for the evolution of bdelloid rotifers without sexual reproduction or genetic exchange. *Science* 288: 1211-1215.

Martens K, Rossetti G, Horne DJ (2003). How ancient are ancient asexuals? Proceedings of the Royal Society of London Series B: *Biological Sciences* 270: 723-729.

Martínez DE, Levinton JS (1992). Asexual metazoans undergo senescence. *Proceedings of the National Academy of Sciences* 89: 9920-9923.

Ott J, Bright M, Bulgheresi S (2004). Symbioses between Marine Nematodes and Sulfur-oxidizing Chemoautotrophic Bacteria. *Symbiosis* 36: 103-126.

Ott JA, Rieger G, Rieger R, Enderes F (1982). New mouthless interstitial worms from the sulfide system: Symbiosis with Prokaryotes. PSZN I: *Mar Ecol* 3: 313-333.

Ott JA, Novak R (1989). Living at an interface: Meiofauna at the oxygen/sulfide boundary of marine sediments. In: Ryland JS, Tyler PA (eds). 23rd European Marine Biology Symposium. Olsen & Olsen. pp 415–422.

Ott JA, Novak R, Schiemer F, Hentschel U, Nebelsick M, Polz M (1991). Tackling the sulfide gradient: A novel strategy involving marine nematodes and chemoautotrophic ectosymbionts. PSZN I: *Mar Ecol* 12: 261-279.

Ott JA (1993). Sulphide symbioses in shallow sands. In: Eleftheriou Aea (ed). Proc 28th Eur Mar Biol Symp. Olsen & Olsen: Fredensburg. pp 143-147.

Schärer L, Littlewood DTJ, Waeschenbach A, Yoshida W, Vizoso DB (2011). Mating behavior and the evolution of sperm design. *Proceedings of the National Academy of Sciences* 108: 1490-1495.

Sterrer W, Rieger R (1974). Retronectidae - a new cosmopolitan marine family of Catenulida (Turbellaria). In: Riser N, Morse M (eds). Biology of the Turbellaria. McGraw-Hill: New York. pp 63-92.

Summary & Zusammenfassung

Summary

Animals engaged in obligate intracellular symbiosis with microbes occur in a wide range of habitats. In the known cases the animal hosts profit from the metabolic capabilities of their symbionts which enable them to utilize additional food and energy resources. A major challenge in animal-microbe symbiosis research is to identify the mechanisms which allow hosts (1) to selectively establish and maintain associations with microbial symbionts inside specific host cells – the bacteriocytes - and (2) to pass these symbionts to the offspring during reproduction (transmission). To date, the investigation of bacteriocyte *de novo* formation (host cell differentiation and uptake of symbionts) was limited by the fact that this process is restricted to early, temporary developmental stages in the available animal model systems. Related to symbiont transmission two principal modes are known: horizontal transmission (each host generation takes up the symbionts anew from the environment) and vertical transmission (the parents transfer the symbionts directly to the offspring). Strict vertical transmission is usually connected with codiversification of the partners (congruent topology of the phylogenetic trees from host and symbiont).

The central objects of research in this thesis were mouth- and gutless marine Platyhelminthes of the genus *Paracatenula* and their bacterial symbionts. The latter are embedded in bacteriocytes that fill up large parts of the worm´s body. In particular it was analyzed how these animals maintain their symbiosis during growth and development and how they transmit the symbionts to the offspring during reproduction. The results summarized hereafter allow a considerably better understanding of the *Paracatenula* symbiosis. In addition they contribute to the understanding of other symbiotic associations possibly right up to the evolution of eukaryotic cell organelles.

The first part of this thesis is the description of a newly discovered *Paracatenula*-species,

Paracatenula galateia, which appeared to be well suited for further experiments that were conducted for this thesis. *P. galateia* could be sampled reliably in the field and even cultivated for up to several weeks, which was not possible with any other *Paracatenula*-species so far. In addition it appeared to be comparatively easy to handle during different staining and labeling procedures.

An important insight resulted from the phylogenetic analysis of numerous *Paracatenula*-species and their symbionts. It did not only identify the symbionts as the first known thiotrophic alphaproteobacterial symbionts, it furthermore revealed that hosts and symbionts coevolve since hundreds of million years.

We identified S-phase cells in *P. galateia* by applying pulse-labeling experiments with the thymidine-analogues BrdU and EdU and we traced their fates in pulse-chase experiments. The experiments revealed that apparently all cells in the animals exclusively derive from so called neoblasts (continuously proliferating pluripotent stem cells of Plathyhelminthes). It was documented in particular, that the S-phase label appears in bacteriocytes and many other differentiated cell types several days after the pulse-labeling. This delay is due to the time which neoblast daughter cells need to migrate and differentiate. The continued *de novo* formation of bacteriocytes in *P. galateia* is unique among all symbiosis models and makes this worm a promising model system to study the developmental detail of this exceptional cell type.

Astonishing was also the strategy of symbiont transmission observed in the animals. *P. galateia* reproduce predominantly asexually by paratomy (transverse fission during which differentiation of new organs occurs prior to separation from the parental animal; see introduction) and regeneration of accidently torn off fragments. Inside these fragments the host transmits numerous symbionts vertically. This kind of transmission is different from the described ones, since the symbionts permanently remain in their familiar environment, the bacteriocytes. In all other known cases of bacteriocyte possessing animals, the symbionts must translocate from the parental bacteriocyte to either a germ cell or directly to the offspring. This translocation bears the risk of detachment for the partners and may also result in host-switching in case other microbes, which do not directly come from the parent, are taken up by the offspring. Furthermore the transmission of low numbers of symbionts deriving from a small enclosed population can lead to an accumulation of deleterious mutations in this population. This effect is termed “transmission bottleneck”. In case of *P. galateia* all these transmission-risks do not come into effect since numerous symbionts

inside of bacteriocytes are transmitted to the asexual offspring. This exceptional transmission strategy may explain the strict codiversification of *Paracatenula* hosts and their respective symbionts.

Both, the *de novo* formation of bacteriocytes and their transmission to the asexual offspring reflect a high degree of symbiont integration into the developmental programs of the *Paracatenula*-host. A further investigation of this especially-tight obligate mutualistic partnership promises not only a better understanding of the interaction between animal and microbe, but it could also open up new insights of eukaryotic cell organelle evolution.

Zusammenfassung

Tiere mit intrazellulären mikrobiellen Symbionten kommen in zahlreichen Lebensräumen vor. In den bekannten Fällen profitieren die Wirtstiere von den umfangreichen metabolischen Fähigkeiten der Symbionten, die es ihnen ermöglichen, zusätzliche Nahrungs- und Energiequellen zu nutzen. Eine besondere Herausforderung in der Erforschung von Tier-Mikroben Symbiosen ist die Identifikation der Mechanismen, die es dem Wirt erlauben (1) spezifische Partnerschaften mit Symbionten in speziellen Wirtszellen – den Bakteriozyten – einzugehen und aufrecht zu halten, sowie (2) diese intrazellulären Symbionten während der Fortpflanzung an die Nachkommenschaft weiterzugeben (Transmission). Bislang war die Erforschung der *de novo* Formation von Bakteriozyten (die Differenzierung der Wirtszelle inklusive der Aufnahme von Symbionten) dadurch limitiert, dass dieser Prozess in den verfügbaren Modellsystemen auf frühe, temporäre Entwicklungsstadien begrenzt ist. In Bezug auf die Transmission von Symbionten sind zwei grundlegende Strategien bekannt: horizontale Transmission (Symbionten werden von jeder Wirtsgeneration neu aus der Umwelt aufgenommen) oder vertikale Transmission (Symbionten werden von den Eltern direkt an den Nachwuchs weitergegeben). Strikt-vertikale Transmission ist in der Regel verbunden mit Kodiversifikation der Partner (kongruente Topologie der Stammbäume von Wirt und Symbiont).

Das zentrale Forschungsobjekt dieser Arbeit waren mund- und darmlose marine Platyhelminthen der Gattung *Paracatenula* und deren bakterielle Symbionten, die eingebettet in Bakteriozyten den Großteil des Tierkörpers füllen. Im Speziellen wurde untersucht, wie diese Tiere ihre Symbiose während Wachstum und Entwicklung aufrecht halten und die Symbionten bei der Fortpflanzung an die Nachkommenschaft weitergeben werden. Die im Folgenden zusammengefassten Ergebnisse zu diesen Fragestellungen erlauben ein sehr viel besseres Verständnis der *Paracatenula* Symbiose und ermöglichen zusätzlich interessante Rückschlüsse auf andere symbiotische Beziehungen bis hin zur Evolution der eukaryotischen Zellorganellen.

Der erste Teil dieser Doktorarbeit ist die Beschreibung einer neu entdeckten *Paracatenula* Art, *Paracatenula galateia*, die sich als äußerst gut geeignet für weitere in dieser Studie durchgeführte Experimente herausstellte. *P. galateia* konnte zuverlässig im Freiland gesammelt und sogar für einige Wochen kultiviert und inkubiert werden. Dies ist bislang mit keiner anderen *Paracatenula* Art gelungen. Weiterhin zeigte sich eine vergleichsweise gute Handhabbarkeit der Tiere bei der Anwendung verschiedener Färbe- und Markierungstechniken.

Eine wichtige Erkenntnis ergab sich durch die phylogenetische Analyse von mehreren *Paracatenula*-Arten und deren Symbionten. Diese zeigte nicht nur, dass in den Bakteriozyten der Würmer die ersten bekannten thiotrophen alphaproteobacteriellen Symbionten leben, sondern es spiegelt sich auch eine strikte, seit mehreren hundert Millionen Jahren andauernde Koevulotion von Wirt und Symbiont wieder.

Durch Markierungsexperimente mit Thymidin-Analoga (BrdU und EdU) konnten S-Phase Zellen in *P. galateia* identifiziert und deren Schicksale verfolgt werden. Dabei zeigte sich, dass offenbar alle Zellen in den Tieren ausschließlich von so genannten Neoblasten (kontinuierlich proliferierende pluripotente Stammzellen in Platyhelminthen) abstammen. Im speziellen konnte dann dokumentiert werden, dass erst mehrere Tage nach dem S-Phase Markierungspuls ein Signal in den Bakteriozyten und vielen anderen differenzierten Zelltypen nachweisbar ist. Diese Verzögerung rührt daher, dass die Tochterzellen der Neoblasten Zeit benötigen um im Körper des Tieres zu ihrer Zielposition zu wandern und zu differenzieren. Die kontinuierliche *de novo* Bildung von Bakteriozyten ist einzigartig unter den bekannten Symbiosen und macht *P. galateia* zu einem vielversprechenden Modellsystem um den Entwicklungsprozess dieses besonderen Zelltyps im Detail zu erforschen.

Als erstaunlich erwies sich auch die Symbionten-Transmissions-Strategie der Tiere. *P. galateia* vermehrt sich hauptsächlich (vielleicht ausschließlich) asexuell durch Paratomie (transversale Teilung, bei der die Differenzierung neuer, zu ersetzender Organe vor der Trennung vom Elterntier eingeleitet wird) oder durch die Regeneration versehentlich abgerissener Fragmente. Mit diesen Fragmenten übertragen die Wirte große Mengen an Symbionten. Diese Art der vertikalen Transmission unterscheidet sich besonders dadurch von allen anderen beschriebenen, dass die Symbionten völlig unbehelligt in ihren gewohnten Lebensraum, dem inneren der Bakteriozyten, verbleiben. In allen anderen untersuchten Symbiosen mit

Bakteriozyten müssen die Symbionten, selbst wenn die Transmission vertikal erfolgt, von der elterlichen Bakteriozyte in eine Keimzelle oder direkt zur Nachkommenschaft wechseln. Dabei kommt es immer wieder zum Kontaktverlust der Partner und gegebenenfalls zum Symbionten-Wechsel im Falle dass andere Mikroben, die nicht direkt von den Eltern kommen, aufgenommen werden. Weiterhin birgt die Weitergabe geringer Symbionten-Mengen aus einer kleinen, abgeschlossenen Population das Risiko der Akkumulation schädlicher Mutationen in diese Population. Dies wird als „Transmissions-Flaschenhals“ bezeichnet. Im Falle von *P. galateia* kommen all diese Transmissionsrisiken nicht zum Tragen, da zahlreiche Symbionten im Inneren der Bakteriozyten direkt an die asexuelle Nachkommenschaft weitergegeben werden. Diese besondere Art der Transmission könnte die strikte Kodiversifikation von *Paracatenula* Wirten mit ihren jeweiligen Symbionten erklären.

Beides, die wiederholte *de novo* Bildung der Bakteriozyten und deren Transmission an die asexuellen Nachkommen in *P. galateia* reflektieren den hohen Grad an Symbionten-Integration in das Entwicklungsprogramm des Wirtes. Die weitere Erforschung dieser besonders engen Partnerschaft verspricht nicht nur ein besseres Verständnis von der Interaktion zwischen Tier und Bakterie, sondern könnte auch neue Erkenntnisse über die Evolution von Zellorganellen eröffnen.

ACKNOWLEDGMENTS / DANKSAGUNG

Ich möchte hiermit meinem Dissertationsbetreuer Jörg Ott dafür danken, dass er mich vor vier Jahren in seine Arbeitsgruppe aufnahm und umgehend das Vertrauen schenkte, mich eigenständig an einem hochinteressanten Thema forschen zu lassen. Gleichzeitig stand Jörg immer mit Rat und Tat unterstützend zur Seite.

Der gesamten Shallow Water Symbiosis Arbeitsgruppe danke ich für jegliche Unterstützung, sowohl im Labor in Wien als auch während der Feldarbeit an den schönsten Stränden der Welt, sowie für die vielen netten Momente abseits der Arbeit.

Besonderer Dank gilt Harald Gruber, der mir auf sechs gemeinsamen Forschungsreisen rund um den Globus, sowie im Wiener Labor und besonders auch am Computer immer helfend zur Seite stand.

Silvia Bulgheresi und Niko Leisch danke ich für deren Umfangreiche Unterstützung im Labor, am Strand und beim Schreiben.

Danken möchte ich auch meinen Initiativkolleg-Kommilitonen Faris Behnam, Jan Dolinsek und Ilias Lagkouvardos, die mit mir und ich mit Ihnen alle Höhen und Tiefen der gesamten Dissertationszeit durchlebte.

Bernhard Egger, Peter Ladurner, Willi Salvenmoser und Gunde Rieger, haben mich mehrmals herzlich in Innsbruck empfangen und mir eine hervorragende Orientierung im Land der Plattwurm-Stammzellen verschafft. Besonders Bernhard möchte ich für seine enorme Hilfsbereitschaft und die unzähligen fachbezogenen und fachfremden Diskussionen in Innsbruck, Wien und Diepenbeek danken.

Auch Wolfgang Sterrer gebührt großer Dank für seine fachmännische Unterstützung bei der Suche nach und der Arbeit mit *Paracatenula*. Genauso wertvoll war aber auch seine humorvolle Art, die auch zähe Tage vor dem Mikroskop kurz erscheinen ließ.

Die größte nicht-wissenschaftliche Unterstützung leisteten zweifelsohne meine Freundin Ariane Marx und im letzten Jahr auch unsere gemeinsame Tochter Luisa. Wenn ich am Ende eines erfolglosen Tages zu den beiden nach Hause kam, waren die Sorgen stets schnell vergessen. Besonders Ariane möchte ich Danken für Ihre nachhaltige Unterstützung meiner Arbeit und der Bereitschaft auch Opfer mit mir zusammen dafür zu bringen.

CURRICULUM VITAE

Personal Data

First- and surname	Ulrich Dirks
Date and place of birth	21.09.1978 in Wesel, Germany
Nationality	German

Education

1999/5	High school diploma at the Andreas-Vesalius-Gymnasium in Wesel, Germany
2000/10-2001/9	Studies of engineering at the Ruhr-University Bochum, Germany

2001/10-2007/3	Studies of Biology at the Heinrich Heine University in Duesseldorf, Germany; main focus on developmental biology, biochemistry and ecophysiology; final Diploma grade: excellent (1,7)
Since autumn 2007	PhD-thesis at the Department of Marine Biology at the University of Vienna; Student in the international graduate school "Symbiotic interactions"

Further scientific education and training

2005/10-2006/1	Trainee at the Max-Planck-Institute for marine Microbiology in Bremen, Germany
2007	Assistant at the HYDRA-Institute for marine science field station on Elba, Italy

Scientific presentations

2008	"12th Symposium of the International Society of Microbial Ecology", Cairns, Australia (poster presentation)
2009	"International Symposium on Flatworm Biology", Diepenbeek, Belgium (Talk)
2010	"Science Day" at Ecology Center of the University of Vienna, Austria (Talk)
2010	"International Symposium on Symbiotic interactions", University Wien, Austria (Talk)

Publications

2011

Sequence variability of the pattern recognition receptor Mermaid mediates specificity of marine nematode symbioses. ISME Journal (2011) Bulgheresi S, Gruber-Vodicka HR, Heindl NR, **Dirks U**, Kostadinova M, Breiteneder H and Ott JA.

A new species of symbiotic flatworms, *Paracatenula galateia* sp. nov. (Platyhelminthes: Catenulida: Retronectidae) from Belize (Central America), MBR (2011) **Dirks U** et al.

Paracatenula, an ancient symbiosis between thiotrophic Alphaproteobacteria and catenulid flatworms. PNAS (2011) Gruber-Vodicka H, **Dirks U** et al.

Microanatomy of the trophosome region of *Paracatenula* cf. *polyhymnia*, a catenulid flatworm with intracellular symbionts. Paper in press in Zoomorphology. Leisch N, **Dirks U**, et al.

in progress

Continued *de novo* formation and asexual transmission of bacteriocytes in the symbiotic flatworm *Paracatenula galateia*. Paper under review at The ISME Journal **Dirks U** et al.

Proliferation pattern of neoblasts during rostrum regeneration of the symbiotic flatworm *Paracatenula galateia* – a pulse-chase pulse analysis. (Ready for submission). **Dirks U** et al.

Further skills

Fieldwork	Research stays at international Field stations in Belize (Central-America), Australia, Egypt and Italy. Sampling of meiofauna und microorganisms; microsensor-measurements under water.
	Sampling of planktonic microbes in the Arendsee, Germany.
Laboratory work	Experienced in various techniques of histology, cell-, micro- and molecular biology.
	Basic knowledge in animal physiology and biochemistry.
	Experienced in dissecting vertebrates (mouse, chicken, fish).
Teaching	Supervision of Diploma-Students
	Teaching assistance in advanced laboratory courses
Language skills	German: native speaker
	English: fluently